



Measurement of the top-quark mass using a leptonic invariant mass in pp collisions at $\sqrt{s} = 13$ TeV with the ATLAS detector

The ATLAS Collaboration

A measurement of the top-quark mass (m_t) in the $t\bar{t} \rightarrow$ lepton + jets channel is presented, with an experimental technique which exploits semileptonic decays of b -hadrons produced in the top-quark decay chain. The distribution of the invariant mass $m_{\ell\mu}$ of the lepton, ℓ (with $\ell = e, \mu$), from the W -boson decay and the muon, μ , originating from the b -hadron decay is reconstructed, and a binned-template profile likelihood fit is performed to extract m_t . The measurement is based on data corresponding to an integrated luminosity of 36.1 fb^{-1} of $\sqrt{s} = 13$ TeV pp collisions provided by the Large Hadron Collider and recorded by the ATLAS detector. The measured value of the top-quark mass is $m_t = 174.41 \pm 0.39$ (stat.) ± 0.66 (syst.) ± 0.25 (recoil) GeV, where the third uncertainty arises from changing the PYTHIA8 parton shower gluon-recoil scheme, used in top-quark decays, to a recently developed setup.

Contents

1	Introduction	2
2	ATLAS experiment	3
3	Data and Simulation	4
3.1	Data sample and object definition	4
3.2	Object and event selections	4
3.3	Signal and background simulations	6
3.4	Modelling of heavy-quark fragmentation, hadron production and decays	7
4	Analysis	12
4.1	Event yields and sample composition	12
4.2	Extraction of the top-quark mass	13
5	Measurement uncertainties	17
5.1	Statistical and datasets	20
5.2	Modelling of the signal process	21
5.3	Modelling of background processes	24
5.4	Detector response	25
6	Conclusions	27

1 Introduction

The large mass of the top-quark plays a role in much of the dynamics of elementary particles via loop diagrams. In the Standard Model (SM), the large top-quark mass significantly affects the radiative corrections to both the Higgs boson and W -boson masses, providing a relationship that can be used for precision tests of the consistency of the SM [1]. Furthermore, a precise measurement of the top-quark mass is required to predict the evolution of the Higgs quartic coupling at high scales [2, 3]. If performed with a precision of the order of a few hundred MeV, the direct determination of the top-quark mass from its decay products, and the indirect measurements from top-quark production cross-sections or kinematic distributions, are important not only for the constraints mentioned above, but also for the challenge of the interpretation of such measurements in the context of a strongly interacting particle theory [4, 5].

A direct measurement of the top-quark mass (m_t) is presented that uses a partial, leptonic-only, invariant mass reconstruction of the top-quark decay products. The analysis is performed from a sample of reconstructed $t\bar{t}$ events in the ℓ +jets channel, where one of the two W -bosons from the top- and antitop-quarks decays leptonically. In the top-quark decay $t \rightarrow Wb$, the invariant mass $m_{\ell\mu}$ of the lepton ℓ (with $\ell = e, \mu$) from the W -boson decay and the muon μ from a semileptonic decay of a b -hadron is constructed as the observable sensitive to the parent m_t value. The advantages of a strategy based on the invariant mass of visible leptonic decay products for the measurement of the top-quark mass rest mainly on the smaller sensitivity to the jet energy calibration and energy resolution, compared to the standard direct reconstruction methods, and on less sensitivity to top-quark production modelling (owing to the boost-invariant construction) than in methods based on the W -decay lepton alone [6]. Moreover, methods

with different types of systematic uncertainties are important when combining measurements, and for testing the consistency of the theoretical interpretation of the top-quark mass.

In this analysis the $m_{\ell\mu}$ distribution from models with different top-quark mass hypotheses is compared with data, and the optimal value of m_t is determined from a binned-template profile likelihood fit. A similar technique was first employed by the CDF Collaboration at the Tevatron collider [7], and a closely related analysis with J/ψ decays has been presented by the CMS Collaboration [8]; however, both these analyses yielded uncertainties in m_t of several GeV. Until now, the most precise measurement of the top-quark mass in the $t\bar{t} \rightarrow \ell\text{jets}$ channel by the ATLAS Collaboration was $m_t = 172.08 \pm 0.39$ (stat.) ± 0.82 (syst.) GeV, whereas combining multiple ATLAS measurements gave $m_t = 172.69 \pm 0.48$ GeV [9]. The CMS Collaboration reports its most precise combination as $m_t = 172.44 \pm 0.49$ GeV [10], and the Tevatron experiments report a combined value of $m_t = 174.30 \pm 0.65$ GeV [11]. Finally, the mass of the top-quark is indirectly determined from global electroweak fits as $m_t = 176.4 \pm 2.1$ GeV [12].

2 ATLAS experiment

The ATLAS experiment [13] at the LHC is a multipurpose particle detector with a forward–backward symmetric cylindrical geometry and a near 4π coverage in solid angle¹. It consists of an inner tracking detector surrounded by a thin superconducting solenoid providing a 2 T axial magnetic field, electromagnetic and hadronic calorimeters, and a muon spectrometer. The inner tracking detector covers the pseudorapidity range $|\eta| < 2.5$ and consists of silicon pixel, silicon microstrip, and transition radiation tracking detectors. The innermost layer, known as the insertable B-layer [14, 15], was added in 2014 and provides high-resolution hits at small radius to improve the tracking performance. Lead/liquid-argon (LAr) sampling calorimeters provide electromagnetic (EM) energy measurements with high granularity. A steel/scintillator-tile hadronic calorimeter covers the central pseudorapidity range ($|\eta| < 1.7$). The endcap and forward regions are instrumented with LAr calorimeters for both the EM and hadronic energy measurements up to $|\eta| = 4.9$. The muon spectrometer surrounds the calorimeters and is based on three large air-core toroid superconducting magnets with eight coils each and a bending power of 2.0 to 7.5 Tm. It includes a system of precision tracking chambers covering the region $|\eta| < 2.7$ and fast detectors for triggering in the range $|\eta| < 2.4$. A two-level trigger system was used to select events [16]. The first-level trigger is implemented in hardware and uses a subset of the detector information to reduce the accepted rate to at most 100 kHz. This is followed by the software-based high-level trigger, which reduces the event rate to around 1 kHz. An extensive software suite [17] is used in the reconstruction and analysis of real and simulated data, in detector operations, and in the trigger and data acquisition systems of the experiment.

¹ ATLAS uses a right-handed coordinate system with its origin at the nominal interaction point (IP) in the centre of the detector and the z -axis along the beam pipe. The x -axis points from the IP to the centre of the LHC ring, and the y -axis points upwards. Cylindrical coordinates (r, ϕ) are used in the transverse plane, ϕ being the azimuthal angle around the z -axis. The pseudorapidity is defined in terms of the polar angle θ as $\eta = -\ln \tan(\theta/2)$. Angular distance is measured in units of $\Delta R \equiv \sqrt{(\Delta\eta)^2 + (\Delta\phi)^2}$.

3 Data and Simulation

3.1 Data sample and object definition

The analysis is performed with the 2015 and 2016 proton–proton collision data sample produced by the LHC at a centre-of-mass energy of $\sqrt{s} = 13$ TeV and collected by the ATLAS experiment, corresponding to an integrated luminosity of 36.1 fb^{-1} [18]. The data sample was recorded during stable beam conditions, and all relevant ATLAS detector subsystems were required to be operational. The average number of pp collisions in the same bunch crossing (referred to as pile-up) in the data sample is 24.1.

Electron candidates are reconstructed from energy deposits (clusters) in the electromagnetic calorimeter matched to reconstructed tracks in the inner detector. Candidates in the transition region $1.37 < |\eta_{\text{cluster}}| < 1.52$ between the calorimeter barrel and endcaps are excluded. Muon candidates are reconstructed from track segments in the layers of the muon spectrometer, and matched to tracks found in the inner detector. The final muon candidates are re-fitted using the complete track information from both detector systems. Jet candidates are reconstructed from three-dimensional topological EM-scale energy clusters [19] in the calorimeter using the anti- k_t jet algorithm [20, 21] with a radius parameter $R = 0.4$. The reconstructed jets are calibrated to the level of stable-particle jets by the application of a jet energy scale (JES) correction derived from simulation and *in situ* corrections based on 13 TeV data [22]. There is no dedicated energy scale correction for jets with semileptonic heavy-flavour hadron decays. The missing transverse momentum, $E_{\text{T}}^{\text{miss}}$, is defined as the magnitude of the negative vector sum of the transverse momentum, p_{T} , of all reconstructed and calibrated physics objects in the event, with an extra term added to account for soft energy in the event that is not associated with any of the reconstructed objects [23]. This soft term is calculated from inner-detector tracks matched to the primary vertex in order to make it more resilient to pile-up contamination.

3.2 Object and event selections

The event selection is designed to collect a sample of $t\bar{t}$ candidate events in the final state $\ell\nu b j j' \bar{b}$, where $\ell = e$ or μ and the $j j'$ are the jets produced in the decay of the W -boson into quarks, and at least one of the b -initiated jets is associated with a muon from the semileptonic decay of a b -hadron. The goal is to select events where the lepton ℓ from the W -boson and the b -initiated jet with the muon from semileptonic decay come from the same top-quark.

Events are required to pass either a single-electron or single-muon trigger. Multiple trigger types were used: the lowest-threshold triggers include isolation requirements to reduce the trigger rate and had p_{T} thresholds of 20 GeV for muons and 24 GeV for electrons in 2015 data, and 26 GeV for both lepton types in 2016 data [16, 24, 25]. These triggers were complemented by others with higher p_{T} thresholds and no isolation requirements to increase event acceptance. Events must have at least one reconstructed vertex, i.e. at least two tracks with $p_{\text{T}} > 0.4$ GeV consistent with the beam-collision region in the x – y plane. If multiple vertices are reconstructed, then the primary vertex is taken to be the one with the largest sum, over the tracks assigned to it, of the transverse momentum squared of each track.

Events are further selected based on the presence of an electron or muon candidate from the decay of a W -boson, called ‘primary’ leptons. Primary-lepton electron candidates must satisfy a ‘tight’ likelihood-based identification criterion [26], be matched to the corresponding trigger, and have $p_{\text{T}} > 27$ GeV, $|\eta| < 2.47$ with the exclusion of $1.37 < |\eta| < 1.52$, longitudinal impact parameter $|z_0 \sin \theta| < 0.5$ mm

and transverse impact parameter significance $|d_0/\sigma(d_0)| < 5$, where $\sigma(d_0)$ is the uncertainty in the transverse impact parameter. Background from photon conversions, hadrons, and electrons produced away from the primary vertex (‘non-prompt’ electrons) is reduced by requiring the primary electron candidates to pass an isolation requirement based on the surrounding tracks and topological clusters in the calorimeter [26]. Primary-lepton muon candidates must satisfy a ‘medium’ quality identification criterion [27], be matched to the corresponding trigger, and have $p_T > 27$ GeV, $|\eta| < 2.5$, longitudinal impact parameter $|z_0 \sin \theta| < 0.5$ mm and transverse impact parameter significance $|d_0/\sigma(d_0)| < 3$. Background from hadrons and from muons produced away from the primary vertex (‘non-prompt’ muons) is reduced by requiring primary muon candidates to pass an isolation requirement based on the surrounding tracks and topological clusters in the calorimeter, and be separated by $\Delta R > 0.4$ from the nearest selected jet. If the nearest selected jet is $\Delta R \leq 0.4$ from the muon and has less than three associated tracks (including the muon track), the muon is kept and the jet is removed from the jet list, to ensure high efficiency for muons undergoing significant energy loss in the calorimeter. Events with more than one candidate primary lepton with $p_T > 25$ GeV are vetoed, in order to reject events from the $t\bar{t}$ dileptonic decay channel.

Jet candidates are required to have $p_T > 25$ GeV and $|\eta| < 2.5$, and a multivariate jet-vertex-tagger (JVT) is applied to suppress jets from pile-up [28]. During jet reconstruction, no distinction is made between identified electrons and jet energy deposits. Therefore, if any of the jets lie within $\Delta R = 0.2$ of a selected electron, the single closest jet is discarded in order to avoid double-counting electrons as jets. After this, electrons that are within $\Delta R = 0.4$ of a remaining jet are removed. Jets are identified as originating from a b -quark (b -tagged) using two techniques, one based on the reconstruction of a displaced jet (DJ tagging) and the other based on the semileptonic decay of a b -hadron into a so-called ‘soft muon’ (SMT tagging). For DJ tagging, multivariate techniques are used to combine information about the impact parameters of displaced tracks and the topological properties of secondary and tertiary decay vertices reconstructed within the jet [29]. The algorithm is trained on simulated $t\bar{t}$ events to discriminate b -jets from a background consisting of light-flavour jets and c -jets. A selection corresponding to an efficiency of 77% for b -jets in $t\bar{t}$ events is employed, with a rejection rate of a factor of 7 (100) for c -jets (light jets). The SMT tagging is performed by requiring the presence of a muon candidate satisfying the ‘tight’ quality identification criterion [27], $p_T > 8$ GeV and $|\eta| < 2.5$, with loose requirements on the impact parameters ($|d_0| < 3$ mm, $|z_0 \sin \theta| < 3$ mm) and with a distance $\Delta R < 0.4$ from a selected jet candidate. The definition of the muon object for the SMT tagging was optimised by maximising the efficiency for muons originating from the semileptonic decays of b - and c -hadrons (selecting approximately 50% of b -jets containing a muon, which are in turn 20% of all b -jets produced in $t\bar{t}$ events), minimising the misidentification rate (about 10^{-3} per light-flavour jet, mostly due to the decays of pions and kaons), and minimising the uncertainty in the measured top-quark mass. If more than one muon satisfying the criteria above is found within a given jet, the muon with the highest p_T is chosen.

Events must have at least one SMT-tagged jet and at least one DJ-tagged jet (which could be the same jet), among a total of at least four jet candidates with $p_T > 30$ GeV (with the exception of the SMT-tagged jet which may have a p_T as low as 25 GeV). If more than one SMT-tagged jet is found in the event, only the one with the highest- p_T muon is considered. The SMT muon and the primary lepton must be separated by $\Delta R_{\ell,\mu} < 2$. The presence of at least one neutrino in the final state is inferred from the requirements that $E_T^{\text{miss}} > 30$ GeV and $E_T^{\text{miss}} + m_T(W) > 60$ GeV.² The requirement that the SMT muon and the primary lepton must be separated by $\Delta R_{\ell,\mu} < 2$ enhances the fraction of events where both leptons come from the same top-quark, in contrast to events where the two leptons originate from different top-quarks.

² The transverse mass is given by $m_T(W) = \sqrt{2p_T^\ell E_T^{\text{miss}}(1 - \cos \Delta\phi)}$, where p_T^ℓ is the transverse momentum of the muon (electron) and $\Delta\phi$ is the azimuthal angle separation between the lepton and the direction of the missing transverse momentum.

The selected events are categorised as same-sign (SS) events or opposite-sign (OS) events according to the charge signs of the primary lepton and the soft muon. When both leptons come from the same top-quark, opposite-sign events are enriched in direct $b \rightarrow \mu X$ decays, while same-sign events have a large contribution from sequential $b \rightarrow cX' \rightarrow \mu X''$ decays; both samples carry information about the mass of the parent top-quark though. Finally, the invariant mass of the primary lepton and the soft muon ($m_{\ell\mu}$) is required to be between 15 and 80 GeV, as this is the region most sensitive to the top-quark mass. This requirement also suppresses the Z -boson, J/ψ and Υ resonances.

3.3 Signal and background simulations

A number of Monte Carlo (MC) simulation samples are used to model the expected signal of top-quark pairs and the background. The MC samples were processed either through the full ATLAS detector simulation [30] based on GEANT4 [31] or through a faster simulation making use of parameterised showers in the calorimeters [32]. Additional simulated pp collisions generated by PYTHIA 8.186 [33] with the MSTW2008 [34, 35] set of leading-order (LO) parton distribution functions (PDFs) and a set of tuned parameters called the A2 tune [36] were used to model the effects of both in-time and out-of-time pile-up. They were superimposed on the MC events, matching the luminosity profile of the recorded data. All simulated samples were processed through the same reconstruction algorithms and analysis chain as the data.

Simulated MC events were corrected so that the object identification efficiencies and energy and momentum scales and resolutions matched those determined from data control samples [22, 27, 28, 37]. The modelling of SMT muons and their misidentification due to light-hadron decays and detector background ('SMT fake') was studied using control samples as well. The efficiency of muon identification in jets was calibrated using muons from J/ψ and Z decays, and checked as a function of nearby track and calorimeter activity, and of the muon's transverse impact parameter d_0 . The calibration of the misidentification rate was performed, using the sample of W +jets events described in the following of the section, with the same approach used in Ref. [38]. A data-driven technique, described in detail in Ref. [39], is used to measure in data the normalisation and flavour composition of such events and to derive corrections that are applied to simulated samples for the calibration. A light-jets dominated sample of W + 1 jet events is then defined by selecting events where the jet is SMT-tagged but is not DJ-tagged, and using the SS category. A data-to-simulation scale factor (SF) of 1.10 ± 0.14 is measured. A slight miscalibration of the p_T of jets that contain a soft muon was observed, and the p_T of these jets was corrected in the simulation with a factor of 0.967 ± 0.024 . It has been measured by studying the distribution of the ratio of the p_T values of the SMT-tagged jet and the average non-SMT-tagged jet in $t\bar{t}$ data and simulation.

The $t\bar{t}$ sample was generated using the $h\nu q$ program [40] in the POWHEG-BOX v2 generator [41, 42] with the NNPDF3.0_{NLO} set of PDFs [43] and the top-quark mass set to 172.5 GeV. Additional samples with different top-quark mass hypotheses were produced in the range of m_t between 165 and 180 GeV, with steps of 0.5 GeV between 170 and 175 GeV. The samples have been produced using the appropriate top-quark decay width values predicted at next-to-next-to-leading order (NNLO) as a function of m_t [44]. The $h\nu q$ program uses on-shell matrix elements for production of $t\bar{t}$ pairs at next-to-leading order (NLO) in quantum chromodynamics (QCD). Off-shell effects and top-quark decays, including spin correlations, were approximated using MADSPIN [45]. Parton showers and hadronisation were modelled by PYTHIA 8.2 [33] using a dedicated 'A14- r_b ' setting of the ATLAS A14 [46] tune, as detailed in Section 3.4. The A14 tune is based on LEP and Tevatron collider data and also uses a combination of ATLAS $\sqrt{s}=7$ TeV measurements of the underlying event, jet production, Z -boson production and top-quark production in order to constrain

the parameters for the showers, multiple parton interactions and colour reconnection effects. Radiation in top-quark decays was handled entirely by the parton-shower generator, which implements matrix-element corrections with an accuracy equivalent to a calculation at the NLO level. The h_{damp} parameter, which controls the p_T of the first additional emission beyond the Born configuration, was set to 1.5 times the top-quark mass of each sample. The main effect of the h_{damp} setting is to regulate the high- p_T emission against which the $t\bar{t}$ system recoils. The EVTGEN v1.2.0 [47] program was used to simulate bottom and charm hadron mixing and decays. The production fractions and the branching ratios (BR) of the decay of b -hadrons and c -hadrons into muons were rescaled to the latest values from the Particle Data Group (PDG) [1], as detailed in Section 3.4. The simulated $t\bar{t}$ event sample was normalised to the Top++2.0 [48] theoretical cross-section of 832^{+46}_{-51} pb, calculated at NNLO in QCD and including resummation of next-to-next-to-leading logarithmic (NNLL) soft gluon terms [49–53].

The main backgrounds to candidate signal events come from the production of a single top-quark, and from a W - or Z -boson in association with jets. A small background contribution arises from diboson (WW , WZ , ZZ) production. Events not containing prompt leptons also contribute to the selected sample via the misidentification of a jet or a photon as an electron, or the presence of non-prompt electrons or muons passing the prompt isolated lepton selection. This contribution is referred to as ‘multijet’ background, and was estimated using data by following the matrix method described in Ref. [54].

The production of V +jets was simulated with the SHERPA 2.2.1 [55] generator using next-to-leading-order (NLO) matrix elements (ME) for up to two partons, and leading-order (LO) matrix elements for up to four partons calculated with the Comix [56] and OPENLOOPS [57–59] libraries. They were matched with the SHERPA parton shower [60] using the MEPS@NLO prescription [61–64] with the set of tuned parameters developed by the SHERPA authors. The NNPDF3.0_{NNLO} set of PDFs [43] was used and the samples were normalised to a next-to-next-to-leading-order (NNLO) prediction [65]. The normalisation of the W +jet background and the fractions of W -bosons produced in association with heavy-flavour quarks are extracted from data, taking advantage of the intrinsic W -boson charge asymmetry in this process [66]. The Z +jets contribution is estimated from MC simulation and checked in a data control sample.

Diboson processes were simulated with the SHERPA 2.1.1 event generator. They were calculated using Comix and OPENLOOPS, and merged with the SHERPA parton shower according to the MEPS@NLO prescription. The CT10_{NLO} PDF set [67] was used in conjunction with dedicated parton shower tuning developed by the SHERPA authors.

Samples of t -, Wt - and s -channel single top-quark background events were generated with POWHEG-Box v1, using the 4-flavour scheme for the NLO matrix element calculations together with the fixed four-flavour PDF set CT10_{F4}. Overlaps between the $t\bar{t}$ and Wt final states were removed with the ‘diagram removal’ prescription [68]. For all top processes, top-quark spin correlations were preserved (for t -channel, top quarks were decayed using MADSPIN). All single top-quark samples were interfaced to PYTHIA 6.428 [69] with the CTEQ6L1 PDF set [70] and the corresponding Perugia 2012 [71] set of tuned parameters. The EVTGEN v1.2.0 program was used to model properties of the bottom and charm hadron decays. The single top-quark t - and s -channel samples were normalised to the approximate NNLO theoretical cross-sections [72–74].

3.4 Modelling of heavy-quark fragmentation, hadron production and decays

The modelling of the momentum transfer between the b -quark and the b -hadron is an important aspect of this analysis. The Monte Carlo event generators, such as the PYTHIA, HERWIG [75, 76] and SHERPA

programs, describe this transfer according to phenomenological models, namely the string and cluster models containing parameters which are tuned to data. The PYTHIA8 program uses parametric functions to describe the b -quark fragmentation function, while HERWIG7 and SHERPA use a non-parametric model which handles the complete parton-shower evolution. The free parameters in those models are typically fit to measurements from e^+e^- colliders, and this analysis assumes that the b -quark fragmentation function is the same in e^+e^- and pp collisions, as supported by dedicated studies.

The Lund–Bowler parameterisation [77, 78] in PYTHIA8 was used. It is given by

$$f(z) = \frac{1}{z^{1+br_b m_b^2}} (1-z)^a \exp(-bm_T^2/z),$$

where a , b and r_b are the function parameters, m_b is the b -quark mass, $m_T = \sqrt{m_B^2 + p_T^2}$ the b -hadron transverse mass (m_B being the b -hadron mass), and z is the fraction of the longitudinal energy carried by the b -hadron with respect to the b -quark, in the light-cone reference frame. The fragmentation function is defined at the hadronisation scale and it is evolved by the parton shower to the process scale through DGLAP evolution equations. In PYTHIA8, the values of a and b were fit to data sensitive to light-quark fragmentation [79], such as charged-particle multiplicities, event shapes and scaled momentum distributions. They are assumed to be universal for light- and heavy-quarks, while the r_b parameter is specific to b -quark fragmentation.

The description of the b -quark fragmentation in the ATLAS A14 tune is improved by fitting for the StringZ:rFactB PYTHIA8 parameter (corresponding to r_b) following the approach given in Refs. [80–83]. The A14 tune sets the parton shower α_s to 0.127, whereas the value of 0.1365 is used in Monash [79]. However, both Monash and A14 set $r_b = 0.855$. Since the b -quark fragmentation is controlled both by α_s and r_b , the procedure described in the following is used to determine a value of r_b more appropriate for a value of $\alpha_s = 0.127$. The fit uses the A14 tune with e^+e^- collision data from the ALEPH, DELPHI and OPAL experiments at the LEP collider, and from the SLD experiment at the SLC collider [84–87]. The distribution of $x_B = 2p_B \cdot p_Z / m_Z^2$ from semileptonically decaying b -hadrons in $e^+e^- \rightarrow Z \rightarrow b\bar{b}$ events is used, where p_B and p_Z are the four-momenta of the b -hadron and the Z -boson, respectively. In the Z rest frame, m_Z is twice the beam energy and therefore $x_B = 2E_B/m_Z$, where E_B is the energy of the b -hadron. The fit is performed using RIVET v3.1.0 [88] to implement the measurements. The effect of the matrix-element corrections for $e^+e^- \rightarrow Z \rightarrow b\bar{b}g$ is taken into account. Eighty simulated samples of 1M $e^+e^- \rightarrow Z \rightarrow b\bar{b}$ events were produced using PYTHIA8 with different values of the r_b parameter in the interval [0.8-1.4] and compared to the experimental data in HEPDATA format. The extraction of the best r_b value is performed through a standard binned χ^2 test on the experimental x_B distribution where statistical and systematic uncertainties are taken into account for each of the four experiments. In addition, for the results of ALEPH, DELPHI and OPAL, bin-by-bin correlations are taken into account in the fit procedure. The SLD experiment did not provide the full covariance matrix for the total uncertainties and therefore the χ^2 fit for this experiment is performed ignoring bin-by-bin correlations. For each experiment, the χ^2 minimisation is performed and the best r_b value and its uncertainty are found. The results are summarised in Table 1. The values of χ^2/ndf for DELPHI and SLD experiments show a poor modelling of the data by the simulated templates. Therefore, before including these results into a global χ^2 combination, the uncertainties found in the r_b parameter for these two cases were rescaled by a factor of $S = \sqrt{\chi^2/\text{ndf}}$ following the procedure outlined in Ref. [1]. After these uncertainties are rescaled, the four χ^2 curves are summed up to produce a single χ^2 curve taking into account the information of all four experiments. In this approach, the four experiments are considered uncorrelated since the dominant uncertainties on

Table 1: Results of a fit of the r_b parameter of the Lund-Bowler b -quark fragmentation function in PYTHIA8 to different experimental data where bin-by-bin correlations for ALEPH, DELPHI and OPAL experiments were considered.

Experiment	r_b	χ^2/ndf
ALEPH	1.070 ± 0.035	21/18
DELPHI	1.094 ± 0.030	73/8
OPAL	1.023 ± 0.019	18/19
SLD	1.092 ± 0.018	58/21

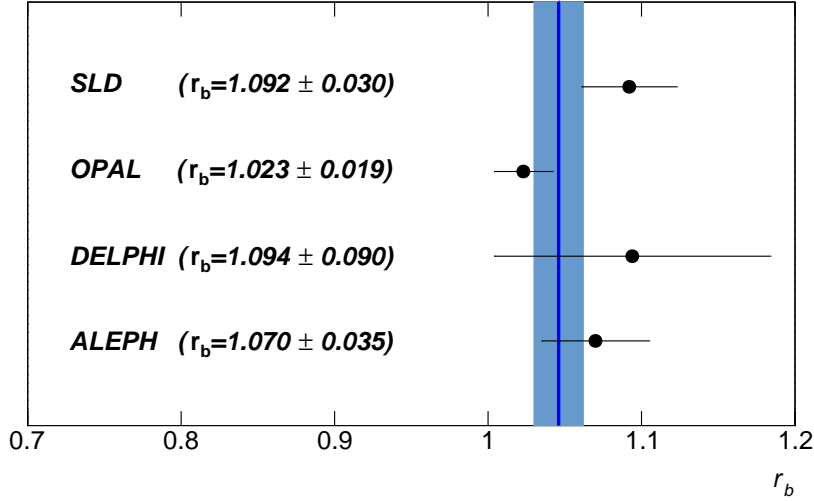


Figure 1: Fit of the r_b PYTHIA parameter to the four experiments considered: SLD, OPAL, DELPHI and ALEPH. For each experiment, the r_b fitted value is shown together with its uncertainty. These results have been obtained including bin-by-bin correlations in the experimental data (except for SLD experiment) and after rescaling the uncertainties on r_b for DELPHI and SLD experiments as explained in the text. The solid blue line represents the value of r_b obtained from the combined fit to the four experiments. The blue band represents the uncertainty from the combined fit to the four experiments.

the measurements come from uncorrelated sources. This curve is then fitted with a parabola to find the minimum of the χ^2 and to extract the best value of the r_b parameter and its uncertainty, yielding $r_b = 1.05 \pm 0.02$. The values of the r_b parameter and its uncertainty for the four experiments, and their combination are shown in Figure 1. A similar procedure is performed, as a cross-check, exploiting the average value $\langle x_B \rangle$ of the four x_B distributions. The experimental $\langle x_B \rangle$ values are compared with the predicted value of the various simulated samples, and the best r_b values and their uncertainties are extracted. A weighted average of the single results is calculated and the result is found to be compatible with the previous method.

The setting with $r_b = 1.05 \pm 0.02$ is referred to as A14- r_b and is applied in this analysis to all signal MC samples using PYTHIA8 for the simulation of the parton shower. The x_B distributions measured by the ALEPH, DELPHI, OPAL and SLD experiments are shown in Figure 2 together with the MC predictions obtained with the A14, the A14- r_b and the POWHEG+HERWIG7 settings respectively. Recent b -fragmentation measurements based on LHC data [89, 90] show reasonable agreement with simulations using the A14- r_b tune.

The production fractions of weakly decaying b - and c -hadrons observed in POWHEG+PYTHIA8 MC

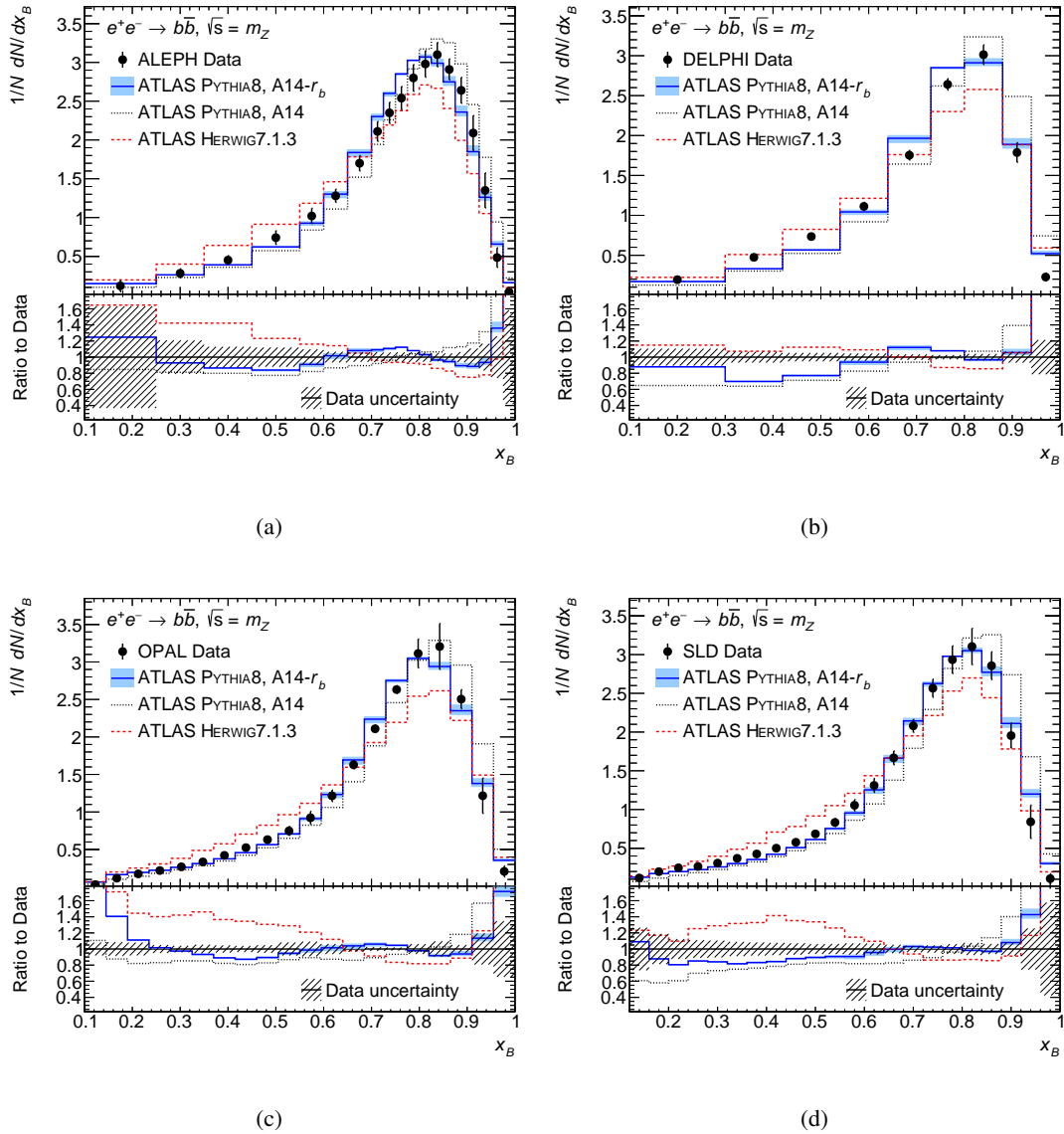


Figure 2: Distributions of x_B from semileptonically decaying b -hadrons in $e^+e^- \rightarrow Z \rightarrow b\bar{b}$ events as measured by the ALEPH, DELPHI and OPAL experiments at the LEP collider, and by the SLD experiment at the SLC collider. Each of the measured spectra is compared with a set of MC predictions. The PYTHIA8 A14- r_b prediction includes a systematic uncertainty band obtained considering the r_b parameter variations described in the text and included as systematic uncertainty in the analysis.

simulation with EVTGEN are rescaled to those from the Heavy Flavour Averaging Group (HFLAV) [91] as reported by the PDG [1] and in Ref. [92]. The production fraction values and corresponding scale factors for POWHEG+PYTHIA8 simulations are shown in Table 2. These scale factors refer only to the first weakly decaying hadron produced in the hadronisation process of b - and c -quarks. The scale factors are applied to each of these hadrons present in a MC simulated event, with the overall event weight given by the product of these scale factors. This procedure assumes that the production fractions of heavy-flavour quarks can be regarded as universal in the kinematic phase space relevant for this analysis, within the uncertainties

Table 2: The production fraction values for b -hadrons and c -hadrons in the PDG and POWHEG+PYTHIA8. The relative scale factors applied to POWHEG+PYTHIA8 are also shown. The values in the PDG column are derived from Refs. [1] and [92]. The same scale factors are applied to the charge-conjugate hadrons.

Hadron	PDG	POWHEG+PYTHIA8	Scale Factor
B^0	0.404 ± 0.006	0.429	0.941 ± 0.014
B^+	0.404 ± 0.006	0.429	0.942 ± 0.014
B_s^0	0.103 ± 0.005	0.095	1.088 ± 0.052
b -baryon	0.088 ± 0.012	0.047	1.87 ± 0.26
D^+	0.226 ± 0.008	0.290	0.780 ± 0.027
D^0	0.564 ± 0.015	0.553	1.020 ± 0.027
D_s^0	0.080 ± 0.005	0.093	0.857 ± 0.054
c -baryon	0.109 ± 0.009	0.038	2.90 ± 0.24

Table 3: Hadron to muon branching ratios from the PDG and in POWHEG+PYTHIA8+EVTGEN. The relative scale factors applied to POWHEG+PYTHIA8 are also shown. The values in the PDG column are derived from Refs. [1] and [92]. The $c \rightarrow \mu$ scale factor is applied only to the semileptonic decays of c -hadrons into muons when the c -hadrons do not come from a cascade b -hadron decay. The same scale factors are applied to the charge conjugate hadrons.

Hadronic Decay Mode	PDG	POWHEG PYTHIA8+EVTGEN	Scale Factor
$b \rightarrow \mu$	$0.1095^{+0.0029}_{-0.0025}$	0.106	$1.032^{+0.0027}_{-0.0023}$
$b \rightarrow \tau$	0.0042 ± 0.0004	0.0064	0.661 ± 0.062
$b \rightarrow c \rightarrow \mu$	0.0802 ± 0.0019	0.085	0.946 ± 0.022
$b \rightarrow \bar{c} \rightarrow \mu$	0.016 ± 0.003	0.018	0.89 ± 0.17
$c \rightarrow \mu$	0.082 ± 0.005	0.084	0.976 ± 0.059

accounted for here, as supported by recent results [93–99] which find deviations from universality only in the very low- p_T regime.

The branching ratios of the b - and c -hadron decays that contain a muon are also adjusted to match those measured by previous experiments [1]. Central values and relative scale factors, along with the corresponding uncertainties, are shown in Table 3; these are measured after applying the corrections for the production fractions described above. The $b \rightarrow \bar{c} \rightarrow \mu$ branching ratio was determined by averaging the direct measurement from DELPHI [100] and the predicted values computed by the LEP Electroweak Heavy Flavour Working Group [101]. The latter prediction is based on flavour-specific $B \rightarrow D$ and $B \rightarrow \Lambda_c^+$ rates measured at CLEO [102–104] in combination with the $B \rightarrow DD(X)$ rates measured in ALEPH [105] to extract the probabilities of producing the different c -hadrons from the initial b -hadron decays. The c -hadron semileptonic branching fractions were also used in the prediction. The $c \rightarrow \mu$ scale factor is applied only to the semileptonic decays of c -hadrons into muons when the c -hadrons do not come from a cascade b -hadron decay.

4 Analysis

4.1 Event yields and sample composition

The number of observed candidate events and the predicted signal and background are shown in Table 4, for both the OS and SS regions. Over 90% of the events in the sample contain a top-quark pair, including cases where the soft muon is erroneously chosen from a $t\bar{t}$ dilepton decay, whereby a muon from the prompt W decay is found near a jet or radiates a near-collinear photon mimicking a soft muon tag, and cases where the soft muon candidate does not originate from a b decay such as in $W \rightarrow cs$ or SMT fakes. The contributions from single top-quark, W - or Z -boson in association with jets, and multijet background are not negligible. The Z +jets background gives a small contribution near the peak of the $m_{\ell\mu}$ distribution, but becomes important for $m_{\ell\mu}$ close to the Z -boson mass peak.

Of the selected $t\bar{t}$ events in the OS class, 83% are cases where the primary lepton and the soft muon belong to the decay of the same top-quark, and 10% are events where the two originate from different top-quarks. The topological requirement $\Delta R_{\ell,\mu} < 2$ is responsible for much of the purity because it is very effective in preferentially selecting the same top-quark decays. For the remaining 7% of cases, the soft muon does not originate from either of the b -quarks produced in the two top-quark decays. In the SS class, the above fractions are 57%, 41% and 2%, respectively. The rate of soft muons that are not from b -quarks is higher in OS events owing to the decay of c -quarks that come from $W \rightarrow cs$ in the top-quark decay chain.

Table 4: Event yields with $m_{\ell\mu}$ between 15 and 80 GeV, separately for OS and SS regions. Uncertainties shown include statistical and systematic contributions but not the recoil uncertainty.

Process	Yield (OS)	Yield (SS)
$t\bar{t}$ (SMT from b - or c -hadron)	55 700 \pm 3400	34 800 \pm 2300
$t\bar{t}$ (SMT from $W \rightarrow \mu\nu$)	2190 \pm 310	4.9 \pm 3.6
$t\bar{t}$ (SMT fake)	1490 \pm 210	1240 \pm 170
Single top t -channel	770 \pm 70	490 \pm 40
Single top s -channel	63 \pm 6	49 \pm 4
Single top Wt channel	1840 \pm 140	1260 \pm 100
W +jets	1600 \pm 400	1080 \pm 240
Z +light jets	210 \pm 80	15 \pm 6
Z +HF jets	550 \pm 180	310 \pm 100
Diboson	17.2 \pm 2.9	6.3 \pm 1.4
Multijet	530 \pm 140	480 \pm 130
Total Expected	65 000 \pm 4000	39 700 \pm 2500
Data	66 891	42 087

In order to better understand the nature of the sample composition in the OS and SS regions, the expected $t\bar{t}$ events shown in the first row of Table 4 are further resolved into components. Table 5 shows the components involving direct and sequential decays, and decays not belonging to the b -quark from the $t \rightarrow Wb$ transition. The direct $t \rightarrow B \rightarrow \mu$ decays are by far the dominant component in the OS sample, while the sequential $t \rightarrow B \rightarrow D \rightarrow \mu$ decays are also suppressed by the kinematic requirement on the soft muon. Decay channels involving τ leptons give a small contribution.

Table 5: Fraction of MC-simulated $t\bar{t}$ events with a soft muon originated by a b - or c -hadron split into components of direct and sequential decays, and decays not belonging to the b -quark from the $t \rightarrow Wb$ transition, separately for the opposite-sign and same-sign event selections. The letters B and D indicate b - and c -hadrons of either charge. Only MC events with two real muons are included.

	OS [%]	SS [%]
Processes involving a μ from a t or \bar{t}		
$t \rightarrow B \rightarrow \mu$	73.6	51.2
$t \rightarrow B \rightarrow D \rightarrow \mu$	16.7	44.2
$t \rightarrow B \rightarrow \tau \rightarrow \mu$	2.0	1.3
$t \rightarrow B \rightarrow D \rightarrow \tau \rightarrow \mu$	0.8	0.8
Processes involving a μ not from a t or \bar{t}		
$B \rightarrow \mu$	0.6	0.9
$D \rightarrow \mu$	5.8	1.4
Other ($\tau \rightarrow \mu$)	0.5	0.1

The data are compared with the sum of the predicted signal and backgrounds in Figures 3 and 4, for an illustrative selection of kinematic distributions of the candidate events for the OS and SS selections: $p_T(\mu^{\text{SMT}})$, $\eta(\mu^{\text{SMT}})$, $p_T(\ell^{\text{primary}})$ and $m_T(W)$. The uncertainties are discussed in detail in Section 5. The compatibility of the data and MC predictions is studied using a χ^2 test involving the bin-by-bin full correlation matrix, and for all distributions the level of agreement is better than 2 standard deviations. The slight excess of SMT muons in regions of high- η is associated with a potential small mismodelling of the efficiency for low- p_T muons in simulation. The corresponding impact on the measurement is negligible.

4.2 Extraction of the top-quark mass

The distribution of the invariant mass of the primary lepton and the soft muon, $m_{\ell\mu}$ is used to determine the mass of the parent top-quark. A binned-template profile likelihood fit is performed, with a Poisson likelihood model and systematic uncertainties included as Gaussian-constrained nuisance parameters [106]. Only the range of $m_{\ell\mu}$ between 15 and 80 GeV is considered in the fit, since the tail of the $m_{\ell\mu}$ distribution is more sensitive to $t\bar{t}$ modelling uncertainties and higher-order corrections, and to the Z +jets background. The fit is performed simultaneously for the OS and SS charge-combination samples, and Figure 5 shows the sensitivity of each of these distributions to variations of the top-quark mass, as well as the binning used by the templates. The SS sample has less sensitivity than the OS sample due to the larger incidence of sequential $b \rightarrow c \rightarrow \mu$ decays, where the SMT muon carries a smaller fraction of the parent b -quark momentum, and due to the larger fraction of events in which the leptons originate from different top-quarks.

The fit uses template histograms simulated as for the nominal $t\bar{t}$ sample but with different values for the input top-quark mass. The templates from the different mass samples are interpolated with piece-wise linear functions built bin by bin. To improve the stability of the method, the templates are smoothed assuming a linear dependence on m_t for the fraction of the total number of events in each bin. A maximum-likelihood fit is performed with three free parameters: m_t , which controls the shape of the $m_{\ell\mu}$ distribution for $t\bar{t}$ events, and the normalisation factors for $t\bar{t}$ events in the OS and SS samples. The normalisation factors ensure that the total of the $t\bar{t}$ signal and background events is always equal to the total number of selected data events, and no m_t information is extracted from the number of events.

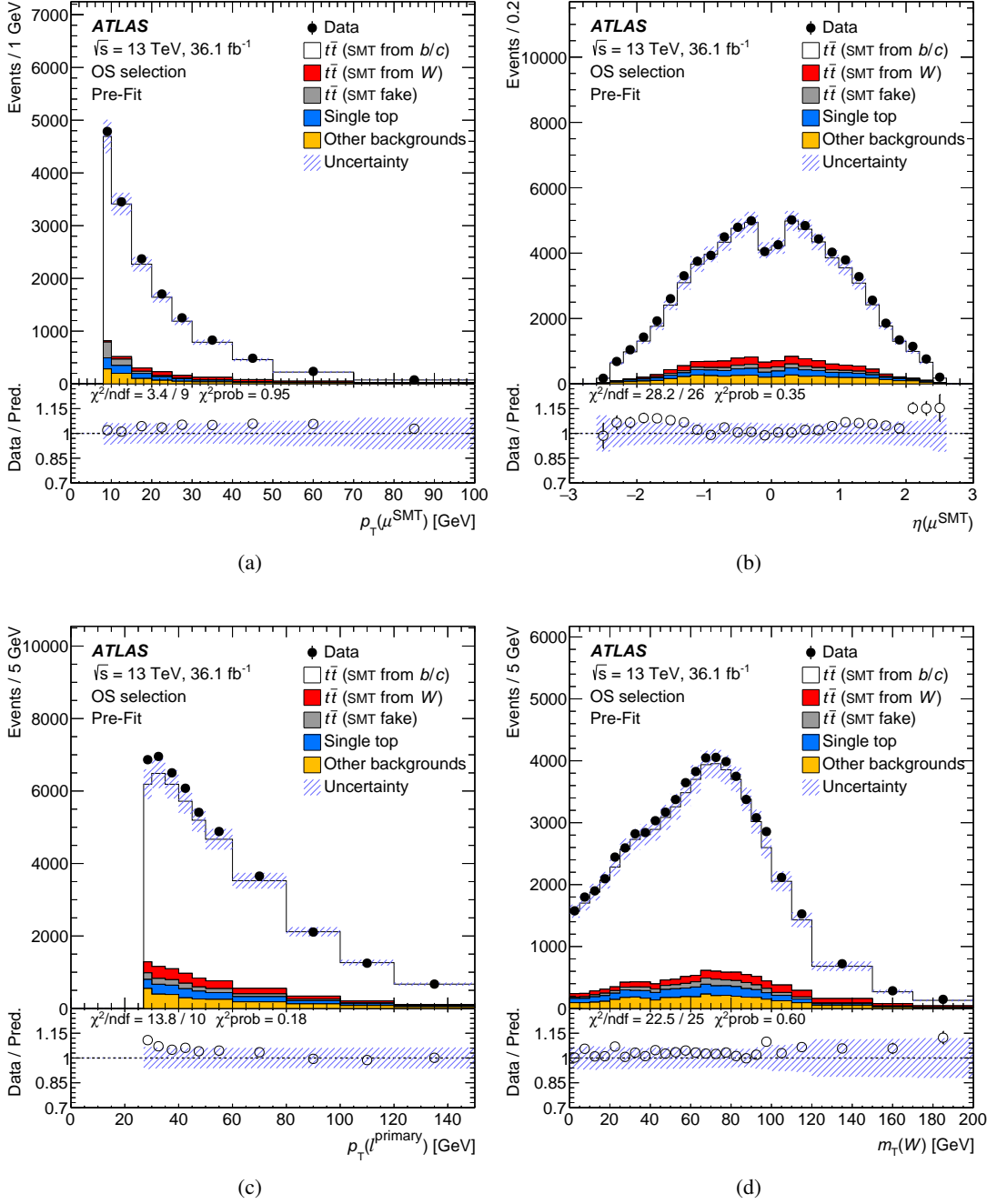


Figure 3: Comparison of data and prediction before the fit described in Section 4.2 in the OS sample, i.e. for events with primary lepton and the soft muon with opposite charges, for the (a) soft muon p_T , (b) soft muon η , (c) primary lepton p_T and (d) W -boson transverse mass. The prediction reports the expected event contribution from the signal and backgrounds. The uncertainty band includes statistical and systematic uncertainties, but does not include the recoil uncertainty.

The uncertainty due to the limited number of simulated events, and due to statistical fluctuations in the background estimates based on control samples, is evaluated by defining a new source of systematic

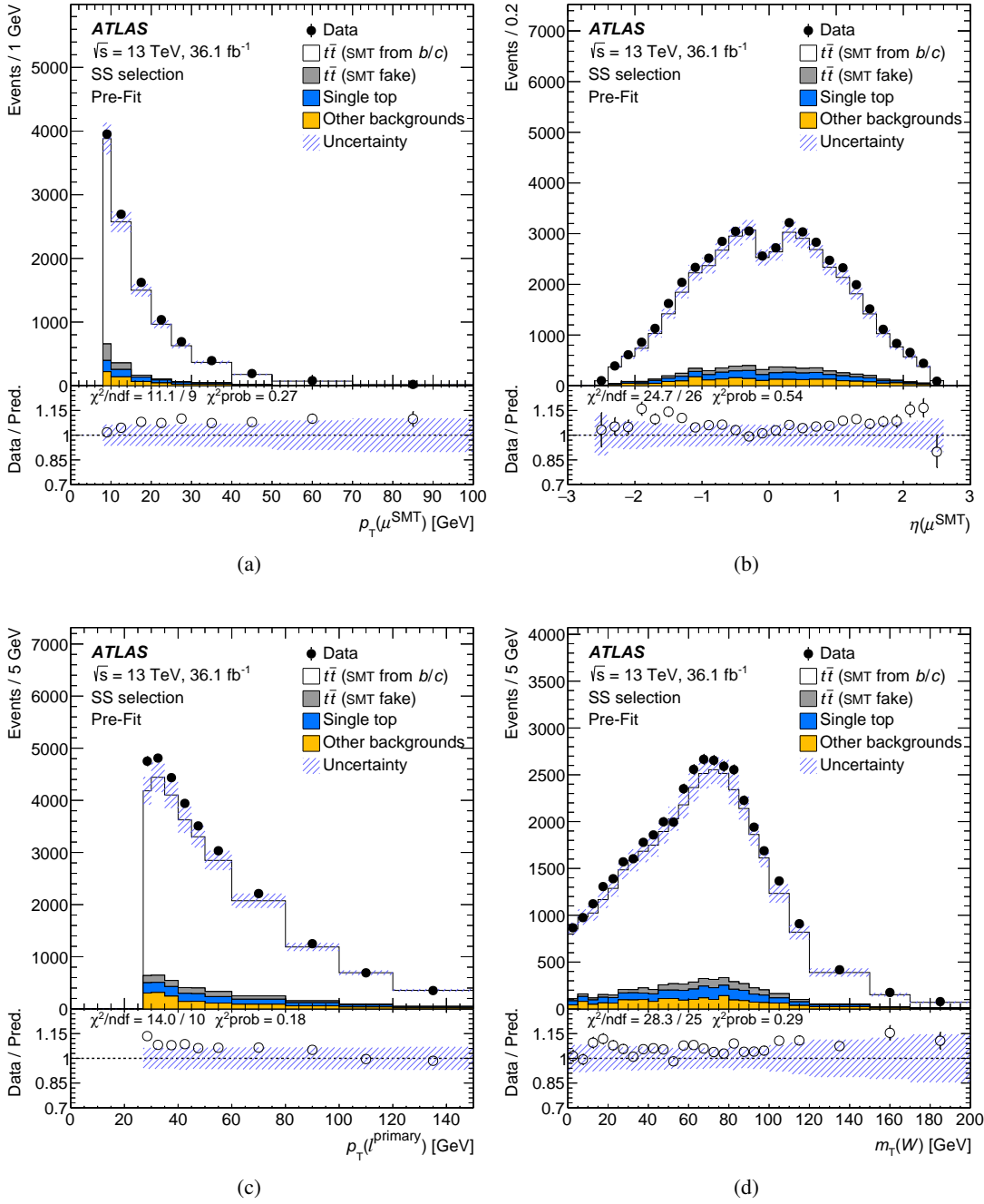


Figure 4: Comparison of data and prediction before the fit described in Section 4.2 in the SS sample, i.e. for events with primary lepton and the soft muon with same charges, for the (a) soft muon p_T , (b) soft muon η , (c) primary lepton p_T and (d) W -boson transverse mass. The prediction reports the expected event contribution from the signal and backgrounds. The uncertainty band includes statistical and systematic uncertainties, but does not include the recoil uncertainty.

uncertainty for each bin of the prediction, which modifies the bin content by its statistical uncertainty. Since a very large number of systematic uncertainties are considered *a priori*, a pruning procedure is applied to

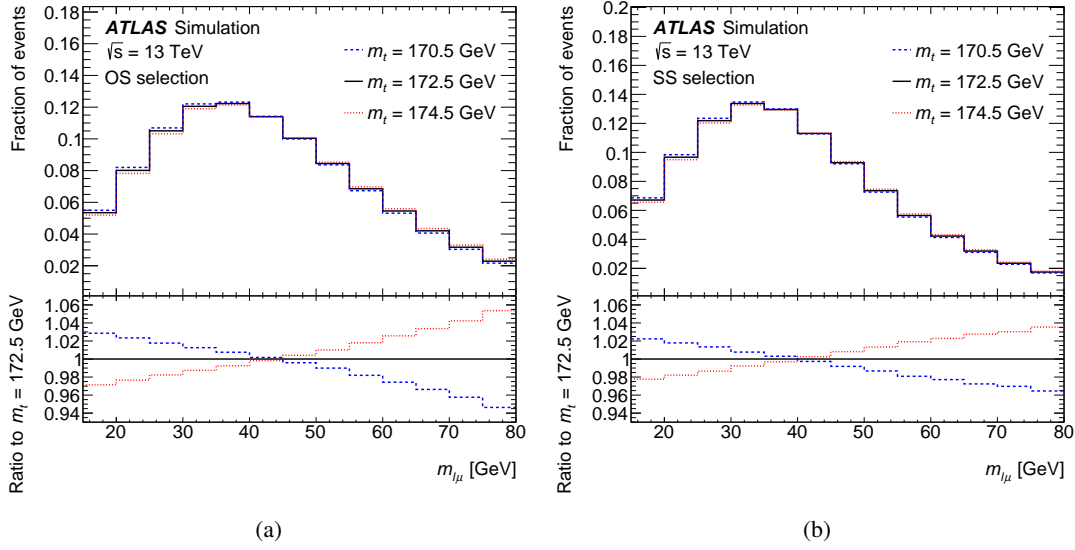


Figure 5: Sensitivity of the $m_{\ell\mu}$ distribution to different input top-quark masses from simulated events, separately for the OS and SS samples.

reduce the number of statistically insignificant systematic uncertainties affecting the prediction of each of the signal and background processes. A systematic variation of the $m_{\ell\mu}$ templates is excluded if the total predicted change is smaller than 0.05% of the nominal bin content for all bins. The impact on the total estimated uncertainty is smaller than 0.03 GeV.

The top-quark mass determination from the fit is found to be linear and unbiased with respect to the input top-quark mass hypothesis by means of pseudo-experiments, and its uncertainty from the likelihood ratio is also checked to ensure it reports the correct statistical coverage. The fit method and the event selection were optimised to minimise the total uncertainty in m_t in a ‘blinded’ approach, i.e. using pseudo-data and data without knowledge of the best-fit top-quark mass. The fit yields:

$$m_t = 174.41 \pm 0.39 \text{ (stat.)} \pm 0.66 \text{ (syst.)} \pm 0.25 \text{ (recoil) GeV,}$$

where the statistical, systematic and recoil uncertainties are described in detail in Section 5. Figure 6 shows the post-fit $m_{\ell\mu}$ distributions in the OS and SS samples; a goodness-of-fit test is performed using the saturated model technique [1, 107] and returns a probability of 56%. Figures 7 and 8 display the corresponding post-fit plots for the kinematic variables of Figures 3 and 4. The data distributions are well described by the prediction, with the primary lepton p_T exhibiting a slight trend which is traced to the boost of the $t\bar{t}$ system, but which has no appreciable impact on the determined top-quark mass. This was confirmed by detailed checks, performed by testing the impact of NNLO corrections on the top quark kinematics, and by performing a test fit including the lepton p_T as a second fit variable. In all cases the impact on the measurement was shown to be well within the quoted modelling uncertainties associated with ISR effects and ME generator choice. The post-fit uncertainties shown in Figures 7 and 8 are significantly reduced with respect to the pre-fit ones shown in Figures 3 and 4 due to the $t\bar{t}$ normalisation being treated as a free parameter in the fit procedure; the normalisation uncertainty considered at pre-fit level is thus

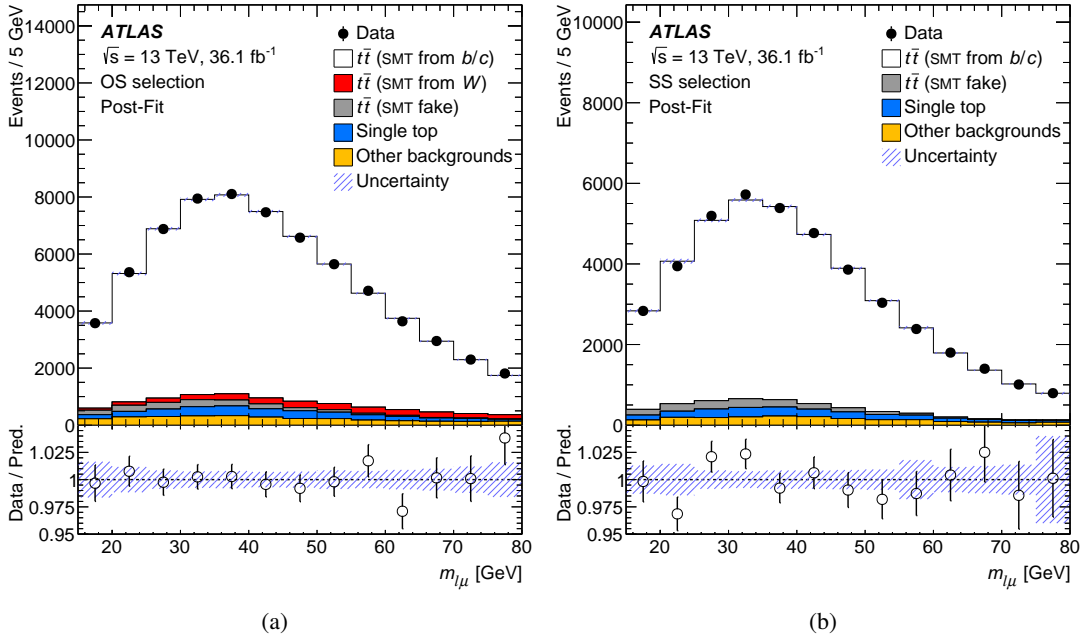


Figure 6: Post-fit $m_{\ell\mu}$ distributions in the (a) OS sample and in the (b) SS sample. The prediction reports the event contribution for the signal and backgrounds. The uncertainty band includes statistical and systematic uncertainties, but does not include the recoil uncertainty. The SS (same sign) or OS (opposite sign) refers to the charge signs of the primary lepton and the soft muon.

removed after the fit procedure. The likelihood scan with the best-fit top-quark mass value is shown in Figure 9.

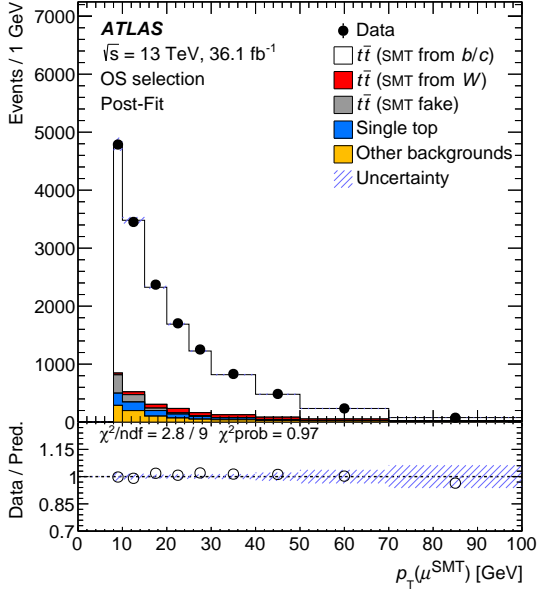
Checks were performed by fitting the OS and SS regions separately, giving $m_t(\text{OS}) = 174.63 \pm 0.47$ (stat.) ± 0.75 (syst.) GeV and $m_t(\text{SS}) = 173.88 \pm 0.74$ (stat.) ± 1.01 (syst.) GeV. Checks were performed by separately fitting the electron and muon channels, different W -decay lepton charges and different configurations of b -tagging and event selection, and were found to all give consistent results. Checks also included the extraction of the top-quark mass with alternative statistical methods, namely using analytic functions for $m_{\ell\mu}$ with a parametric dependence on the top-quark mass, only using the mean value of the $m_{\ell\mu}$ distribution, and using a binned-template likelihood fit without including systematic uncertainties as nuisance parameters. In particular, the inclusion of systematic uncertainties as nuisance parameters in the fit reduces the total uncertainty by 2.6%, in line with reasonable constraints from the fit.

5 Measurement uncertainties

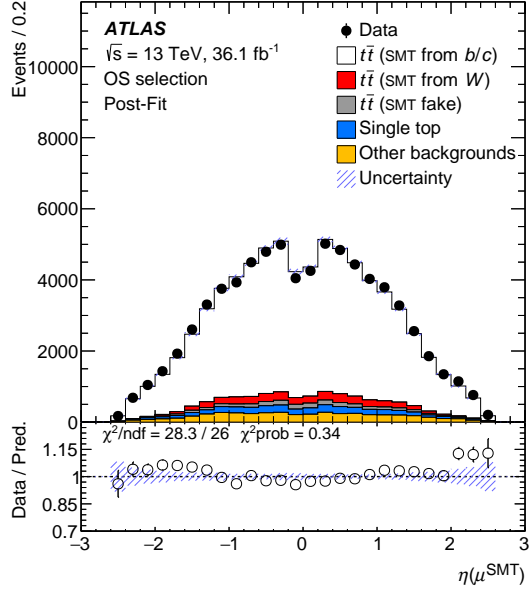
The individual sources of uncertainty and the evaluation of their effect on m_t are described in the following. Many sources of systematic uncertainty are considered, corresponding to a total of 151 individual variations. Table 6 summarises the impact on m_t of the main sources of systematic uncertainty, and each systematic uncertainty is accompanied by an estimate of its statistical precision performed using the bootstrap method [108].

Table 6: Impact of main sources of uncertainty on m_t . Each row of the table corresponds to a group of individual systematic variations. For each uncertainty source the fit is repeated with the corresponding group of nuisance parameters fixed to their best-fit values. The contribution from each source is then evaluated by subtracting in quadrature the uncertainty obtained in this fit from that of the full fit. The total systematic uncertainty is different from the sum in quadrature of the different groups due to correlations among nuisance parameters in the fit. The last column shows the statistical uncertainty on each of the top-quark mass uncertainties as estimated with the bootstrap method [108].

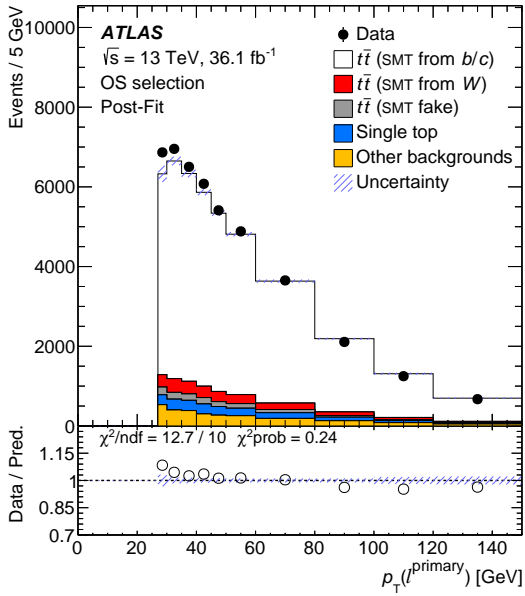
Source	Unc. on m_t [GeV]	Stat. precision [GeV]
Statistical and datasets		
Data statistics	0.39	
Signal and background model statistics	0.17	
Luminosity	< 0.01	± 0.01
Pile-up	0.07	± 0.03
Modelling of signal processes		
Monte Carlo event generator	0.04	± 0.06
b, c -hadron production fractions	0.11	± 0.01
b, c -hadron decay BRs	0.40	± 0.01
b -quark fragmentation r_b	0.19	± 0.06
Parton shower α_S^{FSR}	0.07	± 0.04
Parton shower and hadronisation model	0.06	± 0.07
Initial-state QCD radiation	0.23	± 0.08
Colour reconnection	< 0.01	± 0.02
Choice of PDFs	0.07	± 0.01
Modelling of background processes		
Soft muon fake	0.16	± 0.03
Multijet	0.07	± 0.02
Single top	0.01	± 0.01
W/Z +jets	0.17	± 0.01
Detector response		
Leptons	0.12	± 0.01
Jet energy scale	0.13	± 0.02
Soft muon jet p_T calibration	< 0.01	± 0.01
Jet energy resolution	0.08	± 0.07
b -tagging	0.10	± 0.01
Missing transverse momentum	0.15	± 0.01
<hr/>		
Total stat. and syst. uncertainties (excluding recoil)	0.77	± 0.03
<hr/>		
Recoil uncertainty	0.25	
<hr/>		
Total uncertainty	0.81	
<hr/>		



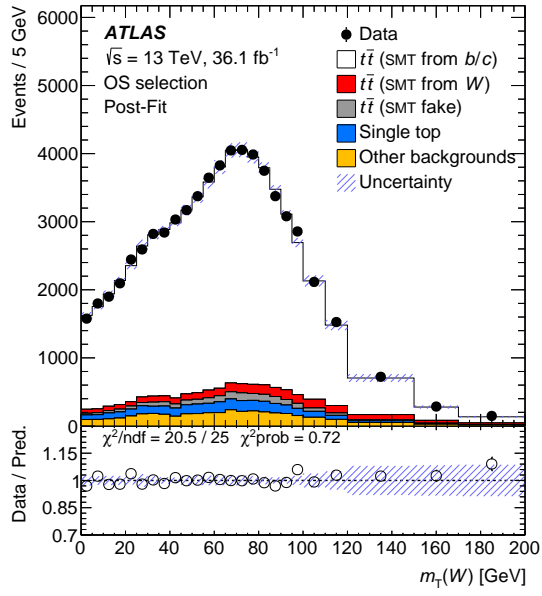
(a)



(b)



(c)



(d)

Figure 7: Post-fit comparison of data and prediction in the OS sample, i.e. for events with primary lepton and the soft muon with opposite charges, for the (a) soft muon p_T , (b) soft muon η , (c) primary lepton p_T and (d) W -boson transverse mass. The prediction reports the event contribution for the signal and backgrounds. The uncertainty band includes statistical and systematic uncertainties, but does not include the recoil uncertainty.

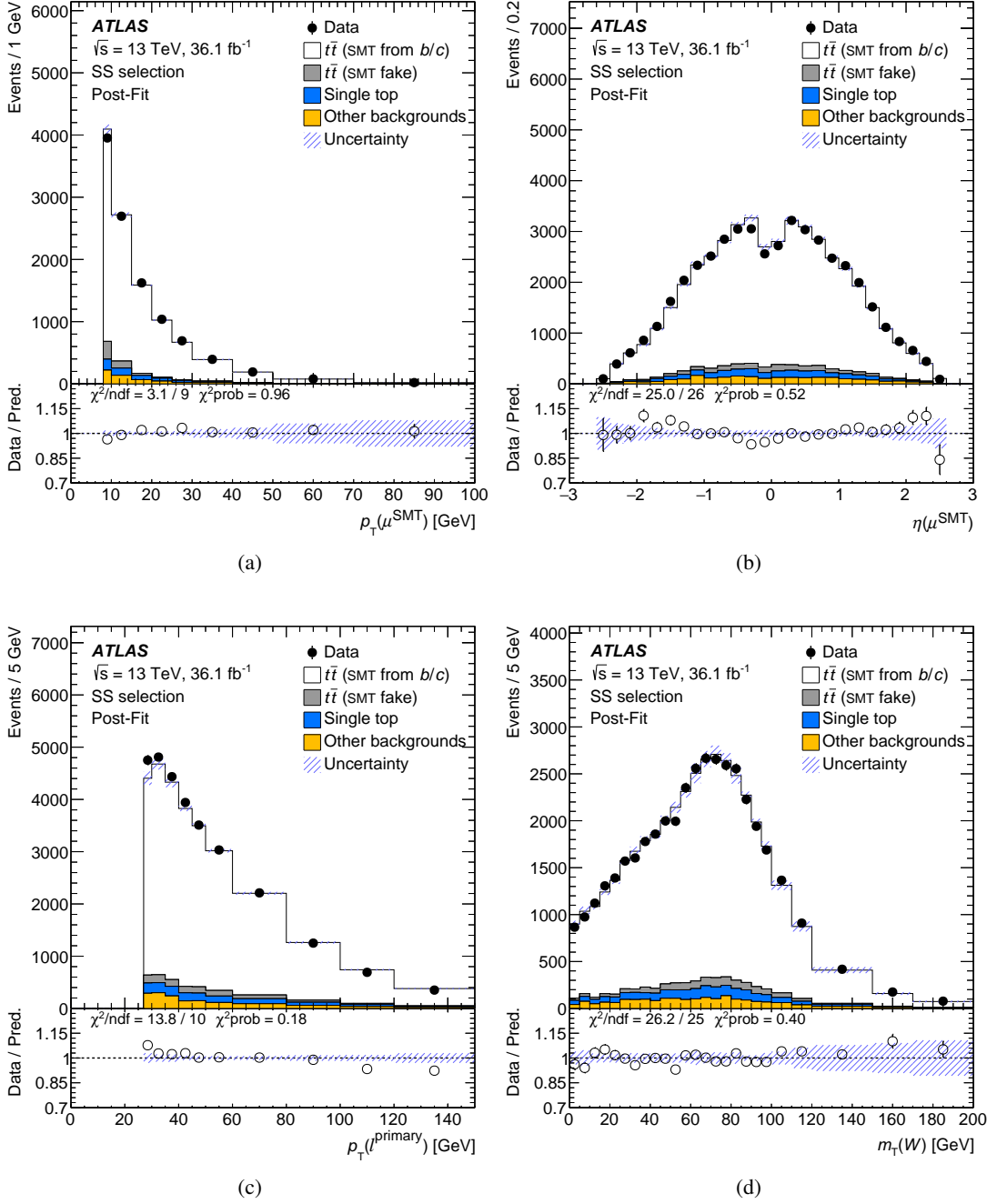


Figure 8: Post-fit comparison of data and prediction in the SS sample, i.e. for events with primary lepton and the soft muon with same charges, for the (a) soft muon p_T , (b) soft muon η , (c) primary lepton p_T and (d) W -boson transverse mass. The prediction reports the event contribution for the signal and backgrounds. The uncertainty band includes statistical and systematic uncertainties, but does not include the recoil uncertainty.

5.1 Statistical and datasets

The uncertainty related to the size of the data sample (data statistical uncertainty) is obtained by performing the fit while keeping constant all of the nuisance parameters associated with the systematic uncertainties.

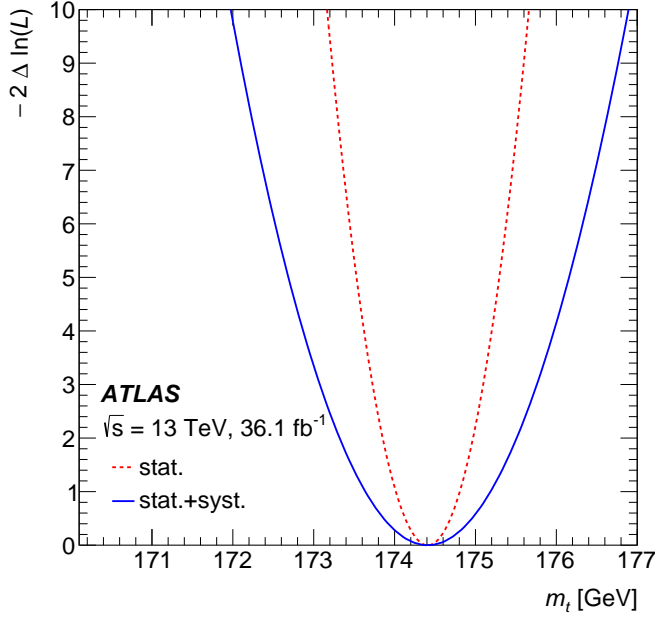


Figure 9: Likelihood scan, showing the best-fit value and the statistical and total uncertainty profiles (excluding the recoil uncertainty).

The data statistical uncertainty obtained by using both the OS and SS selections is ± 0.39 GeV, while the OS sample alone yields ± 0.47 GeV, highlighting the contribution to the sensitivity from the SS sample. The uncertainty due to the limited size of the simulated signal and background samples includes both the impact of the signal samples size on m_t -dependent templates used for the top mass interpolation, and the uncertainty of the backgrounds due to the limited size of the corresponding MC samples. This includes the multijet background, which is estimated with a data control sample. The uncertainty in the combined 2015–2016 integrated luminosity is 2.1% [18], obtained using the LUCID-2 detector [109] for the primary luminosity measurements. The distribution of the average number of interactions per bunch crossing (pile-up activity) in each MC sample is reweighted to match the conditions in data, and a corresponding uncertainty is evaluated according to the uncertainty in the average number of interactions per bunch crossing.

5.2 Modelling of the signal process

Uncertainties in the $t\bar{t}$ signal modelling include all sources that affect the kinematics of the lepton from the W -boson decay and the kinematics of the b -hadron giving rise to the soft muon, and also the fraction of events from different soft-muon flavour components (from b -hadrons, c -hadrons, light jets and W -bosons). The $t\bar{t}$ inclusive cross-section uncertainty does not affect the measurement, since the fit is based only on the shape of the distribution from $t\bar{t}$ events after background subtraction.

Uncertainties that depend on the choice of NLO matching scheme in the $t\bar{t}$ MC generator are estimated by comparing a sample generated with POWHEG+PYTHIA8 with a sample generated with MADGRAPH5_aMC@NLO+PYTHIA8 [110] (referred to hereafter as aMC@NLO+PYTHIA8). The aMC@NLO matching requires specific settings of the PYTHIA8 shower to retain the NLO accuracy. The matrix-element

corrections are switched off for both initial-state radiation and the global-recoil settings that are used for final-state radiation emissions. These settings are different from the nominal POWHEG+PYTHIA8. In order to have a coherent comparison, an alternative POWHEG+PYTHIA8 sample was generated with the same PYTHIA8 configuration as that used to shower aMC@NLO events. Additionally, since aMC@NLO+PYTHIA8 is known to describe poorly the distribution of the boost of the $t\bar{t}$ system ($p_T^{t\bar{t}}$) [111], the $p_T^{t\bar{t}}$ in aMC@NLO+PYTHIA8 is reweighted to that of the POWHEG+PYTHIA8 sample. The full difference between the top-quark masses obtained with the two samples is considered as the positive and negative uncertainty due to the MC generator NLO matching.

Uncertainties in the b -hadron production fractions and the BRs of the inclusive decays of b - and c -hadrons into muons are derived from the uncertainties in the rescaling procedure, described in Section 3.4 and shown in Tables 2 and 3. These uncertainties are propagated through the analysis. In addition, a check was performed to verify that the impact on $m_{\ell\mu}$ due to the different admixture of D -mesons involved in $b \rightarrow c\mu + X$ transitions was within the uncertainty assigned to $b \rightarrow \mu$ inclusive BRs. For this purpose, the exclusive decays $B^0 \rightarrow D^-\mu\nu$, $B^0 \rightarrow D^*(2010)^-\mu\nu$, $B^+ \rightarrow \bar{D}^0\mu\nu$, $B^+ \rightarrow \bar{D}^*(2007)^0\mu\nu$ and their charge conjugates were considered. For each of these decays, a kinematic selection similar to that of the main selection was applied to the events and the BR of each decay was varied within the uncertainty quoted by the PDG. The impact on $m_{\ell\mu}$ was found to be significantly smaller than the effect of varying only the BR of the inclusive $b \rightarrow \mu$ decays. The impact on $m_{\ell\mu}$ from the uncertainties in the $B_{(s)}^0$ mixing parameters is much smaller than the impact from imperfect knowledge of the b -hadron production fractions and from the heavy-quark hadrons BRs. Similarly, the impact of the modelling of the soft-muon kinematics in the exclusive semileptonic decays of b - and c -hadrons in EVTGEN v1.2.0 was tested by varying the various BRs within their uncertainties. The total impact was found to be negligible with respect to the impact of the inclusive b -hadron production fractions and heavy-quark hadrons BRs uncertainties.

Uncertainties in the modelling of the parton shower and hadronisation processes include the estimation of several components. An alternative simulation of the $t\bar{t}$ sample is considered whereby the POWHEG-Box generator is matched to the HERWIG 7.1.3 generator for the modelling of the parton shower and hadronisation. The HERWIG 7.1.3 generator release includes several improvements in the shower description for heavy-quark fragmentation, together with a new tune to e^+e^- data. The angle-ordered shower algorithm is preferred to the dipole shower for this sample, as it better describes both the shower evolution in the 7 TeV ATLAS measurement of jet shapes in $t\bar{t}$ events [112], and the x_B distribution of LEP data, although it does not describe the x_B spectrum of LEP data as well as PYTHIA8. The sample based on HERWIG 7.1.3, when compared with the nominal $t\bar{t}$ simulation used in the fit, allows the effects of changes in the shower algorithm, and therefore in initial- and final-state emissions, to be assessed using alternative but coherent models of b -quark fragmentation and hadronisation, the underlying event and colour reconnection. The full difference between the top-quark masses obtained with the two samples of POWHEG events showered with PYTHIA8 A14- r_b and HERWIG 7.1.3 is considered as the positive and negative uncertainty from variations of the parton shower and hadronisation modelling.

To evaluate the uncertainty on the modelling of the b -quark fragmentation, additional samples were produced with the value of r_b in the fragmentation function varied by its uncertainty of ± 0.02 . Additionally, the uncertainty on the choice of the renormalisation and factorisation scales in the final-state radiation (FSR) description of PYTHIA8 is evaluated using alternative simulated $t\bar{t}$ samples generated with the scale parameters explicitly³ varied up and down by factors of $\sqrt{2}$ [114]. For these alternative settings, the

³ With explicit scale variations, dedicated alternative MC samples are generated with the $\mu_{R,F}$ scales modified in the parton shower settings, as opposed to the automated parton shower variations discussed in Ref. [113], where weights are applied to the MC sample to obtain the systematic shifts. Explicitly changing $\mu_{R,F}$ by a factor $\sqrt{2}$ corresponds approximately to an

appropriate r_b values are determined following the same fit procedure described in Sec. 3.4, in order to still correctly model the x_B distribution for LEP/SLD data. It must be noted that the x_B distribution will however be different for the $t\bar{t}$ samples with varied scales with respect to the nominal one, due to process-dependent effects. This uncertainty is labelled α_S^{FSR} in Tab. 6.

As a check of the separate r_b and α_S^{FSR} uncertainties reported in Table 6, a sample of POWHEG events showered with PYTHIA using the MONASH tune [79] (which has different values of α_S and r_b than the A14- r_b tune), is used to obtain an equivalent systematic uncertainty. The change in the measured top-quark mass obtained with this sample is 0.30 ± 0.06 GeV, consistent with the uncertainties associated with α_S^{FSR} , r_b and the hadronisation model, listed in Table 6.

In the modelling of the parton shower of the b -quark from $t \rightarrow Wb$ with PYTHIA 8.2, there is the possibility to change the default gluon recoil scheme from recoiling against the b -quark (the nominal setting, referred to here as RTB), to recoiling against the W -boson (RECOILTOCOLOURED=OFF, referred to as RTW) [115]. Before PYTHIA version 8.160, the RTW was the only possibility, but it could give unphysical radiation patterns and it is now kept as an option to understand the effect this setting has in view of previous measurements. This setting changes the modelling of second and subsequent gluon emission from quarks produced by coloured resonance decays, such as the b -quark in a $t \rightarrow Wb$ process, but it has no impact for example on $Z \rightarrow b\bar{b}$ decays. A third recoil scheme has been recently made available via the USERHOOK functionality of PYTHIA 8.2 with the top-quark itself serving as recoiler for second and subsequent gluon emission of the b -quark (referred to as RTT)⁴. The RTW and RTT setups give wider-angle gluon radiation, resulting in energy deposits that do not get clustered into the b -jet, and lower gluon-energy emission, altering the modelling of the b -quark fragmentation and hardening the b -hadron momenta. They also mildly change the W -boson p_T and the angle between the W -boson and the b -hadron resulting from the top-quark decay. The recently-developed RTT option has been considered as an additional uncertainty in the measurement, even though the implementation could only be performed based on particle-level simulation and without a dedicated tune that would normally accompany a change of setup of this nature. The change of the recoil model modifies the distribution of the momentum fraction of the b -hadron

$$x_B = \frac{1}{1 - m_W^2/m_t^2 + m_b^2/m_t^2} \frac{2p_B \cdot p_t}{m_t^2},$$

where m_W is the W -boson mass and p_t is the top four-momentum. However, the Mellin moments of this distribution derived with the RTB setup agree well with those predicted by the NLO+NLL resummation convoluted with the Kartvelishvili model tuned on ALEPH, OPAL and SLD data [80]. Therefore, the x_B distribution derived with the RTT shower is reweighted to that of the RTB simulation. The reweighting of x_B is a crude adjustment, since its distribution is controlled by the parameters of the fragmentation function and α_S^{FSR} , which are set in the A14- r_b PYTHIA tune, and bound by the universality of the b -quark fragmentation model. Closure tests demonstrated that the x_B reweighting provides the correct $m_{\ell\mu}$ distribution, and the correct extracted top mass, even though it does not fully address the modelling of other variables of the event. Overall, the analysis performed with the RTT shower setup as above yields a measured top-quark mass value which is larger than the one obtained with the nominal parton shower configuration by approximately 0.25 GeV. The less physically-motivated RTW setup has been also checked, and would have an effect at the same level as RTT. A one-sided shift of the measured top mass is seen with the RTT and RTW setups, but a symmetrised uncertainty of ± 0.25 GeV is assigned and indicated

automated variation of a factor 2, thanks to the implementation of the NLO compensation terms in the latter case.

⁴ The code used for the RTT USERHOOK was provided by the PYTHIA authors directly.

by “recoil”. This uncertainty is considered outside of the profile likelihood fit, and quoted as a separate uncertainty on the result.

The uncertainty in the modelling of initial-state radiation (ISR) is estimated by using four variations: the first two are obtained by independently changing the POWHEG ISR renormalisation and factorisation scales up and down by a factor 2.0, the third by comparing with an alternative sample obtained doubling the h_{damp} parameter with respect to the nominal settings, the fourth one corresponds to the Var3c up and down variations of the PYTHIA8 A14 tune [116].

The modelling of the underlying event and of colour reconnection (CR) can affect the amount of radiation emitted from the b -quark, as well as modify the kinematic distribution of the b -hadron. An underlying-event uncertainty is estimated using the corresponding eigentunes of the A14 PYTHIA8 tune. Variations of colour reconnection parameters are also provided by the A14 eigentunes, determined from measurements of the underlying event in jet production. Samples are generated where the colour reconnection strength in the PYTHIA8 default model is set to its maximum value (all hadrons are reconnected) and are compared with a setting with the colour reconnection switched off. To account for the possibility of colour reconnection also affecting the top-quark decay products, a comparison with the ‘Early Resonance Decay’ (ERD) model is performed [117]. In this model, the top-quarks and W -bosons are allowed to decay before CR takes place, so the top-quark decay products directly participate in CR. The impact on the measured top-quark mass is found to be negligible.

The systematic uncertainty due to the choice of PDFs is evaluated using the PDF4LHC15 error set [118] applied to the nominal $t\bar{t}$ MC settings, and is obtained by means of event reweighting for 30 PDF replicas. The m_t value is extracted for each of the 30 cases, and the total systematic uncertainty due to this effect is computed as the sum in quadrature of the single variations.

5.3 Modelling of background processes

Several sources of uncertainty are considered for the normalisation and shape of the background contributions. The relative uncertainty in the normalisation of the soft-muon component of $t\bar{t}$ events which arises from light-hadron decays and detector background (‘Soft muon fake’) is derived from the uncertainty in the calibration of the misidentification rate. An additional uncertainty is derived from the difference in shape and normalisation of the $m_{\ell\mu}$ distribution of SMT mistags between $t\bar{t}$ samples generated with POWHEG+PYTHIA8 and SHERPA. For the $t\bar{t}$ dilepton component, uncertainties in the modelling of the ISR, in the NLO matching and in the parton shower and hadronisation model are estimated in the same way as for the nominal $t\bar{t}$ sample.

An uncertainty of $+5\%/ -4\%$ is applied to the total cross-section for single top-quark production [72–74]. An additional uncertainty in the amount of initial- and final-state radiation is evaluated in a manner similar to that used for $t\bar{t}$. The uncertainty in the interference between Wt and $t\bar{t}$ production at NLO is assessed by comparing the default ‘diagram removal’ scheme with an alternative ‘diagram subtraction’ scheme [68]. The uncertainty in the event generator for the t -channel is evaluated by comparing it with a sample simulated with aMC@NLO+PYTHIA8. The uncertainty in the parton shower and hadronisation models for the t - and Wt -channels is derived from a comparison with samples showered with HERWIG++. The impact of m_t variations on the single top-quark background has been found to yield negligible effects.

An uncertainty of 30% is applied to the Z +jets background normalisation, for both its light-flavour-jet and heavy-flavour-jet ($Z+c\bar{c}$ and $Z+b\bar{b}$) components. It was validated in a control region around the

Z-boson mass peak, where the normalisations of the Z+light-jet and Z+heavy-flavour-jet are simultaneously extracted with a combined fit and are found to be in agreement with the theoretical expectation for Z+jets. The uncertainty in the normalisation and in the flavour composition of W+jets is assessed using data control regions. The total normalisation and flavour fraction uncertainty is about 22% for $Wb(b)$ and Wcc , approximately 45% for Wc , and about 23% for W+light-jets.

For the multijet background, a 30% systematic uncertainty is assigned to the predicted yields, based on comparisons with data yields in control regions similar to the signal region but enriched in events from the multijet background; the e +jet and μ +jet events are treated as uncorrelated. For the small diboson background, a 50% normalisation uncertainty is assigned and includes uncertainties in the inclusive cross-section and additional jet production [119].

5.4 Detector response

Uncertainties associated with leptons arise from the trigger, reconstruction, identification, and isolation requirements, as well as the lepton momentum scale and resolution. The reconstruction, identification and isolation efficiency for electrons and muons, as well as the efficiency of the trigger, differ slightly between data and simulation and are compensated for by dedicated SFs. Efficiency SFs are derived using data and simulated samples of $Z \rightarrow \ell^+ \ell^-$ ($\ell = e, \mu$), and are applied to the simulation to correct for differences. The effect of uncertainties in these SFs is propagated through the analysis. The total uncertainty in efficiency SFs, for the high- p_T leptons, is $< 0.5\%$ for muons across the entire p_T spectrum [27] and for electrons with $p_T > 30$ GeV, while it exceeds 1% for lower- p_T electrons [37]. The corresponding uncertainties are at the level of few per-mill for the momentum scale both for electrons and muons, and of 5-10% (4-7%) for the electron (muon) momentum resolution, strongly depending on the detector region and on the transverse momentum of the lepton. Additional sources of uncertainty originate from the uncertainty in the corrections applied to adjust the lepton momentum scale and resolution in the simulation to match those in data. They are measured using reconstructed $Z \rightarrow \ell^+ \ell^-$ and $J/\psi \rightarrow \ell^+ \ell^-$ dilepton invariant mass distributions [26, 27]. To evaluate the effect of momentum scale and resolution uncertainties, the analysis is repeated with the lepton momentum varied by $\pm 1\sigma$ and with the lepton momentum smeared, respectively. A systematic uncertainty due to the electron charge misidentification is taken from Ref. [26]. Scale factors correcting for the differences in electron charge misidentification rates between data and simulation are computed using $Z \rightarrow e^+ e^-$ events.

Uncertainties associated with jets arise from the efficiency of jet reconstruction and identification based on the JVT variable, as well as the JES and the jet energy resolution (JER). Although the observable $m_{\ell\mu}$ does not involve jets, the various jet uncertainties impact the analysis through the event selection. The JES and its uncertainty were derived by combining information from test-beam data, LHC collision data and simulation [22]. The JES uncertainty is about 5.5% for jets with $p_T = 25$ GeV and decreases quickly with increasing jet p_T . It is below 1.5% for central jets with p_T in the range of approximately 100 GeV to 1.5 TeV. The highest- p_T jet in this analysis has an average p_T of around 130 GeV, with a typical range between 50 GeV and 450 GeV. The uncertainty from the soft muon jet p_T calibration affects the measured top-quark mass marginally, through the event selection. The magnitude of the JER uncertainty variation is parameterised in jet p_T and η [120], and the uncertainty is propagated by smearing the jet p_T in the simulation. The uncertainty in the efficiency to pass the JVT requirement is evaluated by varying the scale factors within their uncertainties [28].

The efficiencies of DJ tagging in simulated samples are corrected to match efficiencies in data. Correction scale factors are derived for jets originating from b -, c - and light-quarks separately in dedicated calibration analyses [29, 121, 122]. For jets originating from b - and c -quarks, SFs are derived as a function of p_T , whereas the light-jet efficiency is scaled by p_T - and η -dependent factors. Uncertainties in the correction scale factors are estimated by varying each source of uncertainty up and down by one standard deviation and are taken as uncorrelated between b -jets, c -jets, and light-jets. The same SFs are verified to also be applicable to jets containing soft muons by repeating the calibration procedure on a dedicated sample of events. An additional set of MC-to-MC correction factors are introduced to account for the different parton shower and hadronisation model used in the calibration samples compared to those used in this analysis. Furthermore, the efficiency of tagging the hadronic decays of τ -leptons in simulation is treated in the same way as the efficiency of tagging c -jets, and a specific uncertainty is considered for this simplified approach. An additional check is performed by changing the event selection such that there is always a DJ tagged jet other than the SMT tagged jet in the event, and the measured top-quark mass is consistent with the value measured using the nominal event selection.

The E_T^{miss} reconstruction is affected by uncertainties associated with lepton and jet energy scales and resolutions, which are appropriately propagated to the E_T^{miss} calculation. Additional small uncertainties associated with the modelling of the underlying event, in particular its impact on the p_T scale and resolution of unclustered energy, are also taken into account [23].

The total systematic uncertainty is computed from the variance (σ^2) difference between the total uncertainty returned by the fit and the data statistics uncertainty. The plot in Figure 10 shows the ranking of the main systematic uncertainties, including the pulls and the impact of constraining the systematic uncertainties. Uncertainties in Figure 10 are from the individual nuisance parameters. They may be included within a grouped category in Table 6. The leading uncertainties are due to the modelling of the b -quark fragmentation b -hadron and decay. In particular, the BRs for direct and sequential decays are important because the SMT muon p_T is softer when it is produced from c -hadrons in a cascade b -hadron decay, than when it comes directly from a semileptonic b -hadron decay. The BRs also impact the charge-signs combination of the primary lepton and the soft muon. Nearly all of the main systematic uncertainties are largely uncorrelated with those dominant in previous top-quark direct reconstruction measurements [9], and the uncertainty from jet energy calibration is sub-dominant with a value of ± 0.13 GeV.

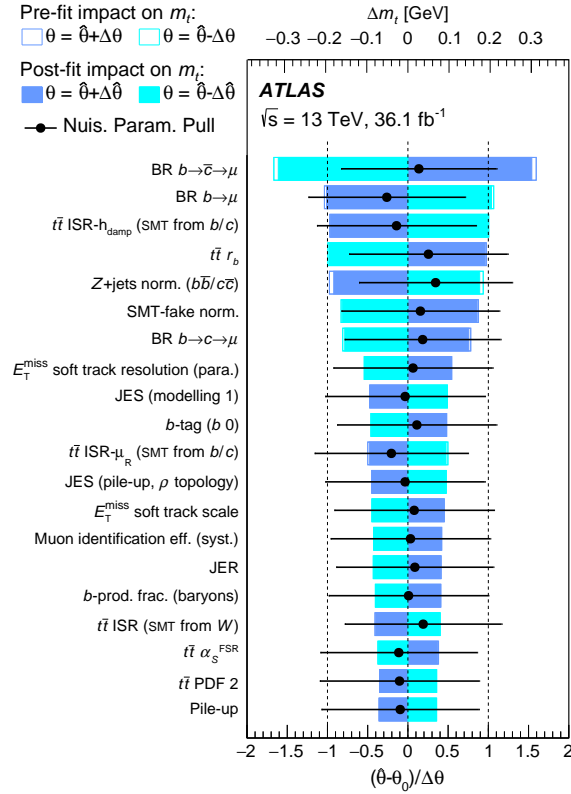


Figure 10: Ranking, from top to bottom, of the main systematic uncertainties (excluding recoil) showing the pulls and the impact of the systematic uncertainties on m_t , from the combined OS and SS binned-template profile likelihood fit to data. The θ 's represent each systematic variation. The upper scale shows the uncertainty contribution to the measured top-quark mass. The PDF 2 is the set number 2 of the PDF4LHC15 error set [118].

6 Conclusions

A direct measurement of the top-quark mass has been performed using a technique that exploits a partial, leptonic-only, invariant mass reconstruction of the top-quark decay products. The analysis uses data corresponding to an integrated luminosity of 36.1 fb^{-1} of $\sqrt{s} = 13 \text{ TeV}$ pp collisions provided by the Large Hadron Collider and recorded by the ATLAS detector, and is based on the invariant mass, $m_{\ell\mu}$, of the lepton ℓ (with $\ell = e, \mu$) from the W -boson decay and the muon μ from a semileptonic decay of a b -hadron. A binned-template profile likelihood fit to the $m_{\ell\mu}$ distribution is performed to determine the most probable top-quark mass value. The result, $m_t = 174.41 \pm 0.39$ (stat.) ± 0.66 (syst.) ± 0.25 (recoil) GeV, corresponds to the most precise single measurement to date of the top-quark mass from the direct reconstruction of its decay products by the ATLAS Collaboration, and more precise than those performed previously with similar techniques [7, 8]. The third uncertainty arises from using a recently developed setup of the PYTHIA8 parton shower gluon-recoil scheme in top quark decays.

Taking into account the correlation between uncertainties, the result is consistent at the level of approximately two standard deviations with the current ATLAS combination of top-quark mass measurements from the reconstruction of the top-quark decay [9]. A similar level of consistency is found with the equivalent combination at CMS [10], while agreement with the latest Tevatron combination [11] is good. Agreement within one standard deviation is also found with the indirect prediction of the top-quark mass from global

electroweak fits [12]. The main sources of systematic uncertainty are due to the modelling of top-quark pair production and b -quark fragmentation and decay, with uncertainties from backgrounds also being significant. On the other hand, the uncertainty due to the calibration of the jet energies is sub-dominant, which is advantageous in future combinations of this result with those from the standard reconstruction of the top-quark decay products.

Acknowledgements

We thank CERN for the very successful operation of the LHC, as well as the support staff from our institutions without whom ATLAS could not be operated efficiently.

We acknowledge the support of ANPCyT, Argentina; YerPhI, Armenia; ARC, Australia; BMWFW and FWF, Austria; ANAS, Azerbaijan; CNPq and FAPESP, Brazil; NSERC, NRC and CFI, Canada; CERN; ANID, Chile; CAS, MOST and NSFC, China; Minciencias, Colombia; MEYS CR, Czech Republic; DNRF and DNSRC, Denmark; IN2P3-CNRS and CEA-DRF/IRFU, France; SRNSFG, Georgia; BMBF, HGF and MPG, Germany; GSRI, Greece; RGC and Hong Kong SAR, China; ISF and Benozziyo Center, Israel; INFN, Italy; MEXT and JSPS, Japan; CNRST, Morocco; NWO, Netherlands; RCN, Norway; MEiN, Poland; FCT, Portugal; MNE/IFA, Romania; MESTD, Serbia; MSSR, Slovakia; ARRS and MIZŠ, Slovenia; DSI/NRF, South Africa; MICINN, Spain; SRC and Wallenberg Foundation, Sweden; SERI, SNSF and Cantons of Bern and Geneva, Switzerland; MOST, Taiwan; TENMAK, Türkiye; STFC, United Kingdom; DOE and NSF, United States of America. In addition, individual groups and members have received support from BCKDF, CANARIE, Compute Canada and CRC, Canada; PRIMUS 21/SCI/017 and UNCE SCI/013, Czech Republic; COST, ERC, ERDF, Horizon 2020 and Marie Skłodowska-Curie Actions, European Union; Investissements d’Avenir Labex, Investissements d’Avenir Idex and ANR, France; DFG and AvH Foundation, Germany; Herakleitos, Thales and Aristeia programmes co-financed by EU-ESF and the Greek NSRF, Greece; BSF-NSF and MINERVA, Israel; Norwegian Financial Mechanism 2014-2021, Norway; NCN and NAWA, Poland; La Caixa Banking Foundation, CERCA Programme Generalitat de Catalunya and PROMETEO and GenT Programmes Generalitat Valenciana, Spain; Göran Gustafssons Stiftelse, Sweden; The Royal Society and Leverhulme Trust, United Kingdom.

The crucial computing support from all WLCG partners is acknowledged gratefully, in particular from CERN, the ATLAS Tier-1 facilities at TRIUMF (Canada), NDGF (Denmark, Norway, Sweden), CC-IN2P3 (France), KIT/GridKA (Germany), INFN-CNAF (Italy), NL-T1 (Netherlands), PIC (Spain), ASGC (Taiwan), RAL (UK) and BNL (USA), the Tier-2 facilities worldwide and large non-WLCG resource providers. Major contributors of computing resources are listed in Ref. [123].

References

- [1] Particle Data Group, *Review of Particle Physics*, *Phys. Rev. D* **98** (2018) 030001.
- [2] G. Degrandi et al., *Higgs mass and vacuum stability in the Standard Model at NNLO*, *JHEP* **08** (2012) 098, arXiv: 1205.6497 [hep-ph].
- [3] S. Alekhin, A. Djouadi and S. Moch, *The top quark and Higgs boson masses and the stability of the electroweak vacuum*, *Phys. Lett. B* **716** (2012) 214, arXiv: 1207.0980 [hep-ph].

- [4] P. Nason, *The Top Mass in Hadronic Collisions*, 2019, arXiv: [1712.02796 \[hep-ph\]](#).
- [5] G. Corcella, *The top-quark mass: challenges in definition and determination*, *Front. in Phys.* **7** (2019) 54, arXiv: [1903.06574 \[hep-ph\]](#).
- [6] ATLAS Collaboration, *Measurement of lepton differential distributions and the top quark mass in $t\bar{t}$ production in pp collisions at $\sqrt{s} = 8$ TeV with the ATLAS detector*, *Eur. Phys. J. C* **77** (2017) 804, arXiv: [1709.09407 \[hep-ex\]](#).
- [7] CDF Collaboration, *Measurement of the Top Quark Mass Using the Invariant Mass of Lepton Pairs in Soft Muon b -tagged Events*, *Phys. Rev. D* **80** (2009) 051104, arXiv: [0906.5371 \[hep-ex\]](#).
- [8] CMS Collaboration, *Measurement of the mass of the top quark in decays with a J/ψ meson in pp collisions at 8 TeV*, *JHEP* **12** (2016) 123, arXiv: [1608.03560 \[hep-ex\]](#).
- [9] ATLAS Collaboration, *Measurement of the top quark mass in the $t\bar{t} \rightarrow$ lepton+jets channel from $\sqrt{s} = 8$ TeV ATLAS data and combination with previous results*, *Eur. Phys. J. C* **79** (2019) 290, arXiv: [1810.01772 \[hep-ex\]](#).
- [10] CMS Collaboration, *Measurement of the top quark mass using proton–proton data at $\sqrt{s} = 7$ and 8 TeV*, *Phys. Rev. D* **93** (2016) 072004, arXiv: [1509.04044 \[hep-ex\]](#).
- [11] The Tevatron Electroweak Working Group, *Combination of CDF and D0 results on the mass of the top quark using up to 9.7 fb^{-1} at the Tevatron*, (2016), arXiv: [1608.01881](#).
- [12] J. Haller et al., *Update of the global electroweak fit and constraints on two-Higgs-doublet models*, *Eur. Phys. J. C* **78** (2018) 675, arXiv: [1803.01853 \[hep-ph\]](#).
- [13] ATLAS Collaboration, *The ATLAS Experiment at the CERN Large Hadron Collider*, *JINST* **3** (2008) S08003.
- [14] ATLAS Collaboration, *ATLAS Insertable B-Layer Technical Design Report*, ATLAS-TDR-19; CERN-LHCC-2010-013, 2010, URL: <https://cds.cern.ch/record/1291633>, Addendum: ATLAS-TDR-19-ADD-1; CERN-LHCC-2012-009, 2012, URL: <https://cds.cern.ch/record/1451888>.
- [15] B. Abbott et al., *Production and integration of the ATLAS Insertable B-Layer*, *JINST* **13** (2018) T05008, arXiv: [1803.00844 \[physics.ins-det\]](#).
- [16] ATLAS Collaboration, *Performance of the ATLAS trigger system in 2015*, *Eur. Phys. J. C* **77** (2017) 317, arXiv: [1611.09661 \[hep-ex\]](#).
- [17] ATLAS Collaboration, *The ATLAS Collaboration Software and Firmware*, ATL-SOFT-PUB-2021-001, 2021, URL: <https://cds.cern.ch/record/2767187>.
- [18] ATLAS Collaboration, *Luminosity determination in pp collisions at $\sqrt{s} = 13$ TeV using the ATLAS detector at the LHC*, ATLAS-CONF-2019-021, 2019, URL: <https://cds.cern.ch/record/2677054>.
- [19] ATLAS Collaboration, *Topological cell clustering in the ATLAS calorimeters and its performance in LHC Run 1*, *Eur. Phys. J. C* **77** (2017) 490, arXiv: [1603.02934 \[hep-ex\]](#).
- [20] M. Cacciari, G. P. Salam and G. Soyez, *The anti- k_t jet clustering algorithm*, *JHEP* **04** (2008) 063, arXiv: [0802.1189 \[hep-ph\]](#).

- [21] M. Cacciari, G. P. Salam and G. Soyez, *FastJet user manual*, *Eur. Phys. J. C* **72** (2012) 1896, arXiv: [1111.6097 \[hep-ph\]](#).
- [22] ATLAS Collaboration, *Jet energy scale measurements and their systematic uncertainties in proton–proton collisions at $\sqrt{s} = 13$ TeV with the ATLAS detector*, *Phys. Rev. D* **96** (2017) 072002, arXiv: [1703.09665 \[hep-ex\]](#).
- [23] ATLAS Collaboration, *Performance of missing transverse momentum reconstruction with the ATLAS detector using proton–proton collisions at $\sqrt{s} = 13$ TeV*, *Eur. Phys. J. C* **78** (2018) 903, arXiv: [1802.08168 \[hep-ex\]](#).
- [24] ATLAS Collaboration, *Performance of electron and photon triggers in ATLAS during LHC Run 2*, *Eur. Phys. J. C* **80** (2020) 47, arXiv: [1909.00761 \[hep-ex\]](#).
- [25] ATLAS Collaboration, *Performance of the ATLAS muon triggers in Run 2*, *JINST* **15** (2020) P09015, arXiv: [2004.13447 \[hep-ex\]](#).
- [26] ATLAS Collaboration, *Electron reconstruction and identification in the ATLAS experiment using the 2015 and 2016 LHC proton–proton collision data at $\sqrt{s} = 13$ TeV*, *Eur. Phys. J. C* **79** (2019) 639, arXiv: [1902.04655 \[hep-ex\]](#).
- [27] ATLAS Collaboration, *Muon reconstruction performance of the ATLAS detector in proton–proton collision data at $\sqrt{s} = 13$ TeV*, *Eur. Phys. J. C* **76** (2016) 292, arXiv: [1603.05598 \[hep-ex\]](#).
- [28] ATLAS Collaboration, *Performance of pile-up mitigation techniques for jets in pp collisions at $\sqrt{s} = 8$ TeV using the ATLAS detector*, *Eur. Phys. J. C* **76** (2016) 581, arXiv: [1510.03823 \[hep-ex\]](#).
- [29] ATLAS Collaboration, *Measurements of b -jet tagging efficiency with the ATLAS detector using $t\bar{t}$ events at $\sqrt{s} = 13$ TeV*, *JHEP* **08** (2018) 089, arXiv: [1805.01845 \[hep-ex\]](#).
- [30] ATLAS Collaboration, *The ATLAS Simulation Infrastructure*, *Eur. Phys. J. C* **70** (2010) 823, arXiv: [1005.4568 \[physics.ins-det\]](#).
- [31] GEANT4 Collaboration, S. Agostinelli et al., *GEANT4 – a simulation toolkit*, *Nucl. Instrum. Meth. A* **506** (2003) 250.
- [32] ATLAS Collaboration, *The simulation principle and performance of the ATLAS fast calorimeter simulation FastCaloSim*, ATL-PHYS-PUB-2010-013, 2010, URL: <https://cds.cern.ch/record/1300517>.
- [33] T. Sjöstrand, S. Mrenna and P. Skands, *A brief introduction to PYTHIA 8.1*, *Comput. Phys. Commun.* **178** (2008) 852, arXiv: [0710.3820 \[hep-ph\]](#).
- [34] A. D. Martin, W. J. Stirling, R. S. Thorne and G. Watt, *Parton distributions for the LHC*, *Eur. Phys. J. C* **63** (2009) 189, arXiv: [0901.0002 \[hep-ph\]](#).
- [35] A. D. Martin, W. J. Stirling, R. S. Thorne and G. Watt, *Uncertainties on α_S in global PDF analyses and implications for predicted hadronic cross sections*, *Eur. Phys. J. C* **64** (2009) 653, arXiv: [0905.3531 \[hep-ph\]](#).
- [36] ATLAS Collaboration, *Summary of ATLAS Pythia 8 tunes*, ATL-PHYS-PUB-2012-003, 2012, URL: <https://cds.cern.ch/record/1474107>.
- [37] ATLAS Collaboration, *Electron and photon energy calibration with the ATLAS detector using 2015–2016 LHC proton–proton collision data*, *JINST* **14** (2019) P03017, arXiv: [1812.03848 \[hep-ex\]](#).

- [38] ATLAS Collaboration, *Measurements of charge and CP asymmetries in b-hadron decays using top-quark events collected by the ATLAS detector in pp collisions at $\sqrt{s} = 8$ TeV*, [JHEP **02** \(2017\) 071](#), arXiv: [1610.07869 \[hep-ex\]](#).
- [39] ATLAS Collaboration, *Measurements of normalized differential cross-sections for $t\bar{t}$ production in pp collisions at $\sqrt{s} = 7$ TeV using the ATLAS detector*, [Phys. Rev. D **90** \(2014\) 072004](#), arXiv: [1407.0371 \[hep-ex\]](#).
- [40] S. Frixione, G. Ridolfi and P. Nason, *A positive-weight next-to-leading-order Monte Carlo for heavy flavour hadroproduction*, [JHEP **09** \(2007\) 126](#), arXiv: [0707.3088 \[hep-ph\]](#).
- [41] P. Nason, *A new method for combining NLO QCD with shower Monte Carlo algorithms*, [JHEP **11** \(2004\) 040](#), arXiv: [hep-ph/0409146](#).
- [42] S. Alioli, P. Nason, C. Oleari and E. Re, *A general framework for implementing NLO calculations in shower Monte Carlo programs: the POWHEG BOX*, [JHEP **06** \(2010\) 043](#), arXiv: [1002.2581 \[hep-ph\]](#).
- [43] R. D. Ball et al., *Parton distributions for the LHC run II*, [JHEP **04** \(2015\) 040](#), arXiv: [1410.8849 \[hep-ph\]](#).
- [44] J. Gao, C. S. Li and H. X. Zhu, *Top-Quark Decay at Next-to-Next-to-Leading Order in QCD*, [Phys. Rev. Lett. **110** \(2013\) 042001](#), arXiv: [1011.3540 \[hep-ph\]](#).
- [45] S. Frixione, E. Laenen, P. Motylinski and B. R. Webber, *Angular correlations of lepton pairs from vector boson and top quark decays in Monte Carlo simulations*, [JHEP **04** \(2007\) 081](#), arXiv: [hep-ph/0702198](#).
- [46] ATLAS Collaboration, *ATLAS Pythia 8 tunes to 7 TeV data*, ATL-PHYS-PUB-2014-021, 2014, URL: <https://cds.cern.ch/record/1966419>.
- [47] D. J. Lange, *The EvtGen particle decay simulation package*, [Nucl. Instrum. Meth. A **462** \(2001\) 152](#).
- [48] M. Czakon and A. Mitov, *Top++: A program for the calculation of the top-pair cross-section at hadron colliders*, [Comput. Phys. Commun. **185** \(2014\) 2930](#), arXiv: [1112.5675 \[hep-ph\]](#).
- [49] M. Cacciari, M. Czakon, M. Mangano, A. Mitov and P. Nason, *Top-pair production at hadron colliders with next-to-next-to-leading logarithmic soft-gluon resummation*, [Phys. Lett. B **710** \(2012\) 612](#), arXiv: [1111.5869 \[hep-ph\]](#).
- [50] P. Bärnreuther, M. Czakon and A. Mitov, *Percent Level Precision Physics at the Tevatron: First Genuine NNLO QCD Corrections to $q\bar{q} \rightarrow t\bar{t}$* , [Phys. Rev. Lett. **109** \(2012\) 132001](#), arXiv: [1204.5201 \[hep-ph\]](#).
- [51] M. Czakon and A. Mitov, *NNLO corrections to top-pair production at hadron colliders: the all-fermionic scattering channels*, [JHEP **12** \(2012\) 54](#), arXiv: [1207.0236 \[hep-ph\]](#).
- [52] M. Czakon and A. Mitov, *NNLO corrections to top-pair production at hadron colliders: the quark-gluon reaction*, [JHEP **01** \(2013\) 80](#), arXiv: [1210.6832 \[hep-ph\]](#).
- [53] M. Czakon, P. Fiedler and A. Mitov, *Total Top-Quark Pair-Production Cross Section at Hadron Colliders Through $O(\alpha_S^4)$* , [Phys. Rev. Lett. **110** \(2013\) 252004](#), arXiv: [1303.6254 \[hep-ph\]](#).

- [54] ATLAS Collaboration, *Estimation of non-prompt and fake lepton backgrounds in final states with top quarks produced in proton–proton collisions at $\sqrt{s} = 8$ TeV with the ATLAS Detector*, ATLAS-CONF-2014-058, 2014, URL: <https://cds.cern.ch/record/1951336>.
- [55] E. Bothmann et al., *Event generation with Sherpa 2.2*, *SciPost Phys.* **7** (2019) 034, arXiv: [1905.09127](https://arxiv.org/abs/1905.09127) [[hep-ph](#)].
- [56] T. Gleisberg and S. Höche, *Comix, a new matrix element generator*, *JHEP* **12** (2008) 039, arXiv: [0808.3674](https://arxiv.org/abs/0808.3674) [[hep-ph](#)].
- [57] F. Buccioni et al., *OpenLoops 2*, *Eur. Phys. J. C* **79** (2019) 866, arXiv: [1907.13071](https://arxiv.org/abs/1907.13071) [[hep-ph](#)].
- [58] F. Cascioli, P. Maierhöfer and S. Pozzorini, *Scattering Amplitudes with Open Loops*, *Phys. Rev. Lett.* **108** (2012) 111601, arXiv: [1111.5206](https://arxiv.org/abs/1111.5206) [[hep-ph](#)].
- [59] A. Denner, S. Dittmaier and L. Hofer, *COLLIER: A fortran-based complex one-loop library in extended regularizations*, *Comput. Phys. Commun.* **212** (2017) 220, arXiv: [1604.06792](https://arxiv.org/abs/1604.06792) [[hep-ph](#)].
- [60] S. Schumann and F. Krauss, *A parton shower algorithm based on Catani–Seymour dipole factorisation*, *JHEP* **03** (2008) 038, arXiv: [0709.1027](https://arxiv.org/abs/0709.1027) [[hep-ph](#)].
- [61] S. Höche, F. Krauss, M. Schönherr and F. Siegert, *A critical appraisal of NLO+PS matching methods*, *JHEP* **09** (2012) 049, arXiv: [1111.1220](https://arxiv.org/abs/1111.1220) [[hep-ph](#)].
- [62] S. Höche, F. Krauss, M. Schönherr and F. Siegert, *QCD matrix elements + parton showers. The NLO case*, *JHEP* **04** (2013) 027, arXiv: [1207.5030](https://arxiv.org/abs/1207.5030) [[hep-ph](#)].
- [63] S. Catani, F. Krauss, B. R. Webber and R. Kuhn, *QCD Matrix Elements + Parton Showers*, *JHEP* **11** (2001) 063, arXiv: [hep-ph/0109231](https://arxiv.org/abs/hep-ph/0109231).
- [64] S. Höche, F. Krauss, S. Schumann and F. Siegert, *QCD matrix elements and truncated showers*, *JHEP* **05** (2009) 053, arXiv: [0903.1219](https://arxiv.org/abs/0903.1219) [[hep-ph](#)].
- [65] C. Anastasiou, L. Dixon, K. Melnikov and F. Petriello, *High-precision QCD at hadron colliders: Electroweak gauge boson rapidity distributions at next-to-next-to leading order*, *Phys. Rev. D* **69** (2004) 094008, arXiv: [hep-ph/0312266](https://arxiv.org/abs/hep-ph/0312266).
- [66] ATLAS Collaboration, *Measurements of differential cross sections of top quark pair production in association with jets in pp collisions at $\sqrt{s} = 13$ TeV using the ATLAS detector*, *JHEP* **10** (2018) 159, arXiv: [1802.06572](https://arxiv.org/abs/1802.06572) [[hep-ex](#)].
- [67] H.-L. Lai et al., *New parton distributions for collider physics*, *Phys. Rev. D* **82** (2010) 074024, arXiv: [1007.2241](https://arxiv.org/abs/1007.2241) [[hep-ph](#)].
- [68] S. Frixione, E. Laenen, P. Motylinski, C. White and B. R. Webber, *Single-top hadroproduction in association with a W boson*, *JHEP* **07** (2008) 029, arXiv: [0805.3067](https://arxiv.org/abs/0805.3067) [[hep-ph](#)].
- [69] T. Sjöstrand, S. Mrenna and P. Z. Skands, *PYTHIA 6.4 physics and manual*, *JHEP* **05** (2006) 026, arXiv: [hep-ph/0603175](https://arxiv.org/abs/hep-ph/0603175).
- [70] J. Pumplin et al., *New Generation of Parton Distributions with Uncertainties from Global QCD Analysis*, *JHEP* **07** (2002) 012, arXiv: [hep-ph/0201195](https://arxiv.org/abs/hep-ph/0201195).

- [71] P. Z. Skands, *Tuning Monte Carlo generators: The Perugia tunes*, *Phys. Rev. D* **82** (2010) 074018, arXiv: [1005.3457 \[hep-ph\]](#).
- [72] N. Kidonakis, *Two-loop soft anomalous dimensions for single top quark associated production with a W^- or H^-* , *Phys. Rev. D* **82** (2010) 054018, arXiv: [1005.4451 \[hep-ph\]](#).
- [73] N. Kidonakis, *NNLL resummation for s-channel single top quark production*, *Phys. Rev. D* **81** (2010) 054028, arXiv: [1001.5034 \[hep-ph\]](#).
- [74] N. Kidonakis, *Next-to-next-to-leading-order collinear and soft gluon corrections for t-channel single top quark production*, *Phys. Rev. D* **83** (2011) 091503, arXiv: [1103.2792 \[hep-ph\]](#).
- [75] M. Bähr et al., *Herwig++ physics and manual*, *Eur. Phys. J. C* **58** (2008) 639, arXiv: [0803.0883 \[hep-ph\]](#).
- [76] J. Bellm et al., *Herwig 7.0/Herwig++ 3.0 release note*, *Eur. Phys. J. C* **76** (2016) 196, arXiv: [1512.01178 \[hep-ph\]](#).
- [77] B. Andersson, G. Gustafson, G. Ingelman and T. Sjöstrand, *Parton fragmentation and string dynamics*, *Phys. Rept.* **97** (1983) 31.
- [78] M.G. Bowler, *e^+e^- Production of heavy quarks in the string model*, *Z. Phys. C* **11** (1981) 169.
- [79] P. Skands, S. Carrazza and J. Rojo, *Tuning PYTHIA 8.1: the Monash 2013 Tune*, *Eur. Phys. J. C* **74** (2014) 3024, arXiv: [1404.5630 \[hep-ph\]](#).
- [80] G. Corcella and V. Drollinger, *Bottom-quark fragmentation: Comparing results from tuned event generators and resummed calculations*, *Nucl. Phys. B* **730** (2005) 82, arXiv: [hep-ph/0508013 \[hep-ph\]](#).
- [81] G. Corcella and F. Mescia, *A phenomenological study of bottom-quark fragmentation in top-quark decay*, *Eur. Phys. J. C* **65** (2010) 171, arXiv: [0907.5158 \[hep-ph\]](#).
- [82] G. Corcella and F. Mescia, *Erratum to: A phenomenological study of bottom-quark fragmentation in top-quark decay*, *Eur. Phys. J. C* **68** (2010) 687.
- [83] G. Corcella, R. Franceschini and D. Kim, *Fragmentation uncertainties in hadronic observables for top-quark mass measurements*, *Nucl. Phys. B* **929** (2018) 485, arXiv: [1712.05801 \[hep-ph\]](#).
- [84] ALEPH Collaboration, *Study of the fragmentation of b quarks into B mesons at the Z peak*, *Phys. Lett. B* **512** (2001) 30, arXiv: [hep-ex/0106051](#).
- [85] DELPHI Collaboration, *A study of the b-quark fragmentation function with the DELPHI detector at LEP I and an averaged distribution obtained at the Z Pole*, *Eur. Phys. J. C* **71** (2011) 1557, arXiv: [1102.4748 \[hep-ex\]](#).
- [86] OPAL Collaboration, *Inclusive analysis of the b quark fragmentation function in Z decays at LEP*, *Eur. Phys. J. C* **29** (2003) 463, arXiv: [hep-ex/0210031 \[hep-ex\]](#).
- [87] SLD Collaboration, *Precise Measurement of the b-Quark Fragmentation Function in Z^0 Boson Decays*, *Phys. Rev. Lett.* **84** (2000) 4300, arXiv: [hep-ex/9912058 \[hep-ex\]](#).
- [88] C. Bierlich et al., *Robust Independent Validation of Experiment and Theory: Rivet version 3*, *SciPost Phys.* **8** (2020) 026, arXiv: [1912.05451 \[hep-ph\]](#).

- [89] ATLAS Collaboration, *Measurement of b -quark fragmentation properties in jets using the decay $B^\pm \rightarrow J/\psi K^\pm$ in pp collisions at $\sqrt{s} = 13$ TeV with the ATLAS detector*, *JHEP* **12** (2021) 131, arXiv: [2108.11650](#) [[hep-ex](#)].
- [90] ATLAS Collaboration, *Measurements of jet observables sensitive to b -quark fragmentation in $t\bar{t}$ events at the LHC with the ATLAS detector*, *Phys. Rev. D* **106** (2022) 032008, arXiv: [2202.13901](#) [[hep-ex](#)].
- [91] Heavy Flavour Averaging Group (HFAG), *Averages of b -hadron, c -hadron, and τ -lepton properties as of summer 2014*, (2014), arXiv: [1412.7515](#) [[hep-ex](#)].
- [92] E. Lohrmann, *A Summary of Charm Hadron Production Fractions*, 2011, arXiv: [1112.3757](#) [[hep-ex](#)].
- [93] LHCb Collaboration, *Evidence for modification of b quark hadronization in high-multiplicity pp collisions at $\sqrt{s} = 13$ TeV*, 2022, arXiv: [2204.13042](#) [[hep-ex](#)].
- [94] LHCb collaboration, *Measurement of the fragmentation fraction ratio f_s/f_d and its dependence on B meson kinematics*, *J. High Energ. Phys.* **04** (2013) 001, arXiv: [1301.5286](#) [[hep-ex](#)].
- [95] LHCb Collaboration, *Measurement of f_s/f_u Variation with Proton-Proton Collision Energy and B -Meson Kinematics*, *Phys. Rev. Lett.* **124** (2020) 122002, arXiv: [1910.09934](#) [[hep-ex](#)].
- [96] LHCb Collaboration, *Precise measurement of the f_s/f_d ratio of fragmentation fractions and of B_s^0 decay branching fractions*, *Phys. Rev. D* **104** (2021) 032005, arXiv: [2103.06810](#) [[hep-ex](#)].
- [97] LHCb Collaboration, *Measurement of b hadron production fractions in 7 TeV pp collisions*, *Phys. Rev. D* **85** (2012) 032008, arXiv: [1111.2357](#) [[hep-ex](#)].
- [98] LHCb Collaboration, *Measurement of b hadron fractions in 13 TeV pp collisions*, *Phys. Rev. D* **100** (2019) 031102, arXiv: [1902.06794](#) [[hep-ex](#)].
- [99] ALICE Collaboration, *Charm-quark fragmentation fractions and production cross section at midrapidity in pp collisions at the LHC*, *Phys. Rev. D* **105** (2022) L011103, arXiv: [2105.06335](#) [[hep-ex](#)].
- [100] DELPHI Collaboration, *Measurement of the semileptonic b branching fractions and average b mixing parameter in Z decays*, *Eur. Phys. J. C* **20** (2001) 455, arXiv: [hep-ex/0105080](#).
- [101] LEP Electroweak Working Group and the SLD Heavy Flavour and Electroweak Groups, *Final input parameters for the LEP/SLD heavy flavour analyses*, LEPHF 2001-01, 2001, URL: <https://www.cern.ch/LEPEWWG/heavy/>.
- [102] CLEO Collaboration, *Flavor-Specific Inclusive B Decays to Charm*, *Phys. Rev. Lett.* **80** (1998) 1150, arXiv: [hep-ex/9710028](#) [[hep-ex](#)].
- [103] CLEO Collaboration, *Measurements of $B \rightarrow D_s^+ X$ decays*, *Phys. Rev. D* **53** (1996) 4734.
- [104] CLEO Collaboration, *Study of flavor-tagged baryon production in B decay*, *Phys. Rev. D* **55** (1997) 13.
- [105] ALEPH Collaboration, *Observation of doubly-charmed B decays at LEP*, *Eur. Phys. J. C* **4** (1998) 387.

- [106] K. Cranmer, G. Lewis, L. Moneta, A. Shibata and W. Verkerke, *HistFactory: A tool for creating statistical models for use with RooFit and RooStats*, CERN-OPEN-2012-016, 2012, URL: <https://cds.cern.ch/record/1456844>.
- [107] S. Baker and R. Cousins, *Clarification of the use of chi-square and likelihood functions in fits to histograms*, *Nucl. Instrum. Meth.* **221** (1984) 437.
- [108] ATLAS Collaboration, *Evaluating statistical uncertainties and correlations using the bootstrap method*, ATL-PHYS-PUB-2021-011, 2021, URL: <https://cds.cern.ch/record/2759945>.
- [109] G. Avoni et al., *The new LUCID-2 detector for luminosity measurement and monitoring in ATLAS*, *JINST* **13** (2018) P07017.
- [110] J. Alwall et al., *The automated computation of tree-level and next-to-leading order differential cross sections, and their matching to parton shower simulations*, *JHEP* **07** (2014) 079, arXiv: [1405.0301](https://arxiv.org/abs/1405.0301) [hep-ph].
- [111] ATLAS Collaboration, *Measurements of top-quark pair differential and double-differential cross-sections in the ℓ +jets channel with pp collisions at $\sqrt{s} = 13$ TeV using the ATLAS detector*, *Eur. Phys. J. C* **79** (2019) 1028, arXiv: [1908.07305](https://arxiv.org/abs/1908.07305) [hep-ex], Erratum: *Eur. Phys. J. C* **80** (2020) 1092.
- [112] ATLAS Collaboration, *Measurement of jet shapes in top-quark pair events at $\sqrt{s} = 7$ TeV using the ATLAS detector*, *Eur. Phys. J. C* **73** (2013) 2676, arXiv: [1307.5749](https://arxiv.org/abs/1307.5749) [hep-ex].
- [113] S. Mrenna and P. Skands, *Automated parton-shower variations in pythia 8*, *Phys. Rev. D* **94** (7 2016) 074005, URL: <https://link.aps.org/doi/10.1103/PhysRevD.94.074005>.
- [114] S. Mrenna and P. Skands, *Automated parton-shower variations in Pythia 8*, *Phys. Rev. D* **94** (2016) 074005, arXiv: [1605.08352](https://arxiv.org/abs/1605.08352) [hep-ph].
- [115] H. Brooks and P. Skands, *Coherent showers in decays of colored resonances*, *Phys. Rev. D* **100** (7 2019) 076006, arXiv: [1907.08980](https://arxiv.org/abs/1907.08980) [hep-ph].
- [116] ATLAS Collaboration, *Simulation of top-quark production for the ATLAS experiment at $\sqrt{s} = 13$ TeV*, ATL-PHYS-PUB-2016-004, 2016, URL: <https://cds.cern.ch/record/2120417>.
- [117] S. Argyropoulos and T. Sjöstrand, *Effects of color reconnection on $t\bar{t}$ final states at the LHC*, *JHEP* **11** (2014) 043, arXiv: [1407.6653](https://arxiv.org/abs/1407.6653) [hep-ph].
- [118] J. Butterworth et al., *PDF4LHC recommendations for LHC Run II*, *J. Phys. G* **43** (2016) 023001, arXiv: [1510.03865](https://arxiv.org/abs/1510.03865) [hep-ph].
- [119] ATLAS Collaboration, *Multi-boson simulation for 13 TeV ATLAS analyses*, ATL-PHYS-PUB-2016-002, 2016, URL: <https://cds.cern.ch/record/2119986>.
- [120] ATLAS Collaboration, *Jet Calibration and Systematic Uncertainties for Jets Reconstructed in the ATLAS Detector at $\sqrt{s} = 13$ TeV*, ATL-PHYS-PUB-2015-015, 2015, URL: <https://cds.cern.ch/record/2037613>.
- [121] ATLAS Collaboration, *Measurement of b -tagging efficiency of c -jets in $t\bar{t}$ events using a likelihood approach with the ATLAS detector*, ATLAS-CONF-2018-001, 2018, URL: <https://cds.cern.ch/record/2306649>.

- [122] ATLAS Collaboration, *Calibration of light-flavour b-jet mistagging rates using ATLAS proton–proton collision data at $\sqrt{s} = 13$ TeV*, ATLAS-CONF-2018-006, 2018,
URL: <https://cds.cern.ch/record/2314418>.
- [123] ATLAS Collaboration, *ATLAS Computing Acknowledgements*, ATL-SOFT-PUB-2021-003, 2021,
URL: <https://cds.cern.ch/record/2776662>.

The ATLAS Collaboration

G. Aad ¹⁰³, B. Abbott ¹²², D.C. Abbott ¹⁰⁴, A. Abed Abud ³⁶, K. Abeling ⁵⁵,
D.K. Abhayasinghe ⁹⁵, S.H. Abidi ¹⁵⁹, O.S. AbouZeid ⁴², N.L. Abraham ¹⁴⁹, H. Abramowicz ¹⁵⁴,
H. Abreu ¹⁵³, Y. Abulaiti ⁶, B.S. Acharya ^{69a,69b,o}, B. Achkar ⁵⁵, S. Adachi ¹⁵⁶, L. Adam ¹⁰¹,
C. Adam Bourdarios ⁵, L. Adamczyk ^{85a}, L. Adamek ¹⁵⁹, J. Adelman ¹¹⁷, M. Adersberger ¹¹⁰,
A. Adiguzel ^{12c,ag}, S. Adorni ⁵⁶, T. Adye ¹³⁶, A.A. Affolder ¹³⁸, Y. Afik ¹⁵³, C. Agapopoulou ⁶⁷,
M.N. Agaras ⁴⁰, A. Aggarwal ¹¹⁵, C. Agheorghiesei ^{27c}, J.A. Aguilar-Saavedra ^{132f,132a,af},
F. Ahmadov ^{38,ad}, W.S. Ahmed ¹⁰⁵, X. Ai ^{18a}, G. Aielli ^{76a,76b}, S. Akatsuka ⁸⁷,
T.P.A. Åkesson ⁹⁸, E. Akilli ⁵⁶, A.V. Akimov ³⁷, K. Al Khoury ⁶⁷, G.L. Alberghi ^{23b},
J. Albert ¹⁶⁸, M.J. Alconada Verzini ¹⁵⁴, S. Alderweireldt ³⁶, M. Aleksa ³⁶, I.N. Aleksandrov ³⁸,
C. Alexa ^{27b}, T. Alexopoulos ¹⁰, A. Alfonsi ¹¹⁶, F. Alfonsi ^{23b,23a}, M. Alhroob ¹²², B. Ali ¹³⁴,
M. Aliev ³⁷, G. Alimonti ^{71a}, C. Allaire ⁶⁷, B.M.M. Allbrooke ¹⁴⁹, B.W. Allen ¹²⁵,
P.P. Allport ²¹, A. Aloisio ^{72a,72b}, F. Alonso ⁹⁰, C. Alpigiani ¹⁴¹, A.A. Alshehri ⁵⁹,
E. Alunno Camelia ^{76a,76b}, M. Alvarez Estevez ¹⁰⁰, M.G. Alviggi ^{72a,72b}, Y. Amaral Coutinho ^{82b},
A. Ambler ¹⁰⁵, L. Ambroz ¹²⁸, C. Amelung ²⁶, D. Amidei ¹⁰⁷, S.P. Amor Dos Santos ^{132a},
S. Amoroso ⁴⁸, C.S. Amrouche ⁵⁶, F. An ⁸¹, C. Anastopoulos ¹⁴², N. Andari ¹³⁷, T. Andeen ¹¹,
C.F. Anders ^{63b}, J.K. Anders ²⁰, A. Andreazza ^{71a,71b}, V. Andrei ^{63a}, C.R. Anelli ¹⁶⁸,
S. Angelidakis ⁴⁰, A. Angerami ⁴¹, A.V. Anisenkov ³⁷, A. Annovi ^{74a}, C. Antel ⁵⁶,
M.T. Anthony ¹⁴², E. Antipov ¹²³, M. Antonelli ⁵³, D.J.A. Antrim ¹⁶³, F. Anulli ^{75a}, M. Aoki ⁸³,
J.A. Aparisi Pozo ¹⁶⁶, L. Aperio Bella ^{15a}, J.P. Araque ^{132a}, V. Araujo Ferraz ^{82b},
R. Araujo Pereira ^{82b}, C. Arcangeletti ⁵³, A.T.H. Arce ⁵¹, F.A. Arduh ⁹⁰, J-F. Arguin ¹⁰⁹,
S. Argyropoulos ⁵⁴, J.-H. Arling ⁴⁸, A.J. Armbruster ³⁶, A. Armstrong ¹⁶³, O. Arnaez ¹⁵⁹,
H. Arnold ¹¹⁶, Z.P. Arrubarrena Tame ¹¹⁰, G. Artoni ¹²⁸, S. Artz ¹⁰¹, S. Asai ¹⁵⁶,
T. Asawatavonvanich ¹⁵⁸, N.A. Asbah ⁶¹, E.M. Asimakopoulou ¹⁶⁴, L. Asquith ¹⁴⁹, J. Assahsah ^{35d},
K. Assamagan ²⁹, R. Astalos ^{28a}, R.J. Atkin ^{33a}, M. Atkinson ¹⁶⁵, N.B. Atlay ¹⁹, H. Atmani ⁶⁷,
K. Augsten ¹³⁴, G. Avolio ³⁶, M.K. Ayoub ^{15a}, G. Azuelos ^{109,ao}, H. Bachacou ¹³⁷,
K. Bachas ^{70a,70b}, M. Backes ¹²⁸, F. Backman ^{47a,47b}, P. Bagnaia ^{75a,75b}, H. Bahrasemani ¹⁴⁵,
A.J. Bailey ¹⁶⁶, V.R. Bailey ¹⁶⁵, J.T. Baines ¹³⁶, C. Bakalis ¹⁰, O.K. Baker ¹⁷⁵, P.J. Bakker ¹¹⁶,
D. Bakshi Gupta ⁸, S. Balaji ¹⁵⁰, E.M. Baldin ³⁷, P. Balek ¹⁷², F. Balli ¹³⁷, W.K. Balunas ¹²⁸,
J. Balz ¹⁰¹, E. Banas ⁸⁶, A. Bandyopadhyay ²⁴, Sw. Banerjee ^{173,j}, A.A.E. Bannoura ¹⁷⁴,
L. Barak ¹⁵⁴, W.M. Barbe ⁴⁰, E.L. Barberio ¹⁰⁶, D. Barberis ^{57b,57a}, M. Barbero ¹⁰³,
G. Barbour ⁹⁶, T. Barillari ¹¹¹, M.-S. Barisits ³⁶, J. Barkeloo ¹²⁵, T. Barklow ¹⁴⁶, R. Barnea ¹⁵³,
B.M. Barnett ¹³⁶, R.M. Barnett ^{18a}, Z. Barnovska-Blenessy ^{62a}, A. Baroncelli ^{62a}, G. Barone ²⁹,
A.J. Barr ¹²⁸, L. Barranco Navarro ^{47a,47b}, F. Barreiro ¹⁰⁰, J. Barreiro Guimarães da Costa ^{15a},
S. Barsov ³⁷, R. Bartoldus ¹⁴⁶, G. Bartolini ¹⁰³, A.E. Barton ⁹¹, P. Bartos ^{28a}, A. Basalae ⁴⁸,
A. Basan ¹⁰¹, A. Bassalat ^{67,aj}, M.J. Basso ¹⁵⁹, R.L. Bates ⁵⁹, S. Batlamous ^{35e}, J.R. Batley ³²,
B. Batool ¹⁴⁴, M. Battaglia ¹³⁸, M. Baucé ^{75a,75b}, F. Bauer ^{137,*}, K.T. Bauer ¹⁶³, H.S. Bawa ³¹,
J.B. Beacham ⁵¹, T. Beau ¹²⁹, P.H. Beauchemin ¹⁶², F. Becherer ⁵⁴, P. Bechtel ²⁴, H.C. Beck ⁵⁵,
H.P. Beck ^{20,r}, K. Becker ¹⁷⁰, C. Becot ⁴⁸, A. Beddall ^{12d}, A.J. Beddall ^{12a}, V.A. Bednyakov ³⁸,
M. Bedognetti ¹¹⁶, C.P. Bee ¹⁴⁸, T.A. Beermann ¹⁷⁴, M. Begalli ^{82b}, M. Begel ²⁹, A. Behera ¹⁴⁸,
J.K. Behr ⁴⁸, F. Beisiegel ²⁴, A.S. Bell ⁹⁶, G. Bella ¹⁵⁴, L. Bellagamba ^{23b}, A. Bellerive ³⁴,
P. Bellos ⁹, K. Beloborodov ³⁷, K. Belotskiy ³⁷, N.L. Belyaev ³⁷, D. Bencheekroun ^{35a},
N. Benekos ¹⁰, Y. Benhammou ¹⁵⁴, D.P. Benjamin ⁶, M. Benoit ⁵⁶, J.R. Bensinger ²⁶,
S. Bentvelsen ¹¹⁶, L. Beresford ¹²⁸, M. Beretta ⁵³, D. Berge ¹⁹, E. Bergeaas Kuutmann ¹⁶⁴,
N. Berger ⁵, B. Bergmann ¹³⁴, L.J. Bergsten ²⁶, J. Beringer ^{18a}, S. Berlendis ⁷, G. Bernardi ¹²⁹,

C. Bernius ¹⁴⁶, F.U. Bernlochner ²⁴, T. Berry ⁹⁵, P. Berta ¹⁰¹, C. Bertella ^{15a}, I.A. Bertram ⁹¹,
 O. Bessidskaia Bylund ¹⁷⁴, N. Besson ¹³⁷, A. Bethani ¹⁰², S. Bethke ¹¹¹, A. Betti ⁴⁴,
 A.J. Bevan ⁹⁴, J. Beyer ¹¹¹, D.S. Bhattacharya ¹⁶⁹, P. Bhattarai ²⁶, R. Bi ¹³¹, R.M. Bianchi ¹³¹,
 O. Biebel ¹¹⁰, D. Biedermann ¹⁹, R. Bielski ³⁶, K. Bierwagen ¹⁰¹, N.V. Biesuz ^{74a,74b},
 M. Biglietti ^{77a}, T.R.V. Billoud ¹⁰⁹, M. Bindi ⁵⁵, A. Bingul ^{12d}, C. Bini ^{75a,75b}, S. Biondi ^{23b,23a},
 M. Birman ¹⁷², T. Bisanz ⁵⁵, D. Biswas ^{173,j}, A. Bitadze ¹⁰², C. Bittrich ⁵⁰, K. Bjørke ¹²⁷,
 T. Blazek ^{28a}, I. Bloch ⁴⁸, C. Blocker ²⁶, A. Blue ⁵⁹, U. Blumenschein ⁹⁴, G.J. Bobbink ¹¹⁶,
 V.S. Bobrovnikov ³⁷, S.S. Bocchetta ⁹⁸, A. Bocci ⁵¹, D. Bogavac ¹⁴, A.G. Bogdanchikov ³⁷,
 C. Bohm ^{47a}, V. Boisvert ⁹⁵, P. Bokan ⁵⁵, T. Bold ^{85a}, A.E. Bolz ^{63b}, M. Bomben ¹²⁹,
 M. Bona ⁹⁴, J.S. Bonilla ¹²⁵, M. Boonekamp ¹³⁷, C.D. Booth ⁹⁵, H.M. Borecka-Bielska ⁹²,
 L.S. Borgna ⁹⁶, A. Borisov ³⁷, G. Borissov ⁹¹, J. Bortfeldt ³⁶, D. Bortoletto ¹²⁸, D. Boscherini ^{23b},
 M. Bosman ¹⁴, J.D. Bossio Sola ¹⁰⁵, K. Bouaouda ^{35a}, J. Boudreau ¹³¹, E.V. Bouhova-Thacker ⁹¹,
 D. Boumediene ⁴⁰, S.K. Boutle ⁵⁹, A. Boveia ¹²⁰, J. Boyd ³⁶, D. Boye ^{33b,ak}, I.R. Boyko ³⁸,
 A.J. Bozson ⁹⁵, J. Bracinik ²¹, N. Brahimy ¹⁰³, G. Brandt ¹⁷⁴, O. Brandt ³², F. Braren ⁴⁸,
 B. Brau ¹⁰⁴, J.E. Brau ¹²⁵, W.D. Breaden Madden ⁵⁹, K. Brendlinger ⁴⁸, L. Brenner ⁴⁸,
 R. Brenner ¹⁶⁴, S. Bressler ¹⁷², B. Brickwedde ¹⁰¹, D.L. Briglin ²¹, D. Britton ⁵⁹,
 D. Britzger ¹¹¹, I. Brock ²⁴, R. Brock ¹⁰⁸, G. Brooijmans ⁴¹, W.K. Brooks ^{139c}, E. Brost ²⁹,
 J.H. Broughton ²¹, P.A. Bruckman de Renstrom ⁸⁶, D. Bruncko ^{28b,*}, A. Bruni ^{23b}, G. Bruni ^{23b},
 L.S. Bruni ¹¹⁶, S. Bruno ^{76a,76b}, M. Bruschi ^{23b}, N. Bruscinò ^{75a,75b}, P. Bryant ³⁹,
 L. Bryngemark ⁹⁸, T. Buanes ¹⁷, Q. Buat ³⁶, P. Buchholz ¹⁴⁴, A.G. Buckley ⁵⁹,
 I.A. Budagov ^{38,*}, M.K. Bugge ¹²⁷, F. Bühner ⁵⁴, O. Bulekov ³⁷, T.J. Burch ¹¹⁷, S. Burdin ⁹²,
 C.D. Burgard ¹¹⁶, A.M. Burger ¹²³, B. Burghgrave ⁸, J.T.P. Burr ⁴⁸, C.D. Burton ¹¹,
 J.C. Burzynski ¹⁰⁴, V. Büscher ¹⁰¹, E. Buschmann ⁵⁵, P.J. Bussey ⁵⁹, J.M. Butler ²⁵,
 C.M. Buttar ⁵⁹, J.M. Butterworth ⁹⁶, P. Butti ³⁶, W. Buttinger ³⁶, C.J. Buxo Vazquez ¹⁰⁸,
 A. Buzatu ¹⁵¹, A.R. Buzykaev ³⁷, G. Cabras ^{23b,23a}, S. Cabrera Urbán ¹⁶⁶, D. Caforio ⁵⁸,
 H. Cai ¹⁶⁵, V.M.M. Cairo ¹⁴⁶, O. Cakir ^{4a}, N. Calace ³⁶, P. Calafiura ^{18a}, A. Calandri ¹⁰³,
 G. Calderini ¹²⁹, P. Calfayan ⁵⁸, G. Callea ⁵⁹, L.P. Caloba ^{82b}, A. Caltabiano ^{76a,76b},
 S. Calvente Lopez ¹⁰⁰, D. Calvet ⁴⁰, S. Calvet ⁴⁰, T.P. Calvet ¹⁴⁸, M. Calvetti ^{74a,74b},
 R. Camacho Toro ¹²⁹, S. Camarda ³⁶, D. Camarero Munoz ¹⁰⁰, P. Camarri ^{76a,76b},
 D. Cameron ¹²⁷, C. Camincher ³⁶, S. Campana ³⁶, M. Campanelli ⁹⁶, A. Camplani ⁴²,
 A. Campoverde ¹⁴⁴, V. Canale ^{72a,72b}, A. Canesse ¹⁰⁵, M. Cano Bret ^{62c}, J. Cantero ¹²³,
 T. Cao ¹⁵⁴, Y. Cao ¹⁶⁵, M.D.M. Capeans Garrido ³⁶, M. Capua ^{43b,43a}, R. Cardarelli ^{76a},
 F. Cardillo ¹⁴², I. Carli ¹³⁵, T. Carli ³⁶, G. Carlino ^{72a}, B.T. Carlson ¹³¹, L. Carminati ^{71a,71b},
 R.M.D. Carney ¹⁴⁶, S. Caron ¹¹⁵, E. Carquin ^{139c}, S. Carrá ⁴⁸, J.W.S. Carter ¹⁵⁹,
 M.P. Casado ^{14,f}, A.F. Casha ¹⁵⁹, D.W. Casper ¹⁶³, R. Castelijns ¹¹⁶, F.L. Castillo ¹⁶⁶,
 L. Castillo Garcia ¹⁴, V. Castillo Gimenez ¹⁶⁶, N.F. Castro ^{132a,132e}, A. Catinaccio ³⁶,
 J.R. Catmore ¹²⁷, A. Cattai ³⁶, V. Cavaliere ²⁹, E. Cavallaro ¹⁴, M. Cavalli-Sforza ¹⁴,
 V. Cavasinni ^{74a,74b}, E. Celebi ^{12b}, L. Cerda Alberich ¹⁶⁶, K. Cerny ¹²⁴, A.S. Cerqueira ^{82a},
 A. Cerri ¹⁴⁹, L. Cerrito ^{76a,76b}, F. Cerutti ^{18a}, A. Cervelli ^{23b}, S.A. Cetin ^{12b}, Z. Chadi ^{35a},
 D. Chakraborty ¹¹⁷, J. Chan ¹⁷³, W.S. Chan ¹¹⁶, W.Y. Chan ⁹², J.D. Chapman ³²,
 B. Chargeishvili ^{152b}, D.G. Charlton ²¹, T.P. Charman ⁹⁴, C.C. Chau ³⁴, S. Che ¹²⁰,
 S. Chekanov ⁶, S.V. Chekulaev ^{160a}, G.A. Chelkov ^{38,a}, B. Chen ⁸¹, C. Chen ^{62a}, C.H. Chen ⁸¹,
 H. Chen ²⁹, J. Chen ^{62a}, J. Chen ⁴¹, J. Chen ²⁶, S. Chen ¹³⁰, S.J. Chen ^{15c}, X. Chen ^{15b,an},
 Y.-H. Chen ⁴⁸, H.C. Cheng ^{65a}, H.J. Cheng ^{15a}, A. Cheplakov ³⁸, E. Cheremushkina ³⁷,
 R. Cherkaoui El Moursli ^{35e}, E. Cheu ⁷, K. Cheung ⁶⁶, T.J.A. Chevalérias ¹³⁷, L. Chevalier ¹³⁷,
 V. Chiarella ⁵³, G. Chiarelli ^{74a}, G. Chiodini ^{70a}, A.S. Chisholm ²¹, A. Chitan ^{27b}, I. Chiu ¹⁵⁶,
 Y.H. Chiu ¹⁶⁸, M.V. Chizhov ³⁸, K. Choi ¹¹, A.R. Chomont ^{75a,75b}, S. Chouridou ¹⁵⁵,

E.Y.S. Chow [ID116](#), M.C. Chu [ID65a](#), X. Chu [ID15a,15d](#), J. Chudoba [ID133](#), J.J. Chwastowski [ID86](#),
 L. Chytka¹²⁴, D. Cieri [ID111](#), K.M. Ciesla [ID86](#), D. Cinca [ID49](#), V. Cindro [ID93](#), I.A. Cioară [ID27b](#),
 A. Ciocio [ID18a](#), F. Cirotto [ID72a,72b](#), Z.H. Citron [ID172,k](#), M. Citterio [ID71a](#), D.A. Ciubotaru^{27b},
 B.M. Ciungu [ID159](#), A. Clark [ID56](#), M.R. Clark [ID41](#), P.J. Clark [ID52](#), C. Clement [ID47a,47b](#), Y. Coadou [ID103](#),
 M. Cobal [ID69a,69c](#), A. Coccaro [ID57b](#), J. Cochran⁸¹, R. Coelho Lopes De Sa [ID104](#), H. Cohen [ID154](#),
 A.E.C. Coimbra [ID36](#), B. Cole [ID41](#), A.P. Colijn¹¹⁶, J. Collot [ID60](#), P. Conde Muiño [ID132a,132h](#),
 S.H. Connell [ID33b](#), I.A. Connelly [ID59](#), S. Constantinescu^{27b}, F. Conventi [ID72a,ap](#),
 A.M. Cooper-Sarkar [ID128](#), G. Corcella^w, F. Cormier [ID167](#), K.J.R. Cormier¹⁵⁹, L.D. Corpe [ID96](#),
 M. Corradi [ID75a,75b](#), E.E. Corrigan [ID98](#), F. Corriveau [ID105,ac](#), M.J. Costa [ID166](#), F. Costanza [ID5](#),
 D. Costanzo [ID142](#), G. Cowan [ID95](#), J.W. Cowley [ID32](#), J. Crane [ID102](#), K. Cranmer [ID118](#), S.J. Crawley⁵⁹,
 R.A. Creager [ID130](#), S. Crépe-Renaudin [ID60](#), F. Crescioli [ID129](#), M. Cristinziani [ID24](#), V. Croft [ID162](#),
 G. Crosetti [ID43b,43a](#), A. Cueto [ID5](#), T. Cuhadar Donszelmann [ID142](#), A.R. Cukierman [ID146](#),
 W.R. Cunningham [ID59](#), S. Czekierda [ID86](#), P. Czodrowski [ID36](#), M.J. Da Cunha Sargedas De Sousa [ID62b](#),
 J.V. Da Fonseca Pinto [ID82b](#), C. Da Via [ID102](#), W. Dabrowski [ID85a](#), F. Dachs [ID36](#), T. Dado [ID28a](#),
 S. Dahbi [ID33d](#), T. Dai [ID107](#), C. Dallapiccola [ID104](#), M. Dam [ID42](#), G. D'amen [ID29](#), V. D'Amico [ID77a,77b](#),
 J. Damp [ID101](#), J.R. Dandoy [ID130](#), M.F. Daneri [ID30](#), N.S. Dann [ID102](#), M. Danninger [ID145](#), V. Dao [ID36](#),
 G. Darbo [ID57b](#), O. Dartsis⁵, A. Dattagupta [ID125](#), T. Daubney⁴⁸, S. D'Auria [ID71a,71b](#), C. David [ID160b](#),
 T. Davidek [ID135](#), D.R. Davis [ID51](#), I. Dawson [ID142](#), K. De [ID8](#), R. De Asmundis [ID72a](#), M. De Beurs [ID116](#),
 S. De Castro [ID23b,23a](#), S. De Cecco [ID75a,75b](#), N. De Groot [ID115](#), P. de Jong [ID116](#), H. De la Torre [ID108](#),
 A. De Maria [ID15c](#), D. De Pedis [ID75a](#), A. De Salvo [ID75a](#), U. De Sanctis [ID76a,76b](#), M. De Santis [ID76a,76b](#),
 A. De Santo [ID149](#), K. De Vasconcelos Corga¹⁰³, J.B. De Vivie De Regie [ID67](#), C. Debenedetti [ID138](#),
 D.V. Dedovich³⁸, A.M. Deiana [ID44](#), J. Del Peso [ID100](#), Y. Delabat Diaz [ID48](#), D. Delgove [ID67](#),
 F. Deliot [ID137,q](#), C.M. Delitzsch [ID7](#), M. Della Pietra [ID72a,72b](#), D. Della Volpe [ID56](#), A. Dell'Acqua [ID36](#),
 L. Dell'Asta [ID76a,76b](#), M. Delmastro [ID5](#), C. Delporte⁶⁷, P.A. Delsart [ID60](#), D.A. DeMarco [ID159](#),
 S. Demers [ID175](#), M. Demichev [ID38](#), G. Demontigny¹⁰⁹, S.P. Denisov [ID37](#), L. D'Eramo [ID129](#),
 D. Derendarz [ID86](#), J.E. Derkaoui [ID35d](#), F. Derue [ID129](#), P. Dervan [ID92](#), K. Desch [ID24](#), C. Deterre [ID48](#),
 K. Dette [ID159](#), C. Deutsch [ID24](#), M.R. Devesa³⁰, P.O. Deviveiros [ID36](#), F.A. Di Bello [ID56](#),
 A. Di Ciaccio [ID76a,76b](#), L. Di Ciaccio [ID5](#), W.K. Di Clemente [ID130](#), C. Di Donato [ID72a,72b](#),
 A. Di Girolamo [ID36](#), G. Di Gregorio [ID74a,74b](#), B. Di Micco [ID77a,77b](#), R. Di Nardo [ID77a,77b](#),
 K.F. Di Petrillo [ID61](#), R. Di Sipio [ID159](#), C. Diaconu [ID103](#), F.A. Dias [ID42](#), T. Dias Do Vale [ID132a](#),
 M.A. Diaz [ID139a](#), J. Dickinson [ID18a](#), E.B. Diehl [ID107](#), J. Dietrich [ID19](#), S. Díez Cornell [ID48](#),
 A. Dimitrievska [ID18a](#), W. Ding [ID15b](#), J. Dingfelder [ID24](#), F. Dittus [ID36](#), F. Djama [ID103](#), T. Djobava [ID152b](#),
 J.I. Djuvsland [ID17](#), M.A.B. Do Vale [ID140](#), M. Dobre [ID27b](#), D. Dodsworth [ID26](#), C. Doglioni [ID98](#),
 J. Dolejsi [ID135](#), Z. Dolezal [ID135](#), M. Donadelli [ID82c](#), B. Dong [ID62c](#), J. Donini [ID40](#), A. D'Onofrio [ID15c](#),
 M. D'Onofrio [ID92](#), J. Dopke [ID136](#), A. Doria [ID72a](#), M.T. Dova [ID90](#), A.T. Doyle [ID59](#), E. Drechsler [ID145](#),
 E. Dreyer [ID145](#), T. Dreyer [ID55](#), A.S. Drobac [ID162](#), D. Du [ID62b](#), Y. Duan [ID62b](#), F. Dubinin [ID37](#),
 M. Dubovsky [ID28a](#), A. Dubreuil [ID56](#), E. Duchovni [ID172](#), G. Duckeck [ID110](#), A. Ducourthial [ID129](#),
 O.A. Ducu [ID109](#), D. Duda [ID111](#), A. Dudarev [ID36](#), A.C. Dudder [ID101](#), E.M. Duffield^{18a}, L. Duflot [ID67](#),
 M. Dührssen [ID36](#), C. Dülsen [ID174](#), M. Dumancic [ID172](#), A.E. Dumitriu [ID27b](#), A.K. Duncan [ID59](#),
 M. Dunford [ID63a](#), A. Duperrin [ID103](#), H. Duran Yildiz [ID4a](#), M. Düren [ID58](#), A. Durglishvili [ID152b](#),
 D. Duschinger⁵⁰, B. Dutta [ID48](#), B.L. Dwyer [ID117](#), G.I. Dyckes [ID130](#), M. Dyndal [ID36](#), S. Dysch [ID102](#),
 B.S. Dziedzic [ID86](#), K.M. Ecker¹¹¹, M.G. Eggleston⁵¹, T. Eifert [ID8](#), G. Eigen [ID17](#), K. Einsweiler [ID18a](#),
 T. Ekelof [ID164](#), H. El Jarrari [ID35e](#), R. El Kosseifi¹⁰³, V. Ellajosyula [ID164](#), M. Ellert [ID164](#),
 F. Ellinghaus [ID174](#), A.A. Elliot [ID94](#), N. Ellis [ID36](#), J. Elmsheuser [ID29](#), M. Elsing [ID36](#), D. Emeliyanov [ID136](#),
 A. Emerman [ID41](#), Y. Enari [ID156](#), M.B. Epland [ID51](#), J. Erdmann [ID49](#), A. Ereditato [ID20](#), P.A. Erland [ID86](#),
 M. Errenst [ID36](#), M. Escalier [ID67](#), C. Escobar [ID166](#), O. Estrada Pastor [ID166](#), E. Etzion [ID154](#), H. Evans [ID68](#),
 A. Ezhilov [ID37](#), F. Fabbri [ID59](#), L. Fabbri [ID23b,23a](#), V. Fabiani [ID115](#), G. Facini [ID170](#),

R.M. Faisca Rodrigues Pereira [ID132a](#), R.M. Fakhruddinov [ID37](#), S. Falciano [ID75a](#), P.J. Falke [ID5](#), S. Falke [ID5](#), J. Faltova [ID135](#), Y. Fang [ID15a](#), Y. Fang [ID15a,15d](#), G. Fanourakis [ID46](#), M. Fanti [ID71a,71b](#), M. Faraj [ID69a,69c,s](#), A. Farbin [ID8](#), A. Farilla [ID77a](#), E.M. Farina [ID73a,73b](#), T. Farooque [ID108](#), S.M. Farrington [ID52](#), P. Farthouat [ID36](#), F. Fassi [ID35e](#), P. Fassnacht [ID36](#), D. Fassouliotis [ID9](#), M. Faucci Giannelli [ID52](#), W.J. Fawcett [ID32](#), L. Fayard [ID67](#), O.L. Fedin [ID37,a](#), W. Fedorko [ID167](#), M. Feickert [ID165](#), L. Feligioni [ID103](#), A. Fell [ID142](#), C. Feng [ID62b](#), M. Feng [ID51](#), M.J. Fenton [ID163](#), A.B. Fenyuk [ID37](#), S.W. Ferguson [ID45](#), J. Ferrando [ID48](#), A. Ferrante [ID165](#), A. Ferrari [ID164](#), P. Ferrari [ID116](#), R. Ferrari [ID73a](#), D.E. Ferreira de Lima [ID63b](#), A. Ferrer [ID166](#), D. Ferrere [ID56](#), C. Ferretti [ID107](#), F. Fiedler [ID101](#), A. Filipčič [ID93](#), F. Filthaut [ID115](#), K.D. Finelli [ID25](#), M.C.N. Fiolhais [ID132a,132c,b](#), L. Fiorini [ID166](#), F. Fischer [ID110](#), W.C. Fisher [ID108](#), I. Fleck [ID144](#), P. Fleischmann [ID107](#), T. Flick [ID174](#), B.M. Flierl [ID110](#), L. Flores [ID130](#), L.R. Flores Castillo [ID65a](#), F.M. Follega [ID78a,78b](#), N. Fomin [ID17](#), J.H. Foo [ID159](#), G.T. Forcolin [ID78a,78b](#), A. Formica [ID137](#), F.A. Förster [ID14](#), A.C. Forti [ID102](#), A.G. Foster [ID21](#), M.G. Foti [ID128](#), D. Fournier [ID67](#), H. Fox [ID91](#), P. Francavilla [ID74a,74b](#), S. Francescato [ID75a,75b](#), M. Franchini [ID23b,23a](#), S. Franchino [ID63a](#), D. Francis [ID36](#), L. Franconi [ID20](#), M. Franklin [ID61](#), A.N. Fray [ID94](#), P.M. Freeman [ID21](#), B. Freund [ID109](#), W.S. Freund [ID82b](#), E.M. Freundlich [ID49](#), D.C. Frizzell [ID122](#), D. Froidevaux [ID36](#), J.A. Frost [ID128](#), C. Fukunaga [ID157](#), E. Fullana Torregrosa [ID166,*](#), T. Fusayasu [ID112](#), J. Fuster [ID166](#), A. Gabrielli [ID23b,23a](#), A. Gabrielli [ID18a](#), S. Gadatsch [ID56](#), P. Gadow [ID111](#), G. Gagliardi [ID57b,57a](#), L.G. Gagnon [ID109](#), B. Galhardo [ID132a](#), G.E. Gallardo [ID128](#), E.J. Gallas [ID128](#), B.J. Gallop [ID136](#), G. Galster [ID42](#), R. Gamboa Goni [ID94](#), K.K. Gan [ID120](#), S. Ganguly [ID172](#), J. Gao [ID62a](#), Y. Gao [ID52](#), Y.S. Gao [ID31,m](#), C. García [ID166](#), J.E. García Navarro [ID166](#), J.A. García Pascual [ID15a](#), C. Garcia-Argos [ID54](#), M. Garcia-Sciveres [ID18a](#), R.W. Gardner [ID39](#), S. Gargiulo [ID54](#), C.A. Garner [ID159](#), V. Garonne [ID127](#), S.J. Gasiorowski [ID141](#), P. Gaspar [ID82b](#), A. Gaudiello [ID57b,57a](#), G. Gaudio [ID73a](#), I.L. Gavrilenko [ID37](#), A. Gavriilyuk [ID37](#), C. Gay [ID167](#), G. Gaycken [ID48](#), E.N. Gazis [ID10](#), A.A. Geanta [ID27b](#), C.M. Gee [ID138](#), C.N.P. Gee [ID136](#), J. Geisen [ID98](#), M. Geisen [ID101](#), C. Gemme [ID57b](#), M.H. Genest [ID60](#), C. Geng [ID107](#), S. Gentile [ID75a,75b](#), S. George [ID95](#), T. Gerialis [ID46](#), L.O. Gerlach [ID55](#), P. Gessinger-Befurt [ID101](#), G. Gessner [ID49](#), S. Ghasemi [ID144](#), M. Ghasemi Bostanabad [ID168](#), M. Ghneimat [ID144](#), A. Ghosh [ID67](#), A. Ghosh [ID80](#), B. Giacobbe [ID23b](#), S. Giagu [ID75a,75b](#), N. Giangiacomi [ID23b,23a](#), P. Giannetti [ID74a](#), A. Giannini [ID72a,72b](#), G. Giannini [ID14](#), S.M. Gibson [ID95](#), M. Gignac [ID138](#), D. Gillberg [ID34](#), G. Gilles [ID174](#), D.M. Gingrich [ID3,ao](#), M.P. Giordani [ID69a,69c](#), P.F. Giraud [ID137](#), G. Giugliarelli [ID69a,69c](#), D. Giugni [ID71a](#), F. Giuli [ID76a,76b](#), S. Gkaitatzis [ID155](#), I. Gkialas [ID9,h](#), E.L. Gkougkousis [ID14](#), P. Gkoutoumis [ID10](#), L.K. Gladilin [ID37](#), C. Glasman [ID100](#), J. Glatzer [ID14](#), P.C.F. Glaysher [ID48](#), A. Glazov [ID48](#), G.R. Gledhill [ID125](#), M. Goblirsch-Kolb [ID26](#), D. Godin [ID109](#), S. Goldfarb [ID106](#), T. Golling [ID56](#), D. Golubkov [ID37](#), A. Gomes [ID132a,132b](#), R. Goncalves Gama [ID55](#), R. Gonçalves [ID132a](#), G. Gonella [ID125](#), L. Gonella [ID21](#), A. Gongadze [ID38](#), F. Gonnella [ID21](#), J.L. Gonski [ID41](#), S. González de la Hoz [ID166](#), S. Gonzalez Fernandez [ID14](#), S. Gonzalez-Sevilla [ID56](#), G.R. Gonzalvo Rodriguez [ID166](#), L. Goossens [ID36](#), N.A. Gorasia [ID21](#), P.A. Gorbounov [ID37](#), B. Gorini [ID36](#), E. Gorini [ID70a,70b](#), A. Gorišek [ID93](#), A.T. Goshaw [ID51](#), M.I. Gostkin [ID38](#), C.A. Gottardo [ID115](#), M. Gouighri [ID35b](#), A.G. Goussiou [ID141](#), N. Govender [ID33b](#), C. Goy [ID5](#), E. Gozani [ID153](#), I. Grabowska-Bold [ID85a](#), E.C. Graham [ID92](#), J. Gramling [ID163](#), E. Gramstad [ID127](#), S. Grancagnolo [ID19](#), M. Grandi [ID149](#), V. Gratchev [ID37,*](#), P.M. Gravila [ID27f](#), F.G. Gravili [ID70a,70b](#), C. Gray [ID59](#), H.M. Gray [ID18a](#), C. Grefe [ID24](#), K. Gregersen [ID98](#), I.M. Gregor [ID48](#), P. Grenier [ID146](#), K. Grevtsov [ID48](#), C. Grieco [ID14](#), N.A. Grieser [ID122](#), A.A. Grillo [ID138](#), K. Grimm [ID31,1](#), S. Grinstein [ID14,x](#), J.-F. Grivaz [ID67](#), S. Groh [ID101](#), E. Gross [ID172](#), J. Grosse-Knetter [ID55](#), Z.J. Grout [ID96](#), C. Grud [ID107](#), A. Grummer [ID114](#), L. Guan [ID107](#), W. Guan [ID173](#), C. Gubbels [ID167](#), J. Guenther [ID36](#), A. Guerguichon [ID67](#), J.G.R. Guerrero Rojas [ID166](#), F. Guescini [ID111](#), R. Gugel [ID54](#), T. Guillemain [ID5](#), S. Guindon [ID36](#), U. Gul [ID59](#), J. Guo [ID62c](#), W. Guo [ID107](#), Y. Guo [ID62a](#), Z. Guo [ID103](#), R. Gupta [ID48](#), S. Gurbuz [ID12c](#), G. Gustavino [ID122](#), M. Guth [ID54](#), P. Gutierrez [ID122](#), C. Gutschow [ID96](#), C. Guyot [ID137](#), C. Gwenlan [ID128](#), C.B. Gwilliam [ID92](#), A. Haas [ID118](#), C. Haber [ID18a](#), H.K. Hadavand [ID8](#), A. Hadeef [ID62a](#),

M. Haleem ¹⁶⁹, J. Haley ¹²³, G. Halladjian ¹⁰⁸, G.D. Hallelwell ¹⁰³, K. Hamacher ¹⁷⁴,
P. Hamal ¹²⁴, K. Hamano ¹⁶⁸, H. Hamdaoui ^{35e}, M. Hamer ²⁴, G.N. Hamity ⁵², K. Han ^{62a,v},
L. Han ^{62a}, S. Han ^{15a}, Y.F. Han ¹⁵⁹, K. Hanagaki ⁸³, M. Hance ¹³⁸, D.M. Handl ¹¹⁰,
B. Haney ¹³⁰, R. Hankache ¹²⁹, E. Hansen ⁹⁸, J.B. Hansen ⁴², J.D. Hansen ⁴², M.C. Hansen ²⁴,
P.H. Hansen ⁴², E.C. Hanson ¹⁰², K. Hara ¹⁶¹, T. Harenberg ¹⁷⁴, S. Harkusha ³⁷, P.F. Harrison ¹⁷⁰,
N.M. Hartmann ¹¹⁰, Y. Hasegawa ¹⁴³, A. Hasib ⁵², S. Hassani ¹³⁷, S. Haug ²⁰, R. Hauser ¹⁰⁸,
L.B. Havener ⁴¹, M. Havranek ¹³⁴, C.M. Hawkes ²¹, R.J. Hawkings ³⁶, D. Hayden ¹⁰⁸,
C. Hayes ¹⁰⁷, R.L. Hayes ¹⁶⁷, C.P. Hays ¹²⁸, J.M. Hays ⁹⁴, H.S. Hayward ⁹², S.J. Haywood ¹³⁶,
F. He ^{62a}, M.P. Heath ⁵², V. Hedberg ⁹⁸, S. Heer ²⁴, K.K. Heidegger ⁵⁴, W.D. Heidorn ⁸¹,
J. Heilman ³⁴, S. Heim ⁴⁸, T. Heim ^{18a}, B. Heinemann ^{48,al}, J.J. Heinrich ¹²⁵, L. Heinrich ³⁶,
J. Hejbal ¹³³, L. Helary ^{63b}, A. Held ¹¹⁸, S. Hellesund ¹²⁷, C.M. Helling ¹³⁸, S. Hellman ^{47a,47b},
C. Helsen ³⁶, R.C.W. Henderson ⁹¹, Y. Heng ¹⁷³, L. Henkelmann ^{63a}, S. Henkelmann ¹⁶⁷,
A.M. Henriques Correia ³⁶, H. Herde ²⁶, V. Herget ¹⁶⁹, Y. Hernández Jiménez ^{33d}, H. Herr ¹⁰¹,
M.G. Herrmann ¹¹⁰, T. Herrmann ⁵⁰, G. Herten ⁵⁴, R. Hertenberger ¹¹⁰, L. Hervas ³⁶,
T.C. Herwig ¹³⁰, G.G. Hesketh ⁹⁶, N.P. Hessey ^{160a}, A. Higashida ¹⁵⁶, S. Higashino ⁸³,
E. Higón-Rodríguez ¹⁶⁶, K. Hildebrand ³⁹, J.C. Hill ³², K.K. Hill ²⁹, K.H. Hiller ⁴⁸, S.J. Hillier ²¹,
M. Hils ⁵⁰, I. Hinchliffe ^{18a}, F. Hinterkeuser ²⁴, M. Hirose ¹²⁶, S. Hirose ⁵⁴, D. Hirschbuehl ¹⁷⁴,
B. Hiti ⁹³, O. Hladik ¹³³, D.R. Hlaluku ^{33d}, X. Hoad ⁵², J. Hobbs ¹⁴⁸, N. Hod ¹⁷²,
M.C. Hodgkinson ¹⁴², A. Hoecker ³⁶, D. Hohn ⁵⁴, D. Hohov ⁶⁷, T. Holm ²⁴, T.R. Holmes ³⁹,
M. Holzbock ¹¹⁰, L.B.A.H. Hommels ³², S. Honda ¹⁶¹, T.M. Hong ¹³¹, J.C. Honig ⁵⁴,
A. Hönlle ¹¹¹, B.H. Hooberman ¹⁶⁵, W.H. Hopkins ⁶, Y. Horii ¹¹³, P. Horn ⁵⁰, L.A. Horyn ³⁹,
S. Hou ¹⁵¹, A. Houmada ^{35a}, J. Howarth ¹⁰², J. Hoya ⁹⁰, M. Hrabovsky ¹²⁴, J. Hrdinka ⁷⁹,
I. Hristova ¹⁹, J. Hrivnac ⁶⁷, A. Hrynevich ³⁷, T. Hryn'ova ⁵, P.J. Hsu ⁶⁶, S.-C. Hsu ¹⁴¹, Q. Hu ²⁹,
S. Hu ^{62c}, Y.F. Hu ^{15a,15d}, D.P. Huang ⁹⁶, Y. Huang ^{62a}, Y. Huang ^{15a}, Z. Hubacek ¹³⁴,
F. Hubaut ¹⁰³, M. Huebner ²⁴, F. Huegging ²⁴, T.B. Huffman ¹²⁸, M. Huhtinen ³⁶,
R.F.H. Hunter ³⁴, P. Huo ¹⁴⁸, N. Huseynov ^{38,ad}, J. Huston ¹⁰⁸, J. Huth ⁶¹, R. Hyneman ¹⁰⁷,
S. Hyrych ^{28a}, G. Iacobucci ⁵⁶, G. Iakovidis ²⁹, I. Ibragimov ¹⁴⁴, L. Iconomidou-Fayard ⁶⁷,
P. Iengo ³⁶, R. Ignazzi ⁴², O. Igonkina ^{116,z,*}, R. Iguchi ¹⁵⁶, T. Iizawa ⁵⁶, Y. Ikegami ⁸³,
M. Ikeno ⁸³, A. Ilg ²⁰, N. Ilic ^{115,159,ac}, F. Iltzsche ⁵⁰, G. Introzzi ^{73a,73b}, M. Iodice ^{77a},
K. Iordanidou ^{160a}, V. Ippolito ^{75a,75b}, M.F. Isacson ¹⁶⁴, M. Ishino ¹⁵⁶, W. Islam ¹²³,
C. Issever ^{19,48}, S. Istin ¹⁵³, F. Ito ¹⁶¹, J.M. Iturbe Ponce ^{65a}, R. Iuppa ^{78a,78b}, A. Ivina ¹⁷²,
H. Iwasaki ⁸³, J.M. Izen ⁴⁵, V. Izzo ^{72a}, P. Jacka ¹³³, P. Jackson ¹, R.M. Jacobs ²⁴,
B.P. Jaeger ¹⁴⁵, V. Jain ², G. Jäkel ¹⁷⁴, K.B. Jakobi ¹⁰¹, K. Jakobs ⁵⁴, T. Jakoubek ¹³³,
J. Jamieson ⁵⁹, K.W. Janas ^{85a}, R. Jansky ⁵⁶, M. Janus ⁵⁵, P.A. Janus ^{85a}, G. Jarlskog ⁹⁸,
N. Javadov ^{38,ad}, T. Javůrek ³⁶, M. Javurkova ¹⁰⁴, F. Jeanneau ¹³⁷, L. Jeanty ¹²⁵, J. Jejelava ^{152a,ae},
A. Jelinskas ¹⁷⁰, P. Jenni ^{54,c}, N. Jeong ⁴⁸, S. Jézéquel ⁵, H. Ji ¹⁷³, J. Jia ¹⁴⁸, H. Jiang ⁸¹, Y. Jiang ^{62a},
Z. Jiang ^{146,p}, S. Jiggins ⁵⁴, F.A. Jimenez Morales ⁴⁰, J. Jimenez Pena ¹¹¹, S. Jin ^{15c}, A. Jinaru ^{27b},
O. Jinnouchi ¹⁵⁸, H. Jivan ^{33d}, P. Johansson ¹⁴², K.A. Johns ⁷, C.A. Johnson ⁶⁸,
R.W.L. Jones ⁹¹, S.D. Jones ¹⁴⁹, S. Jones ⁷, T.J. Jones ⁹², J. Jongmanns ^{63a}, P.M. Jorge ^{132a},
J. Jovicevic ³⁶, X. Ju ^{18a}, J.J. Junggeburth ¹¹¹, A. Juste Rozas ^{14,x}, A. Kaczmarska ⁸⁶,
M. Kado ^{75a,75b}, H. Kagan ¹²⁰, M. Kagan ¹⁴⁶, A. Kahn ⁴¹, C. Kahra ¹⁰¹, T. Kaji ¹⁷¹,
E. Kajomovitz ¹⁵³, C.W. Kalderon ²⁹, A. Kaluza ¹⁰¹, A. Kamenshchikov ³⁷, M. Kaneda ¹⁵⁶,
N.J. Kang ¹³⁸, S. Kang ⁸¹, L. Kanjir ⁹³, Y. Kano ¹¹³, V.A. Kantserov ³⁷, J. Kanzaki ⁸³,
L.S. Kaplan ¹⁷³, D. Kar ^{33d}, K. Karava ¹²⁸, M.J. Kareem ^{160b}, S.N. Karpov ³⁸, Z.M. Karpova ³⁸,
V. Kartvelishvili ⁹¹, A.N. Karyukhin ³⁷, L. Kashif ¹⁷³, A. Kastanas ^{47a,47b}, C. Kato ^{62d,62c},
J. Katzy ⁴⁸, K. Kawade ¹⁴³, K. Kawagoe ⁸⁹, T. Kawaguchi ¹¹³, T. Kawamoto ¹³⁷, G. Kawamura ⁵⁵,
E.F. Kay ¹⁶⁸, V.F. Kazanin ³⁷, R. Keeler ¹⁶⁸, R. Kehoe ⁴⁴, J.S. Keller ³⁴, E. Kellermann ⁹⁸,

D. Kelsey ¹⁴⁹, J.J. Kempster ²¹, J. Kendrick ²¹, K.E. Kennedy ⁴¹, O. Kepka ¹³³, S. Kersten ¹⁷⁴,
 B.P. Kerševan ⁹³, S. Ketabchi Haghighat ¹⁵⁹, M. Khader ¹⁶⁵, F. Khalil-Zada ¹³, M. Khandoga ¹³⁷,
 A. Khanov ¹²³, A.G. Kharlamov ³⁷, T. Kharlamova ³⁷, E.E. Khoda ¹⁶⁷, A. Khodinov ³⁷,
 T.J. Khoo ⁵⁶, J. Khubua ^{152b}, S. Kido ⁸⁴, M. Kiehn ⁵⁶, C.R. Kilby ⁹⁵, E. Kim ¹⁵⁸, Y.K. Kim ³⁹,
 N. Kimura ⁹⁶, O.M. Kind ¹⁹, B.T. King ^{92,*}, D. Kirchmeier ⁵⁰, J. Kirk ¹³⁶, A.E. Kiryunin ¹¹¹,
 T. Kishimoto ¹⁵⁶, D.P. Kisliuk ¹⁵⁹, V. Kitali ⁴⁸, O. Kivernyk ⁵, T. Klapdor-Kleingrothaus ⁵⁴,
 M. Klassen ^{63a}, C. Klein ³², M.H. Klein ¹⁰⁷, M. Klein ⁹², U. Klein ⁹², K. Kleinknecht ¹⁰¹,
 P. Klimek ¹¹⁷, A. Klimentov ²⁹, T. Klingl ²⁴, T. Klioutchnikova ³⁶, F.F. Klitzner ¹¹⁰,
 P. Kluit ¹¹⁶, S. Kluth ¹¹¹, E. Kneringer ⁷⁹, E.B.F.G. Knoops ¹⁰³, A. Knue ⁵⁴, D. Kobayashi ⁸⁹,
 T. Kobayashi ¹⁵⁶, M. Kobel ⁵⁰, M. Kocian ¹⁴⁶, T. Kodama ¹⁵⁶, P. Kodyš ¹³⁵, P.T. Koenig ²⁴,
 T. Koffas ³⁴, N.M. Köhler ³⁶, M. Kolb ¹³⁷, I. Koletsou ⁵, T. Komarek ¹²⁴, T. Kondo ⁸³,
 K. Köneke ⁵⁴, A.X.Y. Kong ¹, A.C. König ¹¹⁵, T. Kono ¹¹⁹, R. Konoplich ^{118,ai},
 V. Konstantinides ⁹⁶, N. Konstantinidis ⁹⁶, B. Konya ⁹⁸, R. Kopeliansky ⁶⁸, S. Koperny ^{85a},
 K. Korcyl ⁸⁶, K. Kordas ¹⁵⁵, G. Koren ¹⁵⁴, A. Korn ⁹⁶, I. Korolkov ¹⁴, E.V. Korolkova ¹⁴²,
 N. Korotkova ³⁷, O. Kortner ¹¹¹, S. Kortner ¹¹¹, T. Kosek ¹³⁵, V.V. Kostyukhin ^{142,37},
 A. Kotsokechagia ⁶⁷, A. Kotwal ⁵¹, A. Koulouris ¹⁰, A. Kourkoumeli-Charalampidi ^{73a,73b},
 C. Kourkoumelis ⁹, E. Kourlitis ¹⁴², V. Kouskoura ²⁹, A.B. Kowalewska ⁸⁶, R. Kowalewski ¹⁶⁸,
 W. Kozanecki ¹⁰², A.S. Kozhin ³⁷, V.A. Kramarenko ³⁷, G. Kramberger ⁹³, D. Krasnopevtsev ^{62a},
 M.W. Krasny ¹²⁹, A. Krasznahorkay ³⁶, D. Krauss ¹¹¹, J.A. Kremer ^{85a}, J. Kretzschmar ⁹²,
 P. Krieger ¹⁵⁹, F. Krieter ¹¹⁰, A. Krishnan ^{63b}, K. Krizka ^{18a}, K. Kroeninger ⁴⁹, H. Kroha ¹¹¹,
 J. Kroll ¹³³, J. Kroll ¹³⁰, K.S. Krowpman ¹⁰⁸, U. Kruchonak ³⁸, H. Krüger ²⁴, N. Krumnack ⁸¹,
 M.C. Kruse ⁵¹, J.A. Krzysiak ⁸⁶, T. Kubota ¹⁰⁶, O. Kuchinskaia ³⁷, S. Kuday ^{4b}, D. Kuechler ⁴⁸,
 J.T. Kuechler ⁴⁸, S. Kuehn ³⁶, A. Kugel ^{63a}, T. Kuhl ⁴⁸, V. Kukhtin ³⁸, R. Kukla ¹⁰³,
 Y. Kulchitsky ^{37,a}, S. Kuleshov ^{139c}, Y.P. Kulinich ¹⁶⁵, M. Kuna ⁶⁰, T. Kunigo ⁸⁷, A. Kupco ¹³³,
 T. Kupfer ⁴⁹, O. Kuprash ⁵⁴, H. Kurashige ⁸⁴, L.L. Kurchaninov ^{160a}, Y.A. Kurochkin ³⁷,
 A. Kurova ³⁷, M.G. Kurth ^{15a,15d}, E.S. Kuwertz ³⁶, M. Kuze ¹⁵⁸, A.K. Kvam ¹⁴¹, J. Kviita ¹²⁴,
 T. Kwan ¹⁰⁵, L. La Rotonda ^{43b,43a}, F. La Ruffa ^{43b,43a}, C. Lacasta ¹⁶⁶, F. Lacava ^{75a,75b},
 D.P.J. Lack ¹⁰², H. Lacker ¹⁹, D. Lacour ¹²⁹, E. Ladygin ³⁸, R. Lafaye ⁵, B. Laforge ¹²⁹,
 T. Lagouri ^{139b}, S. Lai ⁵⁵, I.K. Lakomic ^{85a}, S. Lammers ⁶⁸, W. Lampl ⁷, C. Lampoudis ¹⁵⁵,
 E. Lançon ²⁹, U. Landgraf ⁵⁴, M.P.J. Landon ⁹⁴, M.C. Lanfermann ⁵⁶, V.S. Lang ⁴⁸,
 J.C. Lange ⁵⁵, R.J. Langenberg ¹⁰⁴, A.J. Lankford ¹⁶³, F. Lanni ²⁹, K. Lantzsch ²⁴, A. Lanza ^{73a},
 A. Lapertosa ^{57b,57a}, S. Laplace ¹²⁹, J.F. Laporte ¹³⁷, T. Lari ^{71a}, F. Lasagni Manghi ^{23b},
 M. Lassnig ³⁶, T.S. Lau ^{65a}, A. Laudrain ⁶⁷, A. Laurier ³⁴, M. Lavorgna ^{72a,72b}, S.D. Lawlor ⁹⁵,
 M. Lazzaroni ^{71a,71b}, B. Le ¹⁰⁶, E. Le Guirriec ¹⁰³, A. Lebedev ⁸¹, M. LeBlanc ⁷, T. LeCompte ⁶,
 F. Ledroit-Guillon ⁶⁰, A.C.A. Lee ⁹⁶, C.A. Lee ²⁹, G.R. Lee ¹⁷, L. Lee ⁶¹, S.C. Lee ¹⁵¹,
 S. Lee ⁸¹, B. Lefebvre ^{160a}, H.P. Lefebvre ⁹⁵, M. Lefebvre ¹⁶⁸, C. Leggett ^{18a}, K. Lehmann ¹⁴⁵,
 N. Lehmann ¹⁷⁴, G. Lehmann Miotto ³⁶, W.A. Leight ⁴⁸, A. Leisos ^{155,u}, M.A.L. Leite ^{82c},
 C.E. Leitgeb ¹¹⁰, R. Leitner ¹³⁵, D. Lellouch ^{172,*}, K.J.C. Leney ⁴⁴, T. Lenz ²⁴, R. Leone ⁷,
 S. Leone ^{74a}, C. Leonidopoulos ⁵², A. Leopold ¹²⁹, C. Leroy ¹⁰⁹, R. Les ¹⁵⁹, C.G. Lester ³²,
 M. Levchenko ³⁷, J. Levêque ⁵, D. Levin ¹⁰⁷, L.J. Levinson ¹⁷², D.J. Lewis ²¹, B. Li ^{15b},
 B. Li ¹⁰⁷, C-Q. Li ^{62a}, F. Li ^{62c}, H. Li ^{62a}, H. Li ^{62b}, J. Li ^{62c}, K. Li ¹⁴¹, L. Li ^{62c},
 M. Li ^{15a,15d}, Q. Li ^{15a,15d}, Q.Y. Li ^{62a}, S. Li ^{62d,62c}, X. Li ⁴⁸, Y. Li ⁴⁸, Z. Li ^{62b}, Z. Li ¹⁰⁵,
 Z. Liang ^{15a}, B. Liberti ^{76a}, A. Liblong ¹⁵⁹, K. Lie ^{65c}, S. Lim ²⁹, C.Y. Lin ³², K. Lin ¹⁰⁸,
 T.H. Lin ¹⁰¹, R.A. Linck ⁶⁸, J.H. Lindon ²¹, A.L. Lioni ⁵⁶, E. Lipeles ¹³⁰, A. Lipniacka ¹⁷,
 T.M. Liss ^{165,am}, A. Lister ¹⁶⁷, J.D. Little ⁸, B. Liu ⁸¹, B.X. Liu ⁶, H.B. Liu ²⁹, H. Liu ¹⁰⁷,
 J.B. Liu ^{62a}, J.K.K. Liu ³⁹, K. Liu ^{62d,62c}, M. Liu ^{62a}, P. Liu ^{15a}, Y. Liu ⁴⁸, Y. Liu ^{15a,15d},
 Y.L. Liu ¹⁰⁷, Y.W. Liu ^{62a}, M. Livan ^{73a,73b}, A. Lleres ⁶⁰, J. Llorente Merino ¹⁴⁵, S.L. Lloyd ⁹⁴,

C.Y. Lo ^{65b}, E.M. Lobodzinska ⁴⁸, P. Loch ⁷, S. Loffredo ^{76a,76b}, T. Lohse ¹⁹, K. Lohwasser ¹⁴²,
 M. Lokajicek ^{133,*}, J.D. Long ¹⁶⁵, R.E. Long ⁹¹, L. Longo ³⁶, K.A. Looper ¹²⁰, J.A. Lopez ^{139c},
 I. Lopez Paz ¹⁰², A. Lopez Solis ¹⁴², J. Lorenz ¹¹⁰, N. Lorenzo Martinez ⁵, A.M. Lory ¹¹⁰,
 P.J. Lösel ¹¹⁰, A. Lösle ⁵⁴, X. Lou ⁴⁸, X. Lou ^{15a,15d}, A. Lounis ⁶⁷, J. Love ⁶, P.A. Love ⁹¹,
 J.J. Lozano Bahilo ¹⁶⁶, M. Lu ^{62a}, Y.J. Lu ⁶⁶, H.J. Lubatti ¹⁴¹, C. Luci ^{75a,75b}, A. Lucotte ⁶⁰,
 C. Luedtke ⁵⁴, F. Luehring ⁶⁸, I. Luise ¹²⁹, L. Luminari ^{75a}, B. Lund-Jensen ¹⁴⁷, M.S. Lutz ¹⁰⁴,
 D. Lynn ²⁹, H. Lyons ⁹², R. Lysak ¹³³, E. Lytken ⁹⁸, F. Lyu ^{15a}, V. Lyubushkin ³⁸,
 T. Lyubushkina ³⁸, H. Ma ²⁹, L.L. Ma ^{62b}, Y. Ma ^{62b}, G. Maccarrone ⁵³, A. Macchiolo ¹¹¹,
 C.M. Macdonald ¹⁴², J. Machado Miguens ¹³⁰, D. Madaffari ¹⁶⁶, R. Madar ⁴⁰, W.F. Mader ⁵⁰,
 M. Madugoda Ralalage Don ¹²³, N. Madysa ⁵⁰, J. Maeda ⁸⁴, T. Maeno ²⁹, M. Maerker ⁵⁰,
 V. Magerl ⁵⁴, N. Magini ⁸¹, D.J. Mahon ⁴¹, C. Maidantchik ^{82b}, T. Maier ¹¹⁰, A. Maio ^{132a,132b,132d},
 K. Maj ^{85a}, O. Majersky ^{28a}, S. Majewski ¹²⁵, Y. Makida ⁸³, N. Makovec ⁶⁷, B. Malaescu ¹²⁹,
 Pa. Malecki ⁸⁶, V.P. Maleev ³⁷, F. Malek ⁶⁰, U. Mallik ⁸⁰, D. Malon ⁶, C. Malone ³²,
 S. Maltezos ¹⁰, S. Malyukov ³⁸, J. Mamuzic ¹⁶⁶, G. Mancini ⁵³, I. Mandić ⁹³,
 L. Manhaes de Andrade Filho ^{82a}, I.M. Maniatis ¹⁵⁵, J. Manjarres Ramos ⁵⁰, K.H. Mankinen ⁹⁸,
 A. Mann ¹¹⁰, A. Manousos ⁷⁹, B. Mansoulie ¹³⁷, I. Manthos ¹⁵⁵, S. Manzoni ¹¹⁶,
 A. Marantis ^{155,u}, G. Marceca ³⁰, L. Marchese ¹²⁸, G. Marchiori ¹²⁹, M. Marcisovsky ¹³³,
 L. Marcoccia ^{76a,76b}, C. Marcon ⁹⁸, C.A. Marin Tobon ³⁶, M. Marjanovic ¹²², Z. Marshall ^{18a},
 M.U.F. Martensson ¹⁶⁴, S. Marti-Garcia ¹⁶⁶, C.B. Martin ¹²⁰, T.A. Martin ¹⁷⁰, V.J. Martin ⁵²,
 B. Martin dit Latour ¹⁷, L. Martinelli ^{77a,77b}, M. Martinez ^{14,x}, V.I. Martinez Outschoorn ¹⁰⁴,
 S. Martin-Haugh ¹³⁶, V.S. Martoiu ^{27b}, A.C. Martyniuk ⁹⁶, A. Marzin ³⁶, S.R. Maschek ¹¹¹,
 L. Masetti ¹⁰¹, T. Mashimo ¹⁵⁶, R. Mashinistov ³⁷, J. Masik ¹⁰², A.L. Maslennikov ³⁷,
 L. Massa ^{23b}, P. Massarotti ^{72a,72b}, P. Mastrandrea ^{74a,74b}, A. Mastroberardino ^{43b,43a},
 T. Masubuchi ¹⁵⁶, D. Matakias ²⁹, A. Matic ¹¹⁰, N. Matsuzawa ¹⁵⁶, P. Mättig ²⁴, J. Maurer ^{27b},
 B. Maček ⁹³, D.A. Maximov ³⁷, R. Mazini ¹⁵¹, I. Maznas ¹⁵⁵, S.M. Mazza ¹³⁸, S.P. Mc Kee ¹⁰⁷,
 T.G. McCarthy ¹¹¹, W.P. McCormack ^{18a}, E.F. McDonald ¹⁰⁶, J.A. Mcfayden ³⁶,
 G. Mchedlidze ^{152b}, M.A. McKay ⁴⁴, K.D. McLean ¹⁶⁸, S.J. McMahon ¹³⁶, P.C. McNamara ¹⁰⁶,
 C.J. McNicol ¹⁷⁰, R.A. McPherson ^{168,ac}, J.E. Mdhului ^{33d}, Z.A. Meadows ¹⁰⁴, S. Meehan ³⁶,
 T. Megy ⁵⁴, S. Mehlhase ¹¹⁰, A. Mehta ⁹², T. Meideck ⁶⁰, B. Meirose ⁴⁵, D. Melini ¹⁵³,
 B.R. Mellado Garcia ^{33d}, J.D. Mellenthin ⁵⁵, M. Melo ^{28a}, F. Meloni ⁴⁸, A. Melzer ²⁴,
 S.B. Menary ¹⁰², E.D. Mendes Gouveia ^{132a,132e}, L. Meng ³⁶, X.T. Meng ¹⁰⁷, S. Menke ¹¹¹,
 E. Meoni ^{43b,43a}, S. Mergelmeyer ¹⁹, S.A.M. Merkt ¹³¹, C. Merlassino ¹²⁸, P. Mermod ^{56,*},
 L. Merola ^{72a,72b}, C. Meroni ^{71a}, G. Merz ¹⁰⁷, O. Meshkov ³⁷, J.K.R. Meshreki ¹⁴⁴,
 A. Messina ^{75a,75b}, J. Metcalfe ⁶, A.S. Mete ⁶, C. Meyer ⁶⁸, J-P. Meyer ¹³⁷,
 H. Meyer Zu Theenhausen ^{63a}, F. Miano ¹⁴⁹, M. Michetti ¹⁹, R.P. Middleton ¹³⁶, L. Mijović ⁵²,
 G. Mikenberg ¹⁷², M. Mikestikova ¹³³, M. Mikuz ⁹³, H. Mildner ¹⁴², M. Milesi ¹⁰⁶,
 A. Milic ¹⁵⁹, D.A. Millar ⁹⁴, D.W. Miller ³⁹, A. Milov ¹⁷², D.A. Milstead ^{47a,47b}, R.A. Mina ¹⁴⁶,
 A.A. Minaenko ³⁷, M. Miñano Moya ¹⁶⁶, I.A. Minashvili ^{152b}, A.I. Mincer ¹¹⁸, B. Mindur ^{85a},
 M. Mineev ³⁸, Y. Minegishi ¹⁵⁶, L.M. Mir ¹⁴, A. Mirto ^{70a,70b}, K.P. Mistry ¹³⁰, T. Mitani ¹⁷¹,
 J. Mitrevski ¹¹⁰, V.A. Mitsou ¹⁶⁶, M. Mittal ^{62c}, O. Miu ¹⁵⁹, A. Miucci ²⁰, P.S. Miyagawa ¹⁴²,
 A. Mizukami ⁸³, J.U. Mjörnmark ⁹⁸, T. Mkrtchyan ^{63a}, M. Mlynarikova ¹³⁵, T. Moa ^{47a,47b},
 K. Mochizuki ¹⁰⁹, P. Mogg ⁵⁴, S. Mohapatra ⁴¹, R. Moles-Valls ²⁴, M.C. Mondragon ¹⁰⁸,
 K. Mönig ⁴⁸, J. Monk ⁴², E. Monnier ¹⁰³, A. Montalbano ¹⁴⁵, J. Montejo Berlingen ³⁶,
 M. Montella ⁹⁶, F. Monticelli ⁹⁰, N. Morange ⁶⁷, D. Moreno ²², M. Moreno Llácer ¹⁶⁶,
 C. Moreno Martinez ¹⁴, P. Morettini ^{57b}, M. Morgenstern ¹⁵³, S. Morgenstern ⁵⁰, D. Mori ¹⁴⁵,
 M. Morii ⁶¹, M. Morinaga ¹⁷¹, V. Morisbak ¹²⁷, A.K. Morley ³⁶, G. Mornacchi ³⁶,
 A.P. Morris ⁹⁶, L. Morvaj ¹⁴⁸, P. Moschovakos ³⁶, B. Moser ¹¹⁶, M. Mosidze ^{152b},

T. Moskalets ¹³⁷, H.J. Moss ¹⁴², J. Moss ^{31,n}, E.J.W. Moyse ¹⁰⁴, S. Muanza ¹⁰³, J. Mueller ¹³¹,
 R.S.P. Mueller ¹¹⁰, D. Muenstermann ⁹¹, G.A. Mullier ⁹⁸, D.P. Mungo ^{71a,71b},
 J.L. Munoz Martinez ¹⁴, F.J. Munoz Sanchez ¹⁰², P. Murin ^{28b}, W.J. Murray ^{170,136},
 A. Murrone ^{71a,71b}, M. Muškinja ^{18a}, C. Mwewa ^{33a}, A.G. Myagkov ^{37,a}, A.A. Myers ¹³¹,
 J. Myers ¹²⁵, M. Myska ¹³⁴, B.P. Nachman ^{18a}, O. Nackenhorst ⁴⁹, A. Nag ⁵⁰, K. Nagai ¹²⁸,
 K. Nagano ⁸³, Y. Nagasaka ⁶⁴, J.L. Nagle ²⁹, E. Nagy ¹⁰³, A.M. Nairz ³⁶, Y. Nakahama ¹¹³,
 K. Nakamura ⁸³, T. Nakamura ¹⁵⁶, I. Nakano ¹²¹, H. Nanjo ¹²⁶, F. Napolitano ^{63a},
 R.F. Naranjo Garcia ⁴⁸, R. Narayan ⁴⁴, I. Naryshkin ³⁷, T. Naumann ⁴⁸, G. Navarro ²²,
 P.Y. Nechaeva ³⁷, F. Nechansky ⁴⁸, T.J. Neep ²¹, A. Negri ^{73a,73b}, M. Negrini ^{23b}, C. Nellist ¹¹⁵,
 M.E. Nelson ^{47a,47b}, S. Nemecek ¹³³, M. Nessi ^{36,e}, M.S. Neubauer ¹⁶⁵, F. Neuhaus ¹⁰¹,
 M. Neumann ¹⁷⁴, R. Newhouse ¹⁶⁷, P.R. Newman ²¹, C.W. Ng ¹³¹, Y.S. Ng ¹⁹, Y.W.Y. Ng ¹⁶³,
 B. Ngair ^{35e}, H.D.N. Nguyen ¹⁰³, T. Nguyen Manh ¹⁰⁹, E. Nibigira ⁴⁰, R.B. Nickerson ¹²⁸,
 R. Nicolaidou ¹³⁷, D.S. Nielsen ⁴², J. Nielsen ¹³⁸, N. Nikiforou ¹¹, V. Nikolaenko ^{37,a},
 I. Nikolic-Audit ¹²⁹, K. Nikolopoulos ²¹, P. Nilsson ²⁹, H.R. Nindhito ⁵⁶, Y. Ninomiya ⁸³,
 A. Nisati ^{75a}, N. Nishu ^{62c}, R. Nisius ¹¹¹, I. Nitsche ⁴⁹, T. Nitta ¹⁷¹, T. Nobe ¹⁵⁶, Y. Noguchi ⁸⁷,
 I. Nomidis ¹²⁹, M.A. Nomura ²⁹, M. Nordberg ³⁶, T. Novak ⁹³, O. Novgorodova ⁵⁰, R. Novotny ¹³⁴,
 L. Nozka ¹²⁴, K. Ntekas ¹⁶³, E. Nurse ⁹⁶, F.G. Oakham ^{34,ao}, H. Oberlack ¹¹¹, J. Ocariz ¹²⁹,
 A. Ochi ⁸⁴, I. Ochoa ⁴¹, J.P. Ochoa-Ricoux ^{139a}, K. O'Connor ²⁶, S. Oda ⁸⁹, S. Odaka ⁸³,
 S. Oerdek ⁵⁵, A. Ogrodnik ^{85a}, A. Oh ¹⁰², S.H. Oh ⁵¹, C.C. Ohm ¹⁴⁷, H. Oide ¹⁵⁸,
 M.L. Ojeda ¹⁵⁹, H. Okawa ¹⁶¹, Y. Okazaki ⁸⁷, M.W. O'Keefe ⁹², Y. Okumura ¹⁵⁶, T. Okuyama ⁸³,
 A. Olariu ^{27b}, L.F. Oleiro Seabra ^{132a}, S.A. Olivares Pino ^{139a}, D. Oliveira Damazio ²⁹, J.L. Oliver ¹,
 M.J.R. Olsson ¹⁶³, A. Olszewski ⁸⁶, J. Olszowska ^{86,*}, D.C. O'Neil ¹⁴⁵, A.P. O'Neill ¹²⁸,
 A. Onofre ^{132a,132e}, P.U.E. Onyisi ¹¹, H. Oppen ¹²⁷, M.J. Oreglia ³⁹, G.E. Orellana ⁹⁰,
 D. Orestano ^{77a,77b}, N. Orlando ¹⁴, R.S. Orr ¹⁵⁹, V. O'Shea ⁵⁹, R. Ospanov ^{62a},
 G. Otero y Garzon ³⁰, H. Otono ⁸⁹, P.S. Ott ^{63a}, M. Ouchrif ^{35d}, J. Ouellette ²⁹,
 F. Ould-Saada ¹²⁷, A. Ouraou ^{137,*}, Q. Ouyang ^{15a}, M. Owen ⁵⁹, R.E. Owen ²¹, V.E. Ozcan ^{12c},
 N. Ozturk ⁸, J. Pacalt ¹²⁴, H.A. Pacey ³², K. Pachal ⁵¹, A. Pacheco Pages ¹⁴,
 C. Padilla Aranda ¹⁴, S. Pagan Griso ^{18a}, M. Paganini ¹⁷⁵, G. Palacino ⁶⁸, S. Palazzo ⁵²,
 S. Palestini ³⁶, M. Palka ^{85b}, D. Pallin ⁴⁰, P. Palni ^{85a}, I. Panagoulas ¹⁰, C.E. Pandini ³⁶,
 J.G. Panduro Vazquez ⁹⁵, P. Pani ⁴⁸, G. Panizzo ^{69a,69c}, L. Paolozzi ⁵⁶, C. Papadatos ¹⁰⁹,
 K. Papageorgiou ^{9,h}, S. Parajuli ⁴⁴, A. Paramonov ⁶, D. Paredes Hernandez ^{65b},
 S.R. Paredes Saenz ¹²⁸, B. Parida ³⁷, T.H. Park ¹⁵⁹, A.J. Parker ³¹, M.A. Parker ³²,
 F. Parodi ^{57b,57a}, E.W. Parrish ¹¹⁷, J.A. Parsons ⁴¹, U. Parzefall ⁵⁴, L. Pascual Dominguez ¹²⁹,
 V.R. Pascuzzi ¹⁵⁹, J.M.P. Pasner ¹³⁸, F. Pasquali ¹¹⁶, E. Pasqualucci ^{75a}, S. Passaggio ^{57b},
 F. Pastore ⁹⁵, P. Pasuwan ^{47a,47b}, S. Pataraiia ¹⁰¹, J.R. Pater ¹⁰², A. Pathak ^{173,j}, J. Patton ⁹²,
 T. Pauly ³⁶, J. Pearkes ¹⁴⁶, B. Pearson ¹¹¹, M. Pedersen ¹²⁷, L. Pedraza Diaz ¹¹⁵, R. Pedro ^{132a},
 T. Peiffer ⁵⁵, S.V. Peleganchuk ³⁷, O. Penc ¹³³, H. Peng ^{62a}, B.S. Peralva ^{82a}, M.M. Perego ⁶⁷,
 A.P. Pereira Peixoto ^{132a}, D.V. Perepelitsa ²⁹, F. Peri ¹⁹, L. Perini ^{71a,71b,*}, H. Pernegger ³⁶,
 S. Perrella ^{132a}, A. Perrevoort ¹¹⁶, K. Peters ⁴⁸, R.F.Y. Peters ¹⁰², B.A. Petersen ³⁶,
 T.C. Petersen ⁴², E. Petit ¹⁰³, A. Petridis ¹, C. Petridou ¹⁵⁵, M. Petrov ¹²⁸, F. Petrucci ^{77a,77b},
 M. Pettee ¹⁷⁵, N.E. Pettersson ¹⁰⁴, K. Petukhova ¹³⁵, A. Peyaud ¹³⁷, R. Pezoa ^{139c},
 L. Pezzotti ^{73a,73b}, T. Pham ¹⁰⁶, F.H. Phillips ¹⁰⁸, P.W. Phillips ¹³⁶, M.W. Phipps ¹⁶⁵,
 G. Piacquadio ¹⁴⁸, E. Pianori ^{18a}, A. Picazio ¹⁰⁴, R.H. Pickles ¹⁰², R. Piegaia ³⁰, D. Pietreanu ^{27b},
 J.E. Pilcher ³⁹, A.D. Pilkington ¹⁰², M. Pinamonti ^{69a,69c}, J.L. Pinfold ³, M. Pitt ¹⁵⁴,
 L. Pizzimento ^{76a,76b}, M.-A. Pleier ²⁹, V. Pleskot ¹³⁵, E. Plotnikova ³⁸, P. Podberezko ³⁷,
 R. Poettgen ⁹⁸, R. Poggi ⁵⁶, L. Poggioli ¹²⁹, I. Pogrebnyak ¹⁰⁸, D. Pohl ²⁴, I. Pokharel ⁵⁵,
 G. Polesello ^{73a}, A. Poley ^{18a}, A. Policicchio ^{75a,75b}, R. Polifka ¹³⁵, A. Polini ^{23b},

C.S. Pollard ⁴⁸, V. Polychronakos ²⁹, D. Ponomarenko ³⁷, L. Pontecorvo ³⁶, S. Popa ^{27a},
 G.A. Popeneciu ^{27d}, L. Portales ⁵, D.M. Portillo Quintero ⁶⁰, S. Pospisil ¹³⁴, K. Potamianos ⁴⁸,
 I.N. Potrap ³⁸, C.J. Potter ³², H. Potti ¹¹, T. Poulsen ⁹⁸, J. Poveda ³⁶, T.D. Powell ¹⁴²,
 G. Pownall ⁴⁸, M.E. Pozo Astigarraga ³⁶, P. Pralavorio ¹⁰³, S. Prell ⁸¹, D. Price ¹⁰²,
 M. Primavera ^{70a}, S. Prince ¹⁰⁵, M.L. Proffitt ¹⁴¹, N. Proklova ³⁷, K. Prokofiev ^{65c},
 S. Protopopescu ²⁹, J. Proudfoot ⁶, M. Przybycien ^{85a}, D. Pudzha ³⁷, A. Puri ¹⁶⁵, P. Puzo ⁶⁷,
 J. Qian ¹⁰⁷, Y. Qin ¹⁰², A. Quadt ⁵⁵, M. Queitsch-Maitland ³⁶, A. Qureshi ¹, M. Racko ^{28a},
 F. Ragusa ^{71a,71b}, G. Rahal ⁹⁹, J.A. Raine ⁵⁶, S. Rajagopalan ²⁹, A. Ramirez Morales ⁹⁴,
 K. Ran ^{15a,15d}, T. Rashid ⁶⁷, S. Raspopov ⁵, D.M. Rauch ⁴⁸, F. Rauscher ¹¹⁰, S. Rave ¹⁰¹,
 B. Ravina ¹⁴², I. Ravinovich ¹⁷², J.H. Rawling ¹⁰², M. Raymond ³⁶, A.L. Read ¹²⁷,
 N.P. Readioff ⁶⁰, M. Reale ^{70a,70b}, D.M. Rebuzzi ^{73a,73b}, A. Redelbach ¹⁶⁹, G. Redlinger ²⁹,
 K. Reeves ⁴⁵, L. Rehnisch ¹⁹, J. Reichert ¹³⁰, D. Reikher ¹⁵⁴, A. Reiss ¹⁰¹, A. Rej ¹⁴⁴,
 C. Rembser ³⁶, A. Renardi ⁴⁸, M. Renda ^{27b}, M. Rescigno ^{75a}, S. Resconi ^{71a},
 E.D. Resseguie ^{18a}, S. Rettie ⁹⁶, B. Reynolds ¹²⁰, E. Reynolds ²¹, O.L. Rezanova ³⁷,
 P. Reznicek ¹³⁵, E. Ricci ^{78a,78b}, R. Richter ¹¹¹, S. Richter ⁴⁸, E. Richter-Was ^{85b}, O. Ricken ²⁴,
 M. Ridel ¹²⁹, P. Rieck ¹¹¹, O. Rifki ⁴⁸, M. Rijssenbeek ¹⁴⁸, A. Rimoldi ^{73a,73b}, M. Rimoldi ⁴⁸,
 L. Rinaldi ^{23b,23a}, G. Ripellino ¹⁴⁷, I. Riu ¹⁴, J.C. Rivera Vergara ¹⁶⁸, F. Rizatdinova ¹²³,
 E. Rizvi ⁹⁴, C. Rizzi ³⁶, R.T. Roberts ¹⁰², S.H. Robertson ^{105,ac}, M. Robin ⁴⁸, D. Robinson ³²,
 C.M. Robles Gajardo ^{139c}, M. Robles Manzano ¹⁰¹, A. Robson ⁵⁹, A. Rocchi ^{76a,76b}, E. Rocco ¹⁰¹,
 C. Roda ^{74a,74b}, S. Rodriguez Bosca ¹⁶⁶, A. Rodriguez Perez ¹⁴, D. Rodriguez Rodriguez ¹⁶⁶,
 A.M. Rodríguez Vera ^{160b}, S. Roe ³⁶, O. Røhne ¹²⁷, R. Röhrig ¹¹¹, R.A. Rojas ^{139c}, B. Roland ⁵⁴,
 C.P.A. Roland ⁶⁸, J. Roloff ²⁹, A. Romaniouk ³⁷, M. Romano ^{23b}, N. Rompotis ⁹²,
 M. Ronzani ¹¹⁸, L. Roos ¹²⁹, S. Rosati ^{75a}, G. Rosin ¹⁰⁴, B.J. Rosser ¹³⁰, E. Rossi ⁴⁸,
 E. Rossi ^{77a,77b}, E. Rossi ^{72a,72b}, L.P. Rossi ^{57b}, L. Rossini ^{71a,71b}, R. Rosten ¹⁴, M. Rotaru ^{27b},
 J. Rothberg ^{141,*}, B. Rottler ⁵⁴, D. Rousseau ⁶⁷, G. Rovelli ^{73a,73b}, A. Roy ¹¹, D. Roy ^{33d},
 A. Rozanov ¹⁰³, Y. Rozen ¹⁵³, X. Ruan ^{33d}, F. Rühr ⁵⁴, A. Ruiz-Martinez ¹⁶⁶, A. Rummler ³⁶,
 Z. Rurikova ⁵⁴, N.A. Rusakovich ³⁸, H.L. Russell ¹⁰⁵, L. Rustige ^{40,49}, J.P. Rutherford ⁷,
 E.M. Rüttinger ¹⁴², M. Rybar ⁴¹, G. Rybkin ⁶⁷, E.B. Rye ¹²⁷, A. Ryzhov ³⁷,
 J.A. Sabater Iglesias ⁴⁸, P. Sabatini ⁵⁵, G. Sabato ¹¹⁶, S. Sacerdoti ⁶⁷, H.F-W. Sadrozinski ¹³⁸,
 F. Safai Tehrani ^{75a}, B. Safarzadeh Samani ¹⁴⁹, M. Safdari ¹⁴⁶, P. Saha ¹¹⁷, S. Saha ¹⁰⁵,
 M. Sahinsoy ^{63a}, A. Sahu ¹⁷⁴, M. Saimpert ⁴⁸, M. Saito ¹⁵⁶, T. Saito ¹⁵⁶, H. Sakamoto ¹⁵⁶,
 A. Sakharov ^{118,ai}, D. Salamani ⁵⁶, G. Salamanna ^{77a,77b}, J.E. Salazar Loyola ^{139c}, A. Salnikov ¹⁴⁶,
 J. Salt ¹⁶⁶, D. Salvatore ^{43b,43a}, F. Salvatore ¹⁴⁹, A. Salvucci ^{65a,65b,65c}, A. Salzburger ³⁶,
 J. Samarati ³⁶, D. Sammel ⁵⁴, D. Sampsonidis ¹⁵⁵, D. Sampsonidou ¹⁵⁵, J. Sánchez ¹⁶⁶,
 A. Sanchez Pineda ^{69a,36,69c}, H. Sandaker ¹²⁷, C.O. Sander ⁴⁸, I.G. Sanderswood ⁹¹,
 M. Sandhoff ¹⁷⁴, C. Sandoval ²², D.P.C. Sankey ¹³⁶, M. Sannino ^{57b,57a}, Y. Sano ¹¹³,
 A. Sansoni ⁵³, C. Santoni ⁴⁰, H. Santos ^{132a,132b}, S.N. Santpur ^{18a}, A. Santra ¹⁶⁶,
 J.G. Saraiva ^{132a,132d}, J. Sardain ¹²⁹, O. Sasaki ⁸³, K. Sato ¹⁶¹, F. Sauerburger ⁵⁴, E. Sauvan ⁵,
 P. Savard ^{159,ao}, R. Sawada ¹⁵⁶, C. Sawyer ¹³⁶, L. Sawyer ^{97,ah}, C. Sbarra ^{23b}, A. Sbrizzi ^{23a},
 T. Scanlon ⁹⁶, J. Schaarschmidt ¹⁴¹, P. Schacht ¹¹¹, B.M. Schachtner ¹¹⁰, D. Schaefer ³⁹,
 L. Schaefer ¹³⁰, J. Schaeffer ¹⁰¹, S. Schaepe ³⁶, U. Schäfer ¹⁰¹, A.C. Schaffer ⁶⁷, D. Schaile ¹¹⁰,
 R.D. Chamberger ¹⁴⁸, N. Scharmberg ¹⁰², V.A. Schegelsky ³⁷, D. Scheirich ¹³⁵, F. Schenck ¹⁹,
 M. Schernau ¹⁶³, C. Schiavi ^{57b,57a}, L.K. Schildgen ²⁴, Z.M. Schillaci ²⁶, E.J. Schioppa ³⁶,
 M. Schioppa ^{43b,43a}, K.E. Schleicher ⁵⁴, S. Schlenker ³⁶, K.R. Schmidt-Sommerfeld ¹¹¹,
 K. Schmieden ³⁶, C. Schmitt ¹⁰¹, S. Schmitt ⁴⁸, S. Schmitz ¹⁰¹, J.C. Schmoeckel ⁴⁸,
 L. Schoeffel ¹³⁷, A. Schoening ^{63b}, P.G. Scholer ⁵⁴, E. Schopf ¹²⁸, M. Schott ¹⁰¹,
 J.F.P. Schouwenberg ¹¹⁵, J. Schovancova ³⁶, S. Schramm ⁵⁶, F. Schroeder ¹⁷⁴, A. Schulte ¹⁰¹,

H-C. Schultz-Coulon ^{63a}, M. Schumacher ⁵⁴, B.A. Schumm ¹³⁸, Ph. Schune ¹³⁷,
 A. Schwartzman ¹⁴⁶, T.A. Schwarz ¹⁰⁷, Ph. Schwemling ¹³⁷, R. Schwienhorst ¹⁰⁸,
 A. Sciandra ¹³⁸, G. Sciolla ²⁶, M. Scodreggio ⁴⁸, M. Scornajenghi ^{43b,43a}, F. Scuri ^{74a}, F. Scutti ¹⁰⁶,
 L.M. Scyboz ¹¹¹, C.D. Sebastiani ^{75a,75b}, P. Seema ¹⁹, S.C. Seidel ¹¹⁴, A. Seiden ¹³⁸,
 B.D. Seidlitz ²⁹, T. Seiss ³⁹, J.M. Seixas ^{82b}, G. Sekhniaidze ^{72a}, S.J. Sekula ⁴⁴,
 N. Semprini-Cesari ^{23b,23a}, S. Sen ⁵¹, C. Serfon ⁷⁹, L. Serin ⁶⁷, L. Serkin ^{69a,69b}, M. Sessa ^{62a},
 H. Severini ¹²², S. Sevova ¹⁴⁶, T. Šfiligoj ⁹³, F. Sforza ^{57b,57a}, A. Sfyrla ⁵⁶, E. Shabalina ⁵⁵,
 J.D. Shahinian ¹³⁸, N.W. Shaikh ^{47a,47b}, D. Shaked Renous ¹⁷², L.Y. Shan ^{15a}, J.T. Shank ²⁵,
 M. Shapiro ^{18a}, A. Sharma ¹²⁸, A.S. Sharma ¹, P.B. Shatalov ³⁷, K. Shaw ¹⁴⁹, S.M. Shaw ¹⁰²,
 M. Shehade ¹⁷², Y. Shen ¹²², A.D. Sherman ²⁵, P. Sherwood ⁹⁶, L. Shi ¹⁵¹, S. Shimizu ⁸³,
 C.O. Shimmin ¹⁷⁵, Y. Shimogama ¹⁷¹, M. Shimojima ¹¹², I.P.J. Shipsey ¹²⁸, S. Shirabe ¹⁵⁸,
 M. Shiyakova ^{38,aa}, J. Shlomi ¹⁷², A. Shmeleva ³⁷, M.J. Shochet ³⁹, J. Shojaii ¹⁰⁶, D.R. Shope ¹²²,
 S. Shrestha ¹²⁰, E.M. Shrif ^{33d}, E. Shulga ¹⁷², P. Sicho ¹³³, A.M. Sickles ¹⁶⁵, P.E. Sidebo ¹⁴⁷,
 E. Sideras Haddad ^{33d}, O. Sidiropoulou ³⁶, A. Sidoti ^{23b}, F. Siegert ⁵⁰, Dj. Sijacki ¹⁶,
 M.Jr. Silva ¹⁷³, M.V. Silva Oliveira ^{82a}, S.B. Silverstein ^{47a}, S. Simion ⁶⁷, R. Simoniello ¹⁰¹,
 S. Simsek ^{12b}, P. Sinervo ¹⁵⁹, V. Sinetckii ³⁷, N.B. Sinev ¹²⁵, S. Singh ¹⁴⁵, M. Sioli ^{23b,23a},
 I. Siral ¹²⁵, S.Yu. Sivoklov ^{37,*}, J. Sjölin ^{47a,47b}, E. Skorda ⁹⁸, P. Skubic ¹²², M. Slawinska ⁸⁶,
 K. Sliwa ¹⁶², R. Slovak ¹³⁵, V. Smakhtin ¹⁷², B.H. Smart ¹³⁶, J. Smiesko ^{28b}, N. Smirnov ³⁷,
 S.Yu. Smirnov ³⁷, Y. Smirnov ³⁷, L.N. Smirnova ^{37,a}, O. Smirnova ⁹⁸, J.W. Smith ⁵⁵,
 M. Smizanska ⁹¹, K. Smolek ¹³⁴, A. Smykiewicz ⁸⁶, A.A. Snesarev ³⁷, H.L. Snoek ¹¹⁶,
 I.M. Snyder ¹²⁵, S. Snyder ²⁹, R. Sobie ^{168,ac}, A. Soffer ¹⁵⁴, A. Søggaard ⁵², F. Sohns ⁵⁵,
 C.A. Solans Sanchez ³⁶, E.Yu. Soldatov ³⁷, U. Soldevila ¹⁶⁶, A.A. Solodkov ³⁷, A. Soloshenko ³⁸,
 O.V. Solovyanov ³⁷, V. Solovyev ³⁷, P. Sommer ¹⁴², H. Son ¹⁶², W. Song ¹³⁶, W.Y. Song ^{160b},
 A. Sopczak ¹³⁴, A.L. Soppio ⁹⁶, F. Sopkova ^{28b}, C.L. Sotiropoulou ^{74a,74b}, S. Sottocornola ^{73a,73b},
 R. Soualah ^{69a,69c,g}, D. South ⁴⁸, S. Spagnolo ^{70a,70b}, M. Spalla ¹¹¹, M. Spangenberg ¹⁷⁰,
 F. Spanò ⁹⁵, D. Sperlich ⁵⁴, T.M. Spieker ^{63a}, G. Spigo ³⁶, M. Spina ¹⁴⁹, D.P. Spiteri ⁵⁹,
 M. Spousta ¹³⁵, A. Stabile ^{71a,71b}, R. Stamen ^{63a}, M. Stamenkovic ¹¹⁶, E. Stanecka ⁸⁶,
 B. Stanislaus ¹²⁸, M.M. Stanitzki ⁴⁸, M. Stankaityte ¹²⁸, B. Stapf ¹¹⁶, E.A. Starchenko ³⁷,
 G.H. Stark ¹³⁸, J. Stark ⁶⁰, P. Staroba ¹³³, P. Starovoitov ^{63a}, S. Stärz ¹⁰⁵, R. Staszewski ⁸⁶,
 G. Stavropoulos ⁴⁶, M. Stegler ⁴⁸, P. Steinberg ²⁹, A.L. Steinhebel ¹²⁵, B. Stelzer ¹⁴⁵,
 H.J. Stelzer ¹³¹, O. Stelzer-Chilton ^{160a}, H. Stenzel ⁵⁸, T.J. Stevenson ¹⁴⁹, G.A. Stewart ³⁶,
 M.C. Stockton ³⁶, G. Stoicea ^{27b}, M. Stolarski ^{132a}, S. Stonjek ¹¹¹, A. Straessner ⁵⁰,
 J. Strandberg ¹⁴⁷, S. Strandberg ^{47a,47b}, M. Strauss ¹²², P. Strizenec ^{28b}, R. Ströhmer ¹⁶⁹,
 D.M. Strom ¹²⁵, R. Stroynowski ⁴⁴, A. Strubig ⁵², S.A. Stucci ²⁹, B. Stugu ¹⁷, J. Stupak ¹²²,
 N.A. Styles ⁴⁸, D. Su ¹⁴⁶, W. Su ^{62c}, S. Suchek ^{63a}, V.V. Sulin ³⁷, M.J. Sullivan ⁹²,
 D.M.S. Sultan ⁵⁶, S. Sultansoy ^{4c}, T. Sumida ⁸⁷, S. Sun ¹⁰⁷, X. Sun ¹⁰², K. Suruliz ¹⁴⁹,
 C.J.E. Suster ¹⁵⁰, M.R. Sutton ¹⁴⁹, S. Suzuki ⁸³, M. Svatos ¹³³, M. Swiatlowski ³⁹, S.P. Swift ²,
 T. Swirski ¹⁶⁹, A. Sydorenko ¹⁰¹, I. Sykora ^{28a}, M. Sykora ¹³⁵, T. Sykora ¹³⁵, D. Ta ¹⁰¹,
 K. Tackmann ^{48,y}, J. Taenzer ¹⁵⁴, A. Taffard ¹⁶³, R. Tafirout ^{160a}, H. Takai ²⁹, R. Takashima ⁸⁸,
 K. Takeda ⁸⁴, T. Takeshita ¹⁴³, E.P. Takeva ⁵², Y. Takubo ⁸³, M. Talby ¹⁰³, A.A. Talyshev ³⁷,
 N.M. Tamir ¹⁵⁴, J. Tanaka ¹⁵⁶, M. Tanaka ¹⁵⁸, R. Tanaka ⁶⁷, S. Tapia Araya ¹⁶⁵, S. Tapprogge ¹⁰¹,
 A. Tarek Abouelfadl Mohamed ¹²⁹, S. Tarem ¹⁵³, K. Tariq ^{62b}, G. Tarna ^{27b,d}, G.F. Tartarelli ^{71a},
 P. Tas ¹³⁵, M. Tasevsky ¹³³, T. Tashiro ⁸⁷, E. Tassi ^{43b,43a}, A. Tavares Delgado ^{132a}, Y. Tayalati ^{35e},
 A.J. Taylor ⁵², G.N. Taylor ¹⁰⁶, W. Taylor ^{160b}, A.S. Tee ⁹¹, R. Teixeira De Lima ¹⁴⁶,
 P. Teixeira-Dias ⁹⁵, H. Ten Kate ³⁶, J.J. Teoh ¹¹⁶, S. Terada ⁸³, K. Terashi ¹⁵⁶, J. Terron ¹⁰⁰,
 S. Terzo ¹⁴, M. Testa ⁵³, R.J. Teuscher ^{159,ac}, S.J. Thais ¹⁷⁵, T. Thevenaux-Pelzer ⁴⁸,
 F. Thiele ⁴², D.W. Thomas ⁹⁵, J.O. Thomas ⁴⁴, J.P. Thomas ²¹, P.D. Thompson ²¹,

L.A. Thomsen ¹⁷⁵, E. Thomson ¹³⁰, E.J. Thorpe ⁹⁴, R.E. Ticse Torres ⁵⁵, V. Tikhomirov ^{37,a},
 Yu.A. Tikhonov ³⁷, S. Timoshenko ³⁷, P. Tipton ¹⁷⁵, S. Tisserant ¹⁰³, K. Todome ^{23b,23a},
 S. Todorova-Nova ¹³⁵, S. Todt ⁵⁰, J. Tojo ⁸⁹, S. Tokár ^{28a}, K. Tokushuku ⁸³, E. Tolley ¹²⁰,
 K.G. Tomiwa ^{33d}, M. Tomoto ¹¹³, L. Tompkins ^{146,p}, B. Tong ⁶¹, P. Tornambe ¹⁰⁴,
 E. Torrence ¹²⁵, H. Torres ⁵⁰, E. Torró Pastor ¹⁴¹, C. Tosciri ¹²⁸, J. Toth ^{103,ab}, D.R. Tovey ¹⁴²,
 A. Traeet ¹⁷, C.J. Treado ¹¹⁸, T. Trefzger ¹⁶⁹, F. Tresoldi ¹⁴⁹, A. Tricoli ²⁹, I.M. Trigger ^{160a},
 S. Trincaz-Duvoid ¹²⁹, D.A. Trischuk ¹⁶⁷, B. Trocmé ⁶⁰, A. Trofymov ¹³⁷, C. Troncon ^{71a},
 F. Trovato ¹⁴⁹, L. Truong ^{33b}, M. Trzebinski ⁸⁶, A. Trzupiek ⁸⁶, F. Tsai ⁴⁸, J.C-L. Tseng ¹²⁸,
 P.V. Tsiarehka ^{37,a}, A. Tsirigotis ^{155,u}, V. Tsiskaridze ¹⁴⁸, E.G. Tskhadadze ^{152a}, M. Tsopoulou ¹⁵⁵,
 I.I. Tsukerman ³⁷, V. Tsulaia ^{18a}, S. Tsuno ⁸³, D. Tsybychev ¹⁴⁸, Y. Tu ^{65b}, A. Tudorache ^{27b},
 V. Tudorache ^{27b}, T.T. Tulbure ^{27a}, A.N. Tuna ⁶¹, S. Turchikhin ³⁸, D. Turgeman ¹⁷²,
 I. Turk Cakir ^{4b,t}, R.J. Turner ²¹, R. Turra ^{71a}, P.M. Tuts ⁴¹, S. Tzamarias ¹⁵⁵, E. Tzovara ¹⁰¹,
 G. Uccielli ⁴⁹, K. Uchida ¹⁵⁶, F. Ukegawa ¹⁶¹, G. Unal ³⁶, A. Undrus ²⁹, G. Unel ¹⁶³,
 F.C. Ungaro ¹⁰⁶, Y. Unno ⁸³, K. Uno ¹⁵⁶, J. Urban ^{28b}, P. Urquijo ¹⁰⁶, G. Usai ⁸, Z. Uysal ^{12d},
 V. Vacek ¹³⁴, B. Vachon ¹⁰⁵, K.O.H. Vadla ¹²⁷, A. Vaidya ⁹⁶, C. Valderanis ¹¹⁰,
 E. Valdes Santurio ^{47a,47b}, M. Valente ⁵⁶, S. Valentinetti ^{23b,23a}, A. Valero ¹⁶⁶, L. Valéry ⁴⁸,
 R.A. Vallance ²¹, A. Vallier ³⁶, J.A. Valls Ferrer ¹⁶⁶, T.R. Van Daalen ¹⁴, P. Van Gemmeren ⁶,
 I. Van Vulpen ¹¹⁶, M. Vanadia ^{76a,76b}, W. Vandelli ³⁶, M. Vandenbroucke ¹³⁷, E.R. Vandewall ¹²³,
 A. Vaniachine ³⁷, D. Vannicola ^{75a,75b}, R. Vari ^{75a}, E.W. Varnes ⁷, C. Varni ^{57b,57a}, T. Varol ¹⁵¹,
 D. Varouchas ⁶⁷, K.E. Varvell ¹⁵⁰, M.E. Vasile ^{27b}, G.A. Vasquez ¹⁶⁸, F. Vazeille ⁴⁰,
 D. Vazquez Furelos ¹⁴, T. Vazquez Schroeder ³⁶, J. Veatch ⁵⁵, V. Vecchio ^{77a,77b}, M.J. Veen ¹¹⁶,
 L.M. Veloce ¹⁵⁹, F. Veloso ^{132a,132c}, S. Veneziano ^{75a}, A. Ventura ^{70a,70b}, N. Venturi ³⁶,
 A. Verbytskyi ¹¹¹, V. Vercesi ^{73a}, M. Verducci ^{74a,74b}, C.M. Vergel Infante ⁸¹, C. Vergis ²⁴,
 W. Verkerke ¹¹⁶, A.T. Vermeulen ¹¹⁶, J.C. Vermeulen ¹¹⁶, M.C. Vetterli ^{145,ao},
 N. Viaux Maira ^{139c}, M. Vicente Barreto Pinto ⁵⁶, T. Vickey ¹⁴², O.E. Vickey Boeriu ¹⁴²,
 G.H.A. Viehhauser ¹²⁸, L. Vighani ^{63b}, M. Villa ^{23b,23a}, M. Villaplana Perez ³, E. Vilucchi ⁵³,
 M.G. Vincter ³⁴, G.S. Virdee ²¹, A. Vishwakarma ⁴⁸, C. Vittori ^{23b,23a}, I. Vivarelli ¹⁴⁹,
 M. Vogel ¹⁷⁴, P. Vokac ¹³⁴, S.E. von Buddenbrock ^{33d}, E. Von Toerne ²⁴, V. Vorobel ¹³⁵,
 K. Vorobev ³⁷, M. Vos ¹⁶⁶, J.H. Vosseveld ⁹², M. Vozak ¹⁰², N. Vranjes ¹⁶,
 M. Vranjes Milosavljevic ¹⁶, V. Vrba ^{134,*}, M. Vreeswijk ¹¹⁶, R. Vuillermet ³⁶, I. Vukotic ³⁹,
 P. Wagner ²⁴, W. Wagner ¹⁷⁴, J. Wagner-Kuhr ¹¹⁰, S. Wahdan ¹⁷⁴, H. Wahlberg ⁹⁰,
 V.M. Walbrecht ¹¹¹, J. Walder ⁹¹, R. Walker ¹¹⁰, S.D. Walker ⁹⁵, W. Walkowiak ¹⁴⁴,
 V. Wallangen ^{47a,47b}, A.M. Wang ⁶¹, A.Z. Wang ¹⁷³, C. Wang ^{62c}, F. Wang ¹⁷³, H. Wang ^{18a},
 H. Wang ³, J. Wang ^{65a}, J. Wang ^{63b}, P. Wang ⁴⁴, Q. Wang ¹²², R.-J. Wang ¹⁰¹, R. Wang ^{62a},
 R. Wang ⁶, S.M. Wang ¹⁵¹, W.T. Wang ^{62a}, W.X. Wang ^{62a}, Y. Wang ^{62a}, Z. Wang ^{62c},
 C. Wanotayaroj ⁴⁸, A. Warburton ¹⁰⁵, C.P. Ward ³², D.R. Wardrope ⁹⁶, N. Warrack ⁵⁹,
 A. Washbrook ⁵², A.T. Watson ²¹, M.F. Watson ²¹, G. Watts ¹⁴¹, B.M. Waugh ⁹⁶, A.F. Webb ¹¹,
 S. Webb ¹⁰¹, C. Weber ¹⁷⁵, M.S. Weber ²⁰, S.A. Weber ³⁴, S.M. Weber ^{63a}, A.R. Weidberg ¹²⁸,
 J. Weingarten ⁴⁹, M. Weirich ¹⁰¹, C. Weiser ⁵⁴, P.S. Wells ³⁶, T. Wenaus ²⁹, T. Wengler ³⁶,
 S. Wenig ³⁶, N. Wermes ²⁴, M.D. Werner ⁸¹, M. Wessels ^{63a}, T.D. Weston ²⁰, K. Whalen ¹²⁵,
 N.L. Whallon ¹⁴¹, A.M. Wharton ⁹¹, A.S. White ¹⁰⁷, A. White ⁸, M.J. White ¹, D. Whiteson ¹⁶³,
 B.W. Whitmore ⁹¹, W. Wiedenmann ¹⁷³, C. Wiel ⁵⁰, M. Wielers ¹³⁶, N. Wieseotte ¹⁰¹,
 C. Wiglesworth ⁴², L.A.M. Wiik-Fuchs ⁵⁴, H.G. Wilkens ³⁶, L.J. Wilkins ⁹⁵, H.H. Williams ¹³⁰,
 S. Williams ³², C. Willis ¹⁰⁸, S. Willocq ¹⁰⁴, I. Wingerter-Seez ⁵, E. Winkels ¹⁴⁹,
 F. Winklmeier ¹²⁵, O.J. Winston ¹⁴⁹, B.T. Winter ⁵⁴, M. Wittgen ¹⁴⁶, M. Wobisch ⁹⁷, A. Wolf ¹⁰¹,
 T.M.H. Wolf ¹¹⁶, R. Wolff ¹⁰³, R. Wölker ¹²⁸, J. Wollrath ⁵⁴, M.W. Wolter ⁸⁶, H. Wolters ^{132a,132c},
 V.W.S. Wong ¹⁶⁷, N.L. Woods ¹³⁸, S.D. Worm ²¹, B.K. Wosiek ⁸⁶, K.W. Woźniak ⁸⁶,

K. Wraight ⁵⁹, S.L. Wu ¹⁷³, X. Wu ⁵⁶, Y. Wu ^{62a}, T.R. Wyatt ¹⁰², B.M. Wynne ⁵², S. Xella ⁴², Z. Xi ¹⁰⁷, X. Xiao ¹⁰⁷, I. Xiotidis ¹⁴⁹, D. Xu ^{15a}, H. Xu ^{62a}, H. Xu ^{62a}, L. Xu ²⁹, T. Xu ¹³⁷, W. Xu ¹⁰⁷, Z. Xu ^{62b}, Z. Xu ¹⁴⁶, B. Yabsley ¹⁵⁰, S. Yacoob ^{33a}, K. Yajima ¹²⁶, D.P. Yallup ⁹⁶, N. Yamaguchi ⁸⁹, Y. Yamaguchi ¹⁵⁸, A. Yamamoto ⁸³, M. Yamatani ¹⁵⁶, T. Yamazaki ¹⁵⁶, Y. Yamazaki ⁸⁴, Z. Yan ²⁵, H.J. Yang ^{62c,62d}, H.T. Yang ^{18a}, S. Yang ^{62a}, T. Yang ^{65c}, X. Yang ^{62b,60}, Y. Yang ¹⁵⁶, W-M. Yao ^{18a}, Y.C. Yap ⁴⁸, Y. Yasu ⁸³, E. Yatsenko ^{62c,62d}, H. Ye ^{15c}, J. Ye ⁴⁴, S. Ye ²⁹, I. Yeletsikh ³⁸, M.R. Yexley ⁹¹, E. Yigitbasi ²⁵, K. Yorita ¹⁷¹, K. Yoshihara ¹³⁰, C.J.S. Young ³⁶, C. Young ¹⁴⁶, J. Yu ⁸¹, R. Yuan ^{62b,i}, X. Yue ^{63a}, M. Zaazoua ^{35e}, B. Zabinski ⁸⁶, G. Zacharis ¹⁰, E. Zaffaroni ⁵⁶, T. Zakareishvili ^{152b}, N. Zakharchuk ³⁴, S. Zambito ⁶¹, D. Zanzi ³⁶, D.R. Zaripovas ⁵⁹, S.V. Zeißner ⁴⁹, C. Zeitnitz ¹⁷⁴, G. Zemaityte ¹²⁸, J.C. Zeng ¹⁶⁵, O. Zenin ³⁷, T. Ženiš ^{28a}, D. Zerwas ⁶⁷, M. Zgubić ¹²⁸, B. Zhang ^{15c}, D.F. Zhang ^{15b}, G. Zhang ^{15b}, H. Zhang ^{15c}, J. Zhang ⁶, L. Zhang ^{15c}, L. Zhang ^{62a}, M. Zhang ¹⁶⁵, R. Zhang ¹⁷³, S. Zhang ¹⁰⁷, X. Zhang ^{62b}, Y. Zhang ^{15a,15d}, Z. Zhang ^{65a}, Z. Zhang ⁶⁷, P. Zhao ⁵¹, Z. Zhao ^{62a}, A. Zhemchugov ³⁸, Z. Zheng ¹⁰⁷, D. Zhong ¹⁶⁵, B. Zhou ¹⁰⁷, C. Zhou ¹⁷³, M.S. Zhou ^{15a,15d}, M. Zhou ¹⁴⁸, N. Zhou ^{62c}, Y. Zhou ⁷, C.G. Zhu ^{62b}, C. Zhu ^{15a,15d}, H.L. Zhu ^{62a}, H. Zhu ^{15a}, J. Zhu ¹⁰⁷, Y. Zhu ^{62a}, X. Zhuang ^{15a}, K. Zhukov ³⁷, V. Zhulanov ³⁷, D. Zieminska ⁶⁸, N.I. Zimine ³⁸, S. Zimmermann ^{54,*}, Z. Zinonos ¹¹¹, M. Ziolkowski ¹⁴⁴, L. Živković ¹⁶, G. Zobernig ¹⁷³, A. Zoccoli ^{23b,23a}, K. Zoch ⁵⁵, T.G. Zorbas ¹⁴², R. Zou ³⁹, L. Zwalinski ³⁶.

¹Department of Physics, University of Adelaide, Adelaide; Australia.

²Physics Department, SUNY Albany, Albany NY; United States of America.

³Department of Physics, University of Alberta, Edmonton AB; Canada.

⁴(^a)Department of Physics, Ankara University, Ankara; (^b)Istanbul Aydin University, Application and Research Center for Advanced Studies, Istanbul; (^c)Division of Physics, TOBB University of Economics and Technology, Ankara; Türkiye.

⁵LAPP, Université Savoie Mont Blanc, CNRS/IN2P3, Annecy; France.

⁶High Energy Physics Division, Argonne National Laboratory, Argonne IL; United States of America.

⁷Department of Physics, University of Arizona, Tucson AZ; United States of America.

⁸Department of Physics, University of Texas at Arlington, Arlington TX; United States of America.

⁹Physics Department, National and Kapodistrian University of Athens, Athens; Greece.

¹⁰Physics Department, National Technical University of Athens, Zografou; Greece.

¹¹Department of Physics, University of Texas at Austin, Austin TX; United States of America.

¹²(^a)Bahcesehir University, Faculty of Engineering and Natural Sciences, Istanbul; (^b)Istanbul Bilgi University, Faculty of Engineering and Natural Sciences, Istanbul; (^c)Department of Physics, Bogazici University, Istanbul; (^d)Department of Physics Engineering, Gaziantep University, Gaziantep; Türkiye.

¹³Institute of Physics, Azerbaijan Academy of Sciences, Baku; Azerbaijan.

¹⁴Institut de Física d'Altes Energies (IFAE), Barcelona Institute of Science and Technology, Barcelona; Spain.

¹⁵(^a)Institute of High Energy Physics, Chinese Academy of Sciences, Beijing; (^b)Physics Department, Tsinghua University, Beijing; (^c)Department of Physics, Nanjing University, Nanjing; (^d)University of Chinese Academy of Science (UCAS), Beijing; China.

¹⁶Institute of Physics, University of Belgrade, Belgrade; Serbia.

¹⁷Department for Physics and Technology, University of Bergen, Bergen; Norway.

¹⁸(^a)Physics Division, Lawrence Berkeley National Laboratory, Berkeley CA; (^b)University of California, Berkeley CA; United States of America.

¹⁹Institut für Physik, Humboldt Universität zu Berlin, Berlin; Germany.

- ²⁰Albert Einstein Center for Fundamental Physics and Laboratory for High Energy Physics, University of Bern, Bern; Switzerland.
- ²¹School of Physics and Astronomy, University of Birmingham, Birmingham; United Kingdom.
- ²²Facultad de Ciencias y Centro de Investigaciones, Universidad Antonio Nariño, Bogotá; Colombia.
- ²³(^a)Dipartimento di Fisica e Astronomia A. Righi, Università di Bologna, Bologna; (^b)INFN Sezione di Bologna; Italy.
- ²⁴Physikalisches Institut, Universität Bonn, Bonn; Germany.
- ²⁵Department of Physics, Boston University, Boston MA; United States of America.
- ²⁶Department of Physics, Brandeis University, Waltham MA; United States of America.
- ²⁷(^a)Transilvania University of Brasov, Brasov; (^b)Horia Hulubei National Institute of Physics and Nuclear Engineering, Bucharest; (^c)Department of Physics, Alexandru Ioan Cuza University of Iasi, Iasi; (^d)National Institute for Research and Development of Isotopic and Molecular Technologies, Physics Department, Cluj-Napoca; (^e)University Politehnica Bucharest, Bucharest; (^f)West University in Timisoara, Timisoara; Romania.
- ²⁸(^a)Faculty of Mathematics, Physics and Informatics, Comenius University, Bratislava; (^b)Department of Subnuclear Physics, Institute of Experimental Physics of the Slovak Academy of Sciences, Kosice; Slovak Republic.
- ²⁹Physics Department, Brookhaven National Laboratory, Upton NY; United States of America.
- ³⁰Universidad de Buenos Aires, Facultad de Ciencias Exactas y Naturales, Departamento de Física, y CONICET, Instituto de Física de Buenos Aires (IFIBA), Buenos Aires; Argentina.
- ³¹California State University, CA; United States of America.
- ³²Cavendish Laboratory, University of Cambridge, Cambridge; United Kingdom.
- ³³(^a)Department of Physics, University of Cape Town, Cape Town; (^b)Department of Mechanical Engineering Science, University of Johannesburg, Johannesburg; (^c)University of South Africa, Department of Physics, Pretoria; (^d)School of Physics, University of the Witwatersrand, Johannesburg; South Africa.
- ³⁴Department of Physics, Carleton University, Ottawa ON; Canada.
- ³⁵(^a)Faculté des Sciences Ain Chock, Réseau Universitaire de Physique des Hautes Energies - Université Hassan II, Casablanca; (^b)Faculté des Sciences, Université Ibn-Tofail, Kénitra; (^c)Faculté des Sciences Semlalia, Université Cadi Ayyad, LPHEA-Marrakech; (^d)LPMR, Faculté des Sciences, Université Mohamed Premier, Oujda; (^e)Faculté des sciences, Université Mohammed V, Rabat; Morocco.
- ³⁶CERN, Geneva; Switzerland.
- ³⁷Affiliated with an institute covered by a cooperation agreement with CERN.
- ³⁸Affiliated with an international laboratory covered by a cooperation agreement with CERN.
- ³⁹Enrico Fermi Institute, University of Chicago, Chicago IL; United States of America.
- ⁴⁰LPC, Université Clermont Auvergne, CNRS/IN2P3, Clermont-Ferrand; France.
- ⁴¹Nevis Laboratory, Columbia University, Irvington NY; United States of America.
- ⁴²Niels Bohr Institute, University of Copenhagen, Copenhagen; Denmark.
- ⁴³(^a)Dipartimento di Fisica, Università della Calabria, Rende; (^b)INFN Gruppo Collegato di Cosenza, Laboratori Nazionali di Frascati; Italy.
- ⁴⁴Physics Department, Southern Methodist University, Dallas TX; United States of America.
- ⁴⁵Physics Department, University of Texas at Dallas, Richardson TX; United States of America.
- ⁴⁶National Centre for Scientific Research "Demokritos", Agia Paraskevi; Greece.
- ⁴⁷(^a)Department of Physics, Stockholm University; (^b)Oskar Klein Centre, Stockholm; Sweden.
- ⁴⁸Deutsches Elektronen-Synchrotron DESY, Hamburg and Zeuthen; Germany.
- ⁴⁹Fakultät Physik , Technische Universität Dortmund, Dortmund; Germany.
- ⁵⁰Institut für Kern- und Teilchenphysik, Technische Universität Dresden, Dresden; Germany.

- ⁵¹Department of Physics, Duke University, Durham NC; United States of America.
- ⁵²SUPA - School of Physics and Astronomy, University of Edinburgh, Edinburgh; United Kingdom.
- ⁵³INFN e Laboratori Nazionali di Frascati, Frascati; Italy.
- ⁵⁴Physikalisches Institut, Albert-Ludwigs-Universität Freiburg, Freiburg; Germany.
- ⁵⁵II. Physikalisches Institut, Georg-August-Universität Göttingen, Göttingen; Germany.
- ⁵⁶Département de Physique Nucléaire et Corpusculaire, Université de Genève, Genève; Switzerland.
- ⁵⁷(^a)Dipartimento di Fisica, Università di Genova, Genova; (^b)INFN Sezione di Genova; Italy.
- ⁵⁸II. Physikalisches Institut, Justus-Liebig-Universität Giessen, Giessen; Germany.
- ⁵⁹SUPA - School of Physics and Astronomy, University of Glasgow, Glasgow; United Kingdom.
- ⁶⁰LPSC, Université Grenoble Alpes, CNRS/IN2P3, Grenoble INP, Grenoble; France.
- ⁶¹Laboratory for Particle Physics and Cosmology, Harvard University, Cambridge MA; United States of America.
- ⁶²(^a)Department of Modern Physics and State Key Laboratory of Particle Detection and Electronics, University of Science and Technology of China, Hefei; (^b)Institute of Frontier and Interdisciplinary Science and Key Laboratory of Particle Physics and Particle Irradiation (MOE), Shandong University, Qingdao; (^c)School of Physics and Astronomy, Shanghai Jiao Tong University, Key Laboratory for Particle Astrophysics and Cosmology (MOE), SKLPPC, Shanghai; (^d)Tsung-Dao Lee Institute, Shanghai; China.
- ⁶³(^a)Kirchhoff-Institut für Physik, Ruprecht-Karls-Universität Heidelberg, Heidelberg; (^b)Physikalisches Institut, Ruprecht-Karls-Universität Heidelberg, Heidelberg; Germany.
- ⁶⁴Faculty of Applied Information Science, Hiroshima Institute of Technology, Hiroshima; Japan.
- ⁶⁵(^a)Department of Physics, Chinese University of Hong Kong, Shatin, N.T., Hong Kong; (^b)Department of Physics, University of Hong Kong, Hong Kong; (^c)Department of Physics and Institute for Advanced Study, Hong Kong University of Science and Technology, Clear Water Bay, Kowloon, Hong Kong; China.
- ⁶⁶Department of Physics, National Tsing Hua University, Hsinchu; Taiwan.
- ⁶⁷IJCLab, Université Paris-Saclay, CNRS/IN2P3, 91405, Orsay; France.
- ⁶⁸Department of Physics, Indiana University, Bloomington IN; United States of America.
- ⁶⁹(^a)INFN Gruppo Collegato di Udine, Sezione di Trieste, Udine; (^b)ICTP, Trieste; (^c)Dipartimento Politecnico di Ingegneria e Architettura, Università di Udine, Udine; Italy.
- ⁷⁰(^a)INFN Sezione di Lecce; (^b)Dipartimento di Matematica e Fisica, Università del Salento, Lecce; Italy.
- ⁷¹(^a)INFN Sezione di Milano; (^b)Dipartimento di Fisica, Università di Milano, Milano; Italy.
- ⁷²(^a)INFN Sezione di Napoli; (^b)Dipartimento di Fisica, Università di Napoli, Napoli; Italy.
- ⁷³(^a)INFN Sezione di Pavia; (^b)Dipartimento di Fisica, Università di Pavia, Pavia; Italy.
- ⁷⁴(^a)INFN Sezione di Pisa; (^b)Dipartimento di Fisica E. Fermi, Università di Pisa, Pisa; Italy.
- ⁷⁵(^a)INFN Sezione di Roma; (^b)Dipartimento di Fisica, Sapienza Università di Roma, Roma; Italy.
- ⁷⁶(^a)INFN Sezione di Roma Tor Vergata; (^b)Dipartimento di Fisica, Università di Roma Tor Vergata, Roma; Italy.
- ⁷⁷(^a)INFN Sezione di Roma Tre; (^b)Dipartimento di Matematica e Fisica, Università Roma Tre, Roma; Italy.
- ⁷⁸(^a)INFN-TIFPA; (^b)Università degli Studi di Trento, Trento; Italy.
- ⁷⁹Universität Innsbruck, Department of Astro and Particle Physics, Innsbruck; Austria.
- ⁸⁰University of Iowa, Iowa City IA; United States of America.
- ⁸¹Department of Physics and Astronomy, Iowa State University, Ames IA; United States of America.
- ⁸²(^a)Departamento de Engenharia Elétrica, Universidade Federal de Juiz de Fora (UFJF), Juiz de Fora; (^b)Universidade Federal do Rio De Janeiro COPPE/EE/IF, Rio de Janeiro; (^c)Instituto de Física, Universidade de São Paulo, São Paulo; Brazil.
- ⁸³KEK, High Energy Accelerator Research Organization, Tsukuba; Japan.
- ⁸⁴Graduate School of Science, Kobe University, Kobe; Japan.

- ⁸⁵(*a*) AGH University of Science and Technology, Faculty of Physics and Applied Computer Science, Krakow; (*b*) Marian Smoluchowski Institute of Physics, Jagiellonian University, Krakow; Poland.
- ⁸⁶Institute of Nuclear Physics Polish Academy of Sciences, Krakow; Poland.
- ⁸⁷Faculty of Science, Kyoto University, Kyoto; Japan.
- ⁸⁸Kyoto University of Education, Kyoto; Japan.
- ⁸⁹Research Center for Advanced Particle Physics and Department of Physics, Kyushu University, Fukuoka ; Japan.
- ⁹⁰Instituto de Física La Plata, Universidad Nacional de La Plata and CONICET, La Plata; Argentina.
- ⁹¹Physics Department, Lancaster University, Lancaster; United Kingdom.
- ⁹²Oliver Lodge Laboratory, University of Liverpool, Liverpool; United Kingdom.
- ⁹³Department of Experimental Particle Physics, Jožef Stefan Institute and Department of Physics, University of Ljubljana, Ljubljana; Slovenia.
- ⁹⁴School of Physics and Astronomy, Queen Mary University of London, London; United Kingdom.
- ⁹⁵Department of Physics, Royal Holloway University of London, Egham; United Kingdom.
- ⁹⁶Department of Physics and Astronomy, University College London, London; United Kingdom.
- ⁹⁷Louisiana Tech University, Ruston LA; United States of America.
- ⁹⁸Fysiska institutionen, Lunds universitet, Lund; Sweden.
- ⁹⁹Centre de Calcul de l'Institut National de Physique Nucléaire et de Physique des Particules (IN2P3), Villeurbanne; France.
- ¹⁰⁰Departamento de Física Teórica C-15 and CIAFF, Universidad Autónoma de Madrid, Madrid; Spain.
- ¹⁰¹Institut für Physik, Universität Mainz, Mainz; Germany.
- ¹⁰²School of Physics and Astronomy, University of Manchester, Manchester; United Kingdom.
- ¹⁰³CPPM, Aix-Marseille Université, CNRS/IN2P3, Marseille; France.
- ¹⁰⁴Department of Physics, University of Massachusetts, Amherst MA; United States of America.
- ¹⁰⁵Department of Physics, McGill University, Montreal QC; Canada.
- ¹⁰⁶School of Physics, University of Melbourne, Victoria; Australia.
- ¹⁰⁷Department of Physics, University of Michigan, Ann Arbor MI; United States of America.
- ¹⁰⁸Department of Physics and Astronomy, Michigan State University, East Lansing MI; United States of America.
- ¹⁰⁹Group of Particle Physics, University of Montreal, Montreal QC; Canada.
- ¹¹⁰Fakultät für Physik, Ludwig-Maximilians-Universität München, München; Germany.
- ¹¹¹Max-Planck-Institut für Physik (Werner-Heisenberg-Institut), München; Germany.
- ¹¹²Nagasaki Institute of Applied Science, Nagasaki; Japan.
- ¹¹³Graduate School of Science and Kobayashi-Maskawa Institute, Nagoya University, Nagoya; Japan.
- ¹¹⁴Department of Physics and Astronomy, University of New Mexico, Albuquerque NM; United States of America.
- ¹¹⁵Institute for Mathematics, Astrophysics and Particle Physics, Radboud University/Nikhef, Nijmegen; Netherlands.
- ¹¹⁶Nikhef National Institute for Subatomic Physics and University of Amsterdam, Amsterdam; Netherlands.
- ¹¹⁷Department of Physics, Northern Illinois University, DeKalb IL; United States of America.
- ¹¹⁸Department of Physics, New York University, New York NY; United States of America.
- ¹¹⁹Ochanomizu University, Otsuka, Bunkyo-ku, Tokyo; Japan.
- ¹²⁰Ohio State University, Columbus OH; United States of America.
- ¹²¹Faculty of Science, Okayama University, Okayama; Japan.
- ¹²²Homer L. Dodge Department of Physics and Astronomy, University of Oklahoma, Norman OK; United States of America.

- ¹²³Department of Physics, Oklahoma State University, Stillwater OK; United States of America.
- ¹²⁴Palacký University, Joint Laboratory of Optics, Olomouc; Czech Republic.
- ¹²⁵Institute for Fundamental Science, University of Oregon, Eugene, OR; United States of America.
- ¹²⁶Graduate School of Science, Osaka University, Osaka; Japan.
- ¹²⁷Department of Physics, University of Oslo, Oslo; Norway.
- ¹²⁸Department of Physics, Oxford University, Oxford; United Kingdom.
- ¹²⁹LPNHE, Sorbonne Université, Université Paris Cité, CNRS/IN2P3, Paris; France.
- ¹³⁰Department of Physics, University of Pennsylvania, Philadelphia PA; United States of America.
- ¹³¹Department of Physics and Astronomy, University of Pittsburgh, Pittsburgh PA; United States of America.
- ¹³²(^a)Laboratório de Instrumentação e Física Experimental de Partículas - LIP, Lisboa; (^b)Departamento de Física, Faculdade de Ciências, Universidade de Lisboa, Lisboa; (^c)Departamento de Física, Universidade de Coimbra, Coimbra; (^d)Centro de Física Nuclear da Universidade de Lisboa, Lisboa; (^e)Departamento de Física, Universidade do Minho, Braga; (^f)Departamento de Física Teórica y del Cosmos, Universidad de Granada, Granada (Spain); (^g)Dep Física and CEFITEC of Faculdade de Ciências e Tecnologia, Universidade Nova de Lisboa, Caparica; (^h)Departamento de Física, Instituto Superior Técnico, Universidade de Lisboa, Lisboa; Portugal.
- ¹³³Institute of Physics of the Czech Academy of Sciences, Prague; Czech Republic.
- ¹³⁴Czech Technical University in Prague, Prague; Czech Republic.
- ¹³⁵Charles University, Faculty of Mathematics and Physics, Prague; Czech Republic.
- ¹³⁶Particle Physics Department, Rutherford Appleton Laboratory, Didcot; United Kingdom.
- ¹³⁷IRFU, CEA, Université Paris-Saclay, Gif-sur-Yvette; France.
- ¹³⁸Santa Cruz Institute for Particle Physics, University of California Santa Cruz, Santa Cruz CA; United States of America.
- ¹³⁹(^a)Departamento de Física, Pontificia Universidad Católica de Chile, Santiago; (^b)Universidad Andres Bello, Department of Physics, Santiago; (^c)Departamento de Física, Universidad Técnica Federico Santa María, Valparaíso; Chile.
- ¹⁴⁰Universidade Federal de São João del Rei (UFSJ), São João del Rei; Brazil.
- ¹⁴¹Department of Physics, University of Washington, Seattle WA; United States of America.
- ¹⁴²Department of Physics and Astronomy, University of Sheffield, Sheffield; United Kingdom.
- ¹⁴³Department of Physics, Shinshu University, Nagano; Japan.
- ¹⁴⁴Department Physik, Universität Siegen, Siegen; Germany.
- ¹⁴⁵Department of Physics, Simon Fraser University, Burnaby BC; Canada.
- ¹⁴⁶SLAC National Accelerator Laboratory, Stanford CA; United States of America.
- ¹⁴⁷Department of Physics, Royal Institute of Technology, Stockholm; Sweden.
- ¹⁴⁸Departments of Physics and Astronomy, Stony Brook University, Stony Brook NY; United States of America.
- ¹⁴⁹Department of Physics and Astronomy, University of Sussex, Brighton; United Kingdom.
- ¹⁵⁰School of Physics, University of Sydney, Sydney; Australia.
- ¹⁵¹Institute of Physics, Academia Sinica, Taipei; Taiwan.
- ¹⁵²(^a)E. Andronikashvili Institute of Physics, Iv. Javakhishvili Tbilisi State University, Tbilisi; (^b)High Energy Physics Institute, Tbilisi State University, Tbilisi; Georgia.
- ¹⁵³Department of Physics, Technion, Israel Institute of Technology, Haifa; Israel.
- ¹⁵⁴Raymond and Beverly Sackler School of Physics and Astronomy, Tel Aviv University, Tel Aviv; Israel.
- ¹⁵⁵Department of Physics, Aristotle University of Thessaloniki, Thessaloniki; Greece.
- ¹⁵⁶International Center for Elementary Particle Physics and Department of Physics, University of Tokyo, Tokyo; Japan.

- ¹⁵⁷Graduate School of Science and Technology, Tokyo Metropolitan University, Tokyo; Japan.
- ¹⁵⁸Department of Physics, Tokyo Institute of Technology, Tokyo; Japan.
- ¹⁵⁹Department of Physics, University of Toronto, Toronto ON; Canada.
- ¹⁶⁰(^a)TRIUMF, Vancouver BC; (^b)Department of Physics and Astronomy, York University, Toronto ON; Canada.
- ¹⁶¹Division of Physics and Tomonaga Center for the History of the Universe, Faculty of Pure and Applied Sciences, University of Tsukuba, Tsukuba; Japan.
- ¹⁶²Department of Physics and Astronomy, Tufts University, Medford MA; United States of America.
- ¹⁶³Department of Physics and Astronomy, University of California Irvine, Irvine CA; United States of America.
- ¹⁶⁴Department of Physics and Astronomy, University of Uppsala, Uppsala; Sweden.
- ¹⁶⁵Department of Physics, University of Illinois, Urbana IL; United States of America.
- ¹⁶⁶Instituto de Física Corpuscular (IFIC), Centro Mixto Universidad de Valencia - CSIC, Valencia; Spain.
- ¹⁶⁷Department of Physics, University of British Columbia, Vancouver BC; Canada.
- ¹⁶⁸Department of Physics and Astronomy, University of Victoria, Victoria BC; Canada.
- ¹⁶⁹Fakultät für Physik und Astronomie, Julius-Maximilians-Universität Würzburg, Würzburg; Germany.
- ¹⁷⁰Department of Physics, University of Warwick, Coventry; United Kingdom.
- ¹⁷¹Waseda University, Tokyo; Japan.
- ¹⁷²Department of Particle Physics and Astrophysics, Weizmann Institute of Science, Rehovot; Israel.
- ¹⁷³Department of Physics, University of Wisconsin, Madison WI; United States of America.
- ¹⁷⁴Fakultät für Mathematik und Naturwissenschaften, Fachgruppe Physik, Bergische Universität Wuppertal, Wuppertal; Germany.
- ¹⁷⁵Department of Physics, Yale University, New Haven CT; United States of America.
- ^a Also Affiliated with an institute covered by a cooperation agreement with CERN.
- ^b Also at Borough of Manhattan Community College, City University of New York, New York NY; United States of America.
- ^c Also at CERN, Geneva; Switzerland.
- ^d Also at CPPM, Aix-Marseille Université, CNRS/IN2P3, Marseille; France.
- ^e Also at Département de Physique Nucléaire et Corpusculaire, Université de Genève, Genève; Switzerland.
- ^f Also at Departament de Física de la Universitat Autònoma de Barcelona, Barcelona; Spain.
- ^g Also at Department of Applied Physics and Astronomy, University of Sharjah, Sharjah; United Arab Emirates.
- ^h Also at Department of Financial and Management Engineering, University of the Aegean, Chios; Greece.
- ⁱ Also at Department of Physics and Astronomy, Michigan State University, East Lansing MI; United States of America.
- ^j Also at Department of Physics and Astronomy, University of Louisville, Louisville, KY; United States of America.
- ^k Also at Department of Physics, Ben Gurion University of the Negev, Beer Sheva; Israel.
- ^l Also at Department of Physics, California State University, East Bay; United States of America.
- ^m Also at Department of Physics, California State University, Fresno; United States of America.
- ⁿ Also at Department of Physics, California State University, Sacramento; United States of America.
- ^o Also at Department of Physics, King's College London, London; United Kingdom.
- ^p Also at Department of Physics, Stanford University, Stanford CA; United States of America.
- ^q Also at Department of Physics, University of Adelaide, Adelaide; Australia.
- ^r Also at Department of Physics, University of Fribourg, Fribourg; Switzerland.
- ^s Also at Dipartimento di Matematica, Informatica e Fisica, Università di Udine, Udine; Italy.

- ^t Also at Giresun University, Faculty of Engineering, Giresun; Türkiye.
- ^u Also at Hellenic Open University, Patras; Greece.
- ^v Also at IJCLab, Université Paris-Saclay, CNRS/IN2P3, 91405, Orsay; France.
- ^w Associated at INFN e Laboratori Nazionali di Frascati, Frascati; Italy.
- ^x Also at Institucio Catalana de Recerca i Estudis Avancats, ICREA, Barcelona; Spain.
- ^y Also at Institut für Experimentalphysik, Universität Hamburg, Hamburg; Germany.
- ^z Also at Institute for Mathematics, Astrophysics and Particle Physics, Radboud University/Nikhef, Nijmegen; Netherlands.
- ^{aa} Also at Institute for Nuclear Research and Nuclear Energy (INRNE) of the Bulgarian Academy of Sciences, Sofia; Bulgaria.
- ^{ab} Also at Institute for Particle and Nuclear Physics, Wigner Research Centre for Physics, Budapest; Hungary.
- ^{ac} Also at Institute of Particle Physics (IPP); Canada.
- ^{ad} Also at Institute of Physics, Azerbaijan Academy of Sciences, Baku; Azerbaijan.
- ^{ae} Also at Institute of Theoretical Physics, Ilia State University, Tbilisi; Georgia.
- ^{af} Also at Instituto de Fisica Teorica, IFT-UAM/CSIC, Madrid; Spain.
- ^{ag} Also at Istanbul University, Dept. of Physics, Istanbul; Türkiye.
- ^{ah} Also at Louisiana Tech University, Ruston LA; United States of America.
- ^{ai} Also at Manhattan College, New York NY; United States of America.
- ^{aj} Also at Physics Department, An-Najah National University, Nablus; Palestine.
- ^{ak} Also at Physics Dept, University of South Africa, Pretoria; South Africa.
- ^{al} Also at Physikalisches Institut, Albert-Ludwigs-Universität Freiburg, Freiburg; Germany.
- ^{am} Also at The City College of New York, New York NY; United States of America.
- ^{an} Also at The Collaborative Innovation Center of Quantum Matter (CICQM), Beijing; China.
- ^{ao} Also at TRIUMF, Vancouver BC; Canada.
- ^{ap} Also at Università di Napoli Parthenope, Napoli; Italy.
- * Deceased